Theory of the weakly interacting Bose gas

Jens O. Andersen*

Nordita, Blegdamsvej 17, 2100 Copenhagen, Denmark

(Published 1 July 2004)

This article reviews recent advances in the theory of the three-dimensional dilute homogeneous Bose gas at zero and finite temperature. Effective-field-theory methods are used to formulate a systematic perturbative framework that can be used to calculate the properties of a system at $T=0$. The perturbative expansion of these properties is essentially an expansion in the gas parameter $\sqrt{na^3}$, where a is the s-wave scattering length and n is the number density. In particular, the leading quantum corrections to the ground-state energy density, the condensate depletion, and long-wavelength collective excitations are rederived in an efficient and economical manner. Nonuniversal effects are also discussed. These effects are higher-order corrections that depend on properties of the interatomic potential other than the scattering length, such as the effective range. The article critically examines various approaches to the dilute Bose gas in equilibrium at finite temperature. These include the Bogoliubov approximation, the Popov approximation, the Hartree-Fock-Bogoliubov approximation, the Φ-derivable approach, optimized perturbation theory, and renormalization-group techniques. The article ends with a look at recent calculations of the critical temperature of the dilute Bose gas, which include $1/N$ techniques, lattice simulations, self-consistent calculations, and variational perturbation theory.

CONTENTS

---

*Electronic address: jensoa@nordita.dk

I. INTRODUCTION

The remarkable realization of Bose-Einstein condensation (BEC) of trapped alkali atoms (Anderson *et al.*, 1995; Bradley *et al.*, 1995; Davis *et al.*, 1995) has created an enormous interest in the properties of the weakly interacting Bose gas. Although the experiments are carried out in magnetic and optical harmonic traps, the homogeneous Bose gas has also received renewed interest (Shi and Griffin, 1998). The homogeneous Bose gas is interesting in its own right, and it may prove useful to go back to this somewhat simpler system to gain insight that carries over to the trapped case.

Bose-Einstein condensation has a very long history dating back to the early days of quantum mechanics and the papers by Bose and Einstein (Bose, 1924; Einstein, 1924). The canonical example of a system that exhibits BEC is liquid ^{4}He. At very low atmospheric pressure, ^{4}He becomes superfluid below a temperature of 2.17 K, which is called the λ point. The fluid then consists of two components, namely, a normal and a superfluid component. The superfluid component has zero viscosity, and it has the remarkable property that it can flow through narrow tubes without friction. In modern terminology, the phase transition from a normal fluid to a superfluid is described as spontaneous breaking of the global U(1) symmetry and the occurrence of a condensate of atoms residing in the zero-momentum state. This description also explains the experimental fact that the spectrum is gapless and linear in the long-wavelength limit; the existence of a gapless and linear dispersion relation follows from the Goldstone theorem (Goldstone, 1961). It turns out that ^{4}He is strongly interacting, and this reduces the density of the condensate to a rather small fraction of the total number density. At very low temperature and pressure, the condensate density is approximately 10% of the total number density. Thus the condensate density and superfluid density are very different at low tempera-

ture. Liquid ^{4}He consists of extended objects with very complicated nonlocal interactions. Moreover, the fact that it is strongly interacting makes it impossible to apply perturbative methods. This has led to the search for weakly interacting Bose gases. The trapped alkali gases are such systems, and their advantage over liquid ^{4}He is that they behave like systems of point particles with simple local interactions. The study of these gases has therefore become a very active field of research in the past decade. Interested readers may consult the books by Pethick and Smith (2002), and by Pitaevskii and Stringari (2003), as well as the review papers by Dalfovo *et al.* (1999) and by Leggett (2001).

The concept of Bose-Einstein condensation has been applied in many areas of physics other than ^{4}He, and thus a thorough understanding of it is important. For instance, many properties of a superconductor can be understood in terms of a condensate of pairs of electrons with opposite spin and momenta. Similarly, many properties of the QCD vacuum can be understood on the basis of a condensate of quark-antiquark pairs with zero total momentum. This condensate is called the chiral condensate, and, in massless QCD, it breaks the chiral symmetry of the QCD Lagrangian. The pions are interpreted as the corresponding Goldstone particles.

The homogeneous Bose gas at zero temperature has been studied extensively for over 50 years, starting with the classic paper by Bogoliubov (1947). At zero temperature, the quantum loop expansion is essentially an expansion in the gas parameter $\sqrt{na^3}$, where n is the number density and a is the (positive) s-wave scattering length. The leading quantum corrections to the chemical potential, energy density, and speed of sound were calculated many years ago by Lee and Yang using the pseudopotential method (Lee and Yang, 1957). Part of the second quantum correction to the energy density was obtained by Wu (1959), by Hugenholz and Pines (1959), and by Sawada (1959). Only recently, a complete two-loop result has been obtained by Braaten and Nieto (1997). The result depends not only on the scattering length a, but also on an energy-independent term in the scattering amplitude for $3 \rightarrow 3$ scattering. The fact that physical quantities depend on properties other than the s-wave scattering length was already pointed out by Hugenholz and Pines (1959). These effects are called *nonuniversal effects*. In the past decades effective field theory has been established as an ideal tool for systematically calculating low-energy observables of a physical system (Lepage, 1989; Georgi, 1993; Kaplan, 1995). Effective-field-theory methods have also proven very useful for calculating higher-order corrections in powers of $\sqrt{na^3}$ as well as nonuniversal effects in the weakly interacting Bose gas (Braaten *et al.*, 2001).

Finite-temperature corrections to the pressure of a dilute Bose gas were first calculated by Lee and Yang (1958). Performing an expansion of the pressure about zero temperature, they showed that the leading term goes as T^4. This shows that the thermodynamics at low temperature are completely determined by the linear part of the spectrum. Similarly, the low-temperature expansion of the number density was calculated by Glassgold *et al.* (1960) and shows a T^2 behavior. These calculations were all based on the Bogoliubov approximation and are therefore valid only at low temperature, where the depletion of the condensate is small. The first approach to take into account the excited states, and thus to be usable over the whole temperature range up to T_c, is the Popov theory (Popov, 1983, 1987; Shi and Griffin, 1998). Very recently, an improved many-body T-matrix approximation was developed (Al Khawaja *et al.*, 2002; Andersen *et al.*, 2002), which does not suffer from the infrared divergences in lower dimensions that plague the Bogoliubov and Popov approximations. While the approach can be applied in any dimension, its main application is in one and two dimensions, since the predictions in three dimensions are very similar to those of established approaches. For instance, it predicts the same zero-temperature depletion of the condensate as the Bogoliubov approximation and the same critical temperature as the Popov approximation.

The most recent extensive review on the homogeneous Bose gas was written by Shi and Griffin (1998), six years ago. In the meantime, significant progress has been made, and a new review paper summarizing recent advances is appropriate. There will of course be an overlap between the review of Shi and Griffin and the present paper, but some new material is covered. This includes nonuniversal effects (Braaten *et al.*, 2001), renormalization-group calculations (Bijlsma and Stoof, 1996a, 1996b; Andersen and Strickland, 1999; Metikas and Alber, 2002), some of the variational approaches (Lundh and Rammer, 2002), and calculations of the critical temperature T_c.[1] Traditionally, the theory of dilute Bose gases is presented using creation and annihilation operators as well as normal and anomalous self-energies. The present review is different in this respect, since we are using modern functional methods, and only occasionally will we present the material in terms of normal and anomalous averages. This also implies that we are working with Lagrangians and actions, rather than with Hamiltonians. We are largely going to base our discussion on effective-field-theory methods (Lepage, 1989; Georgi, 1993; Kaplan, 1995). The virtue of effective field theory is that it allows one to systematically calculate physical quantities efficiently by taking advantage of the separation of length scales in a particular problem. We shall return to these issues in some detail later.

Much of the theoretical research on trapped Bose gases in recent years has been on dynamical issues, e.g., condensate formation, damping of collective excitations, and collapse of the condensate. There is also a large body of literature on the nonequilibrium dynamics of

---

[1]See, for example, Grüter *et al.*, 1997; Baym *et al.*, 1999, 2000, 2001; Holzmann and Krauth, 1999; Arnold and Tomasik, 2000; Arnold and Moore, 2001a, 2001b; de Souza Cruz *et al.*, 2001, 2002; Kashurnikov *et al.*, 2001; Arnold *et al.*, 2002; Braaten and Radescu, 2002; Davis and Morgan, 2003; Kastening, 2003, 2004; Kleinert, 2003; Ledowski *et al.*, 2003.

the dilute Bose gas, but these topics deserve a separate review. Similarly, there has been significant progress in the understanding of low-dimensional Bose gases, following their experimental realization (Petrov, Holzmann, and Shlyapnikov, 2000; Al Khawaja *et al.*, 2002; Andersen *et al.*, 2002). In order to limit the material, we shall focus entirely on the three-dimensional Bose gas in this review. For the same reason, we also restrict ourselves to the spinless Bose gas.

The paper is organized as follows: In Sec. II, the ideal Bose gas at finite temperature is briefly reviewed. Section III discusses the weakly interacting Bose gas at zero temperature. A perturbative framework using effective-field-theory methods is set up. This framework is used to rederive the leading quantum corrections to various quantities and discuss nonuniversal effects. Section IV treats the weakly interacting Bose gas at finite temperature. We discuss the Hartree-Fock-Bogoliubov approximation, the Bogoliubov approximation, and the Popov approximation. Then we consider the Φ-derivable approach and optimized perturbation theory, which are variational approaches. Finally, renormalization-group techniques are reviewed. Section V discusses the calculation of the critical temperature T_c using a variety of different techniques. In Sec. VI, we summarize and conclude. Calculational details, as well as notation and conventions, are included in the Appendix.

II. THE IDEAL BOSE GAS

In this section, we review the ideal Bose gas at finite temperature. Although this is standard textbook material, a discussion is included to make the paper self-contained. In the remainder of the paper, we set $\hbar = 2m = k_B = 1$. Factors of $\hbar$, $2m$, and k_B can be reinserted using dimensional analysis.

Consider N bosons at temperature T in a box of volume V, so that the number density is $n = N/V$. We impose periodic boundary conditions. We are always working in the thermodynamic limit, meaning $N, V \to \infty$ in such a manner that n is fixed.

At high temperature, where the thermal wavelength $\lambda_T = 2\sqrt{\pi/T}$ is much shorter than the interparticle spacing, the atoms behave classically, and their statistics are not important. As the temperature is lowered, the atoms can be viewed as little wave packets with extent of the order λ_T. Bose-Einstein condensation takes place when the thermal wavelength of a particle is on the order of the interparticle spacing $n^{-1/3}$, and the wave functions of the bosons start to overlap. The particles then accumulate in the zero-momentum state. At $T = 0$, all the particles reside in this state. Since fermions behave very differently at low temperatures due to the Pauli exclusion principle, BEC is truly a quantum phenomenon.

We can estimate T_c^0 by equating the thermal wavelength λ_T with the average distance between the bosons $n^{-1/3}$:

$$2\sqrt{\pi/T_c^0} \sim n^{-1/3}. \tag{1}$$

The estimate for the critical temperature T_c^0 then becomes

$$T_c^0 \sim 4\pi n^{2/3}. \tag{2}$$

Having estimated T_c, we next discuss the thermodynamics in more detail. In the functional approach to the imaginary-time formalism, the grand-canonical partition function $\mathcal{Z}$ is given by a path integral (Negele and Orland, 1988):

$$\mathcal{Z} = \int \mathcal{D}\psi^* \mathcal{D}\psi e^{-S[\psi^*, \psi]}, \tag{3}$$

where the action S is given by

$$S[\psi^*, \psi] = \int_0^\beta d\tau \int d^3x \, \psi^*(\mathbf{x}, \tau) \left[\frac{\partial}{\partial \tau} - \nabla^2 - \mu \right] \psi(\mathbf{x}, \tau). \tag{4}$$

Here, $\beta = 1/T$ and μ is the chemical potential. The complex fields ψ^* and ψ satisfy the standard bosonic periodicity condition that $\psi(\mathbf{x}, \tau)$ and $\psi^*(\mathbf{x}, \tau)$ are periodic in τ with period β. We next write the complex field in terms of two real fields,[2]

$$\psi = \frac{1}{\sqrt{2}}(\psi_1 + i\psi_2). \tag{5}$$

After inserting Eq. (5) into the action (4), we find the corresponding Green's function or propagator to be

$$D_0(\omega_n, p) = \frac{1}{\omega_n^2 + (p^2 - \mu)^2} \begin{pmatrix} p^2 - \mu & \omega_n \\ -\omega_n & p^2 - \mu \end{pmatrix}, \tag{6}$$

where $\omega_n = 2\pi n T$ is the nth Matsubara frequency. The path integral (3) is Gaussian and can therefore be evaluated exactly. The result is

$$\mathcal{Z} = e^{-\int_0^\beta d\tau \int d^3x \, \det D_0^{-1}(\omega_n, p)}, \tag{7}$$

where $D_0^{-1}(\omega_n, p)$ is the inverse of the propagator (6) and det denotes a determinant in the functional sense. The free-energy density is given by

$$\mathcal{F} = -\frac{1}{V\beta} \ln \mathcal{Z}$$

$$= \frac{1}{2} \text{Tr} \ln D_0^{-1}(\omega_n, p), \tag{8}$$

where we have used that $\ln \det A = \text{Tr} \ln A$ for any matrix A where Tr denotes the trace. Inverting Eq. (6) and taking the trace, we obtain

$$\mathcal{F} = \frac{1}{2} \sum_P \!\!\!\!\!\!\!\int \ln[\omega_n^2 + (p^2 - \mu)^2], \tag{9}$$

where the sum-integral means

---

[2] In traditional approaches, one uses the single complex field ψ instead of two real fields. This is merely a matter of taste. See also the comments at the end of this section.

$$\sum_{P}\!\!\!\!\!\!\!\!\int \equiv M^{2\epsilon}T\sum_{\omega_n=2n\pi T}\int\frac{d^dp}{(2\pi)^d}. \qquad (10)$$

The sum-integral involves a summation over Matsubara frequencies and a regularized integral over $d=3-2\epsilon$ dimensions. M is a renormalization scale that ensures that the integral also has the canonical dimensions for $d\neq3$. In the following, we absorb the factor $M^{2\epsilon}$ in the measure, and so it will not appear explicitly. We discuss the details further in the Appendix. After summing over Matsubara frequencies, we obtain

$$\mathcal{F}=\int\frac{d^dp}{(2\pi)^d}\left\{\frac{1}{2}(p^2-\mu)+T\ln[1-e^{-\beta(p^2-\mu)}]\right\}. \qquad (11)$$

The first term inside the brackets is an infinite constant that is independent of temperature. It represents the zero-point fluctuations and can be removed by a vacuum energy counterterm $\Delta\mathcal{E}$. The second term is the standard finite-temperature free energy of an ideal gas of nonrelativistic bosons.

In the operator approach, the starting point would be the grand-canonical Hamiltonian which corresponds to the action (4):

$$\mathcal{H}=\frac{1}{2}\int\frac{d^3p}{(2\pi)^3}(p^2-\mu)a_{\mathbf{p}}^\dagger a_{\mathbf{p}}. \qquad (12)$$

Using the Hamiltonian (12) to calculate physical quantities, one does not encounter zero-point fluctuation terms, since it has been normal ordered; the operator $a_{\mathbf{p}}$ annihilates the vacuum. If it had not been normal ordered, one would find the same divergent terms as with the path-integral approach. This is the usual ambiguity of the quantization procedure in going from classical field theory to quantum field theory.

We have replaced momentum sums by integrals over p. Due to the measure d^dp, the integrand always vanishes at $p=0$, and the contribution from the ground state is not accounted for. If we denote the condensate density of particles in the lowest-energy state by n_0, and the number density of particles in the excited states by n_{ex}, we have $n=n_0+n_{\text{ex}}$. The density of excited particles is then given by minus the derivative of $\mathcal{F}$ with respect to the chemical potential:

$$n_{\text{ex}}=\int\frac{d^dp}{(2\pi)^d}n(p^2-\mu), \qquad (13)$$

where

$$n(\omega)=\frac{1}{e^{\beta\omega}-1} \qquad (14)$$

is the Bose-Einstein distribution function. Equation (13) makes sense only for $\mu\leq0$. If $\mu>p^2$ for some p^*, the occupation number of the states with $p<p^*$ would become negative. Clearly, this is unphysical. Below the transition temperature, the number of particles in the excited states is given by the integral (13) with $\mu=0$. One finds

$$n_{\text{ex}}=\frac{\zeta\!\left(\dfrac{3}{2}\right)}{(4\pi)^{3/2}}T^{3/2}, \qquad (15)$$

where $\zeta(x)$ is the Riemann zeta function with argument x. The critical temperature is the temperature at which all the particles can be accommodated in the excited states, that is, $n=n_{\text{ex}}$. This yields

$$T_c^0=4\pi\left[\frac{n}{\zeta\!\left(\dfrac{3}{2}\right)}\right]^{2/3}. \qquad (16)$$

The quantity $n\lambda_T^3$ is called the *degeneracy parameter*. For an ideal Bose gas, the critical number density n_c satisfies $n_c\lambda_T^3=\zeta(\frac{3}{2})$. We see that the estimate (2) is correct within a factor of $[\zeta(\frac{3}{2})]^{-2/3}\approx0.527$ of the exact result (16). Using Eqs. (15) and (16), we can write the condensate density n_0 as a function of the temperature T,

$$n_0=n\left[1-\left(\frac{T}{T_c}\right)^{3/2}\right]. \qquad (17)$$

The exponent 3/2 in Eq. (17) is determined solely by the density of states. For an ideal Bose gas in a three-dimensional isotropic harmonic trap, the exponent is 3 (Dalfovo *et al.*, 1999).

III. WEAKLY INTERACTING BOSE GAS AT ZERO TEMPERATURE

In this section, we discuss in some detail the weakly interacting Bose gas at $T=0$. We begin with a description using effective field theory and formulate a perturbative framework that can be used for practical calculations. We then calculate the leading corrections in the low-density expansion to the energy density, depletion, and long-wavelength excitations. Finally, we discuss nonuniversal effects.

A. Effective field theory

Effective field theory is a general approach that can be used to analyze the low-energy behavior of a physical system in a systematic way (Lepage, 1989; Georgi, 1993; Kaplan, 1995). One takes advantage of the separation of scales in a system to make model-independent predictions at low energy. The effective Lagrangian $\mathcal{L}_{\text{eff}}$ that describes the low-energy physics is written in terms only of the long-wavelength degrees of freedom, and the operators that appear are determined by these degrees of freedom and the symmetries present at low energy. The effective Lagrangian generally includes an infinite tower of nonrenormalizable interactions, but they can be organized according to their importance at low energy. To a certain order in a low-energy expansion, only a finite number of operators contribute to a physical quantity and one can carry out renormalization in the standard

way, order by order in this expansion.[3] Since the coefficients of these operators encode the short-wavelength physics, we do not need to make any detailed assumptions about the high-energy dynamics to make predictions at low energy.

In some cases, one can determine the coefficients of the low-energy theory as functions of the coupling constants in the underlying theory by a perturbative matching procedure. One calculates physical observables at low energies perturbatively and demands they be the same both in the full and in the effective theory. The coefficients of the effective theory then encode the short-distance physics. If one cannot determine these short-distance coefficients by matching, they can be taken as phenomenological parameters that are determined by experiment.

A classic example of an effective field theory is chiral perturbation theory, which is a low-energy field theory for pions (Gasser and Leutwyler, 1984, 1985). Pions are interacting particles whose fundamental description is provided by QCD. However, QCD is strongly interacting and confining at low energies, and so perturbative calculations using the QCD Lagrangian are hopeless. Instead of using the quark and gluon degrees of freedom in QCD, one writes down the most general Lagrangian for the pions, which are the relevant low-energy degrees of freedom. The terms that appear in the chiral Lagrangian are determined by the global symmetries of QCD. The coefficients of the chiral Lagrangian cannot be determined as functions of the couplings and masses in QCD using perturbative methods. They can, in principle, be determined using a nonperturbative method such as lattice gauge theory, but in practice they are normally determined by experiment.

Nonrelativistic QED (Caswell and Lepage, 1986) is an example of an effective field theory whose coefficients are tuned so they reproduce a set of low-energy scattering amplitudes of full QED. Nonrelativistic QED is tailored to perform low-energy (bound-state) calculations, where one takes advantage of the nonrelativistic nature of the bound states by isolating the contributions from the relativistic momentum scales. These are encoded in the coefficients of the various local operators in the effective Lagrangian. Traditional approaches involving the Bethe-Salpeter equation do not take advantage of the separation of scales in bound-state problems and are therefore much more difficult to solve.

Landau's quasiparticle model for ^{4}He can also be viewed as an effective field theory. In order to explain that the specific heat varies as T^3 for temperatures much smaller than T_c, he suggested that the low-lying excitations are phonons with a linear dispersion relation. More generally, he proposed a spectrum that is linear for small wave vectors and has a local minimum around $p = p_0$. This part of the spectrum behaves like

$$\epsilon(p) = \Delta + \frac{(p - p_0)^2}{2m_0},$$ (18)

where Δ, p_0, and m_0 are phenomenological parameters. Excitations near p_0 are referred to as *rotons*. Assuming that the elementary excitations are noninteracting, one can use the spectrum to calculate the specific heat. Landau determined the parameters by fitting the calculated specific heat to experimental data (Landau, 1947).

The weakly interacting Bose gas is a system in which effective-field-theory methods can be applied successfully. The starting point is the action

$$S[\psi^*, \psi] = \int dt \left\{ \int d^d x \, \psi^*(\mathbf{x}, t) \right.$$

$$\times \left[i \frac{\partial}{\partial t} + \nabla^2 + \mu \right] \psi(\mathbf{x}, t)$$

$$- \frac{1}{2} \int d^d x \int d^d x' \, \psi^*(\mathbf{x}, t) \psi^*(\mathbf{x}', t)$$

$$\left. \times V_0(\mathbf{x} - \mathbf{x}') \psi(\mathbf{x}, t) \psi(\mathbf{x}', t) + \cdots \right\}.$$ (19)

Here, $\psi^*(\mathbf{x}, t)$ is a complex field operator that creates a boson at the position $\mathbf{x}$ at time t, μ is the chemical potential, and $V_0(\mathbf{x})$ is the two-body potential. The ellipses indicate terms that describe possible interactions between three or more bosons. The chemical potential μ must be adjusted to get the correct number density n.

The interatomic potential can be divided into a central part $V_0^c(x)$ and a remainder. The central part of the potential depends only on the separation x of the atoms and their electronic spins. It conserves separately the total orbital angular momentum and the total electronic spin of the atoms. The noncentral part of the interaction conserves the total angular momentum, but does not separately conserve the orbital angular momentum and the total electronic spin of the atoms. An example of a term in the noncentral part of the interaction is the magnetic dipole-dipole interaction.

The central part of the potential consists of a short-range part with range x_0 and a long-range van der Waals tail. The latter goes as $1/x^6$ as $x \to \infty$. A typical two-body potential is shown in Fig. 1. A model potential of this kind is the sum of a hard-core potential with range x_0 and a van der Waals potential:

$$V_0^c(x) = \begin{cases} +\infty, & x < x_0 \\ -\dfrac{C_6}{x^6}, & x > x_0, \end{cases}$$ (20)

where C_6 and x_0 are constants. Another example is the hard-core square-well potential:

$$V_0^c(x) = \begin{cases} +\infty, & x < x_c \\ -V_0, & x_c < x < x_0 \\ 0, & x < x_0, \end{cases}$$ (21)

---

[3]The counterterms that are used to cancel the divergences in the calculations of one physical quantity are the same as those required in the calculations of another. Thus, having determined the counterterms once and for all, we can use the effective theory to make predictions about other physical quantities.
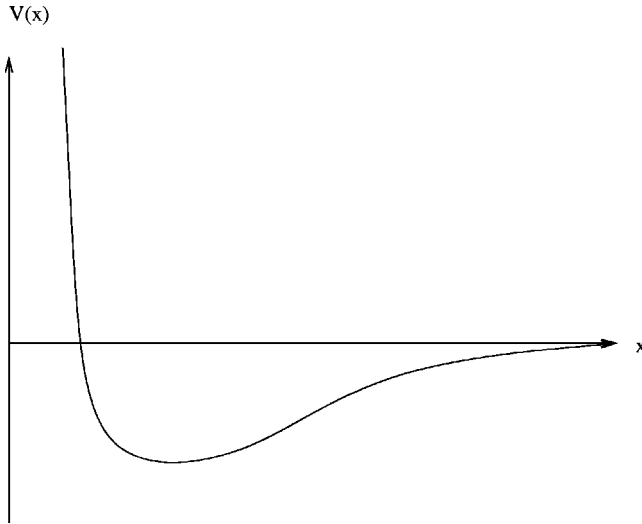
V(x)

FIG. 1. Typical behavior of a two-body potential $V_0^c(x)$.

where x_0 and x_c are constants. This potential sustains a number of two-body bound states depending on the values of x_0 and x_c. Many real potentials used in experiments sustain bound states, and the ground state of the system is no longer a homogeneoues gas, but rather a state of clusters of atoms. However, if the scattering length is positive, the homogeneous Bose gas can exist as a long-lived metastable state.

In Fig. 2, we have shown the Fourier transform $V(\mathbf{k})$ of a typical short-range two-body potential with range x_0. Since a true interatomic potential vanishes for large momenta k, one will never face ultraviolet divergences using it in actual (perturbative) calculations.

In this paper we restrict our calculations to the spinless Bose gas. In experiments with trapped alkali atoms (e.g., ^{7}Li, ^{23}Na, ^{85}Rb, ^{87}Rb, and ^{133}Cs), the situation is more complicated. In all these atoms, there is a single s
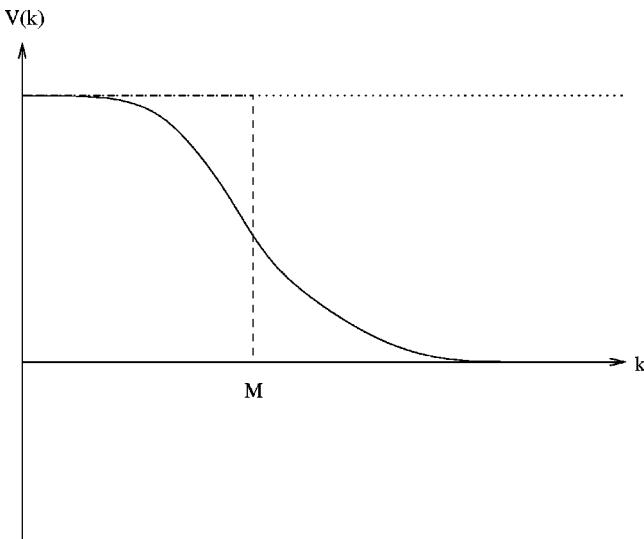
V(k)

FIG. 2. Short-range two-body potential with range x_0: solid line, typical behavior of the potential in momentum space $V(\mathbf{k})$; dotted line, Fourier transform of a contact potential. M is an ultraviolet cutoff.

electron outside closed shells. Consequently these atoms have electron spin $S=1/2$. The total spin of a colliding pair of alkali atoms is therefore either $S=0$ or $S=1$. The central part of the potential $V_0^c(x)$ depends on the total spin, and one refers to these potentials as the *singlet* and *triplet potentials*, respectively. The singlet potential is generally much deeper and sustains many more bound states than does the triplet potential. For example, the singlet potential of ^{87}Rb is deeper than the triplet potential by more than one order of magnitude. The scattering lengths are denoted by a_s and a_t. In the case of atomic hydrogen, they have been calculated from first principles; $a_s=0.3a_0$ and $a_t=1.3a_0$, where a_0 is the Bohr radius. Similarly, the coefficient of the van der Waals tail has also been determined; $C_6=6.499a_0$ (Yan *et al.*, 1996).

One can associate a natural length scale l with any atomic potential $V_0^c(x)$. For a short-range potential, this length is the range x_0 itself. For a long-range potential, it is a little more complicated. The length scale associated with the van der Waals tail is $l_{\mathrm{vdW}} \sim C_6^{1/4}$. In this case, the length scale l is either the range or l_{vdW}, whichever is larger. For a generic potential, the low-energy observables such as the scattering length and the effective range are of the order l. There is nothing that forbids these quantities being much larger than l, but it is unnatural and typically requires fine-tuning of one or more parameters in the potential. In the case of the alkali atoms, l_{vdW} is much larger than the range of the short-range part of the potential and is thus the natural length scale for these atoms. The spin-singlet scattering length for ^{85}Rb is $a_s=+2800a_0$, which is more than an order of magnitude larger than $l=l_{\mathrm{vdW}}=164a_0$. This can be viewed as a fine-tuning of the mass of the atom, as can be seen from the fact that the mass of ^{87}Rb is only 2.3% larger, and the spin-singlet scattering length has the more natural value $a_s=+90.4a_0$. One can also obtain unnaturally large scattering lengths by tuning an external parameter in experiments. One way of doing this is to tune an external magnetic field to a Feshbach resonance (Feshbach, 1962), which is currently receiving a lot of attention both theoretically (Stwalley, 1976; Tiesinga, Verhaar, and Stoof, 1993) and experimentally (Inouye *et al.*, 1998).

In the remainder of this work, we do not specify the magntiude of the scattering length. We require only that the *diluteness condition* be satisfied, namely, that

$$na^3 \ll 1. \tag{22}$$

We now return to the action (19), which is invariant under a global phase transformation

$$\psi(\mathbf{x},t) \to e^{i\alpha}\psi(\mathbf{x},t). \tag{23}$$

The global U(1) symmetry reflects the conservation of atoms. It also ensures that the number density n and current density $\mathbf{j}$ satisfy the continuity equation,

$$\dot{n} + \nabla \cdot \mathbf{j} = 0, \tag{24}$$

where the dot denotes differentiation with respect to time.

The nonlocal evolution equation that follows from the action (19) cannot always be used for practical calculations, but can be replaced by a local one. Suppose we are interested in the properties of the system at momenta k such that the de Broglie wavelength $1/k$ is much longer than the range of the interatomic potential $V_0(\mathbf{x})$. The interactions therefore appear pointlike on the scale of the de Broglie wavelength, and they can be mimicked by local interactions. The parameters of these local interactions must be tuned so that they reproduce low-energy observables to sufficient accuracy. However, if the potential is long range, the scattering amplitude depends in a nonanalytic way on the wave vector $\mathbf{k}$ characterizing the incoming atoms in the center-of-mass frame. Such behavior cannot be reproduced by local operators. If $V_0^c(x)$ falls off like $1/x^6$, this nonanalytic behavior enters first at order k^4 (Braaten and Hammer, 2003).

The effective Lagrangian for the bosons can be constructed using the methods of effective field theory. Once the symmetries have been identified, one writes down the most general local effective Lagrangian consistent with these symmetries. At zero temperature, the symmetries are Galilean invariance, time-reversal symmetry, and the global phase symmetry (23). These symmetries severely restrict the possible terms in the effective action. One finds (Braaten and Nieto, 1997)

$$S[\psi^*,\psi] = \int dt \int d^d x \left\{ \psi^* \left[i\frac{\partial}{\partial t} + \nabla^2 + \mu \right] \psi \right.$$
$$- \frac{1}{2} g(\psi^*\psi)^2 - \frac{1}{2} h[\nabla(\psi^*\psi)]^2$$
$$\left. - \frac{g_3}{36}(\psi^*\psi)^3 + \cdots \right\}, \tag{25}$$

where g, h, and g_3 are coupling constants that can be determined by a matching procedure. The dots denote operators that are higher order in the field ψ or its derivative $\nabla\psi$ and that respect the symmetries. One demands that the effective field theory represented by the action (25) reproduce a set of low-energy observables to some desired accuracy. Examples are the coefficients of the expansions in $\sqrt{na^3}$ of the ground-state energy density or the coefficients in the low-energy expansions for the scattering amplitudes in the n-body sector. When the coefficients in the action (25) have been determined to some accuracy in a low-energy expansion, effective field theory guarantees that all other observables can be determined with the same accuracy.

The quantum field theory defined by the action (25) has ultraviolet divergences that must be removed by renormalization of the parameters $\mu, g, h, g_3, \ldots$. They arise because we are treating the interactions between the atoms as pointlike down to arbitrarily short distances. For instance, the operator $g(\psi^\dagger\psi)^2$ can be thought of as a contact potential with strength g; $V_0(\mathbf{x} - \mathbf{x}') = g\delta(\mathbf{x} - \mathbf{x}')$. The Fourier transform is then a constant in momentum space; $V_0(\mathbf{k}) = g$. This is illustrated

in Fig. 2, where the dotted line shows $V(\mathbf{k})$. Thus $V(\mathbf{k})$ does not vanish for large momenta, and this is the reason why one encounters ultraviolet divergences in the calculation of Feynman diagrams. In order to make the theory well defined, we must introduce an ultraviolet cutoff. This is indicated in Fig. 2, where we exclude wave numbers $k > M$ in momentum integrals.

If we use a simple momentum cutoff M to cut off the ultraviolet divergences, there will be terms that are proportional to M^n, where n is a positive integer. There are also terms that are proportional to $\ln(M)$. The coefficients of the power divergences depend on the method we use to regulate the integrals, while the coefficients of $\ln(M)$ do not. Thus the power divergence are artifacts of the regulator, while the logarithmic divergences represent real physics. In this paper, we shall be using dimensional regularization ('t Hooft and Veltman, 1972) to regulate infrared as well as ultraviolet divergences in the loop integrals. In dimensional regularization, one calculates the loop integrals in $d = 3 - 2\epsilon$ dimensions for values of ϵ for which the integrals converge. One finally continues analytically back to $d = 3$ dimensions. In dimensional regularization, an arbitrary momentum scale M is introduced to ensure that loop integrals also have their canonical dimensions away from three dimensions. This scale can be identified with the simple momentum cutoff mentioned above. Advantages of dimensional regularization are that it respects symmetries such as rotational symmetry and gauge invariance. Dimensional regularization sets power divergences to zero, and logarithmic divergences show up as poles in ϵ. With dimensional regularization, therefore, the only ultraviolet divergences that require explicit renormalization are logarithmic divergences. This simplifies calculations significantly, as we shall see. In fact, all the divergences encountered in the one-loop calculations that we present here can be removed by the renormalization of μ, g, and the vacuum energy $\mathcal{E}$, which, in three dimensions, are power divergences. Thus no explicit renormalization is required.

We now return to the determination of the parameters $g, h, g_3, \ldots$. We follow Braaten $et~al.$ (2001) and determine the parameters by demanding that the effective-field theory (25) reproduce the low-momentum expansions for the scattering amplitudes in the vacuum for $2 \to 2$ scattering, $3 \to 3$ scattering, etc. to some desired accuracy.

To calculate the coupling constant g, consider the scattering of two atoms in the vacuum with initial wave numbers $\mathbf{k}_1$ and $\mathbf{k}_2$, and final wave numbers $\mathbf{k}_1'$ and $\mathbf{k}_2'$. The probability amplitude for the $2 \to 2$ scattering is given by the T-matrix element $\mathcal{T}$. The tree-level contribution to $\mathcal{T}$ comes from the leftmost diagram in Fig. 3 and is given by

$$\mathcal{T}_0 = -2g, \tag{26}$$

where the subscript indicates the number of loops. The quantum corrections to the tree-level result come from the loop diagrams in Fig. 3. The leading quantum correction comes from the one-loop diagram and reads
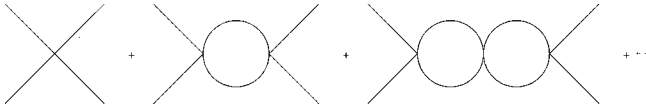
FIG. 3. Diagrams contributing to the $2 \to 2$ scattering amplitude.

$$\mathcal{T}_1(q) = -2ig^2 \int \frac{d\omega}{2\pi} \int \frac{d^d k}{(2\pi)^d} \frac{1}{\omega - k^2 + i\varepsilon}$$

$$\times \frac{1}{(\omega - k_1^2 - k_2^2) + (\mathbf{k} - \mathbf{k}_1 - \mathbf{k}_2)^2 + i\varepsilon}, \qquad (27)$$

where $q = \frac{1}{2}|\mathbf{k}_1 - \mathbf{k}_2|$, and we have used that the free propagator $\Delta_0(\omega, \mathbf{k})$ in the vacuum corresponding to the action (25) is

$$\Delta_0(\omega, \mathbf{k}) = \frac{i}{\omega - k^2 + i\epsilon}. \qquad (28)$$

The integral over ω is performed using contour integration. After changing variables $\mathbf{k} \to \mathbf{k} + |\mathbf{k}_1 + \mathbf{k}_2|/2$, we obtain

$$\mathcal{T}_1(q) = g^2 \int \frac{d^d k}{(2\pi)^d} \frac{1}{k^2 - q^2 - i\varepsilon}. \qquad (29)$$

Note that the integral over k is linearly divergent in the ultraviolet. This divergence is set to zero in dimensional regularization. Using dimensional regularization, the result of the integration of k can be written as

$$\mathcal{T}_1(q) = g^2 M^{2\epsilon} \frac{\Gamma\left(1 - \dfrac{d}{2}\right)}{(4\pi)^{d/2}} [-q^2 - i\varepsilon]^{(d-2)/2}, \qquad (30)$$

where $\Gamma(x)$ is the gamma function. The limit $d \to 3$ is regular, and Eq. (30) reduces to

$$\mathcal{T}_1(q) = i \frac{g^2 q}{4\pi}. \qquad (31)$$

This expression is simply Fermi's golden rule. The quantum corrections from higher orders are given by the diagrams like the two-loop graph in Fig. 3. They form a geometric series that can be summed up exactly, and the exact $2 \to 2$ amplitude becomes

$$\mathcal{T}(q) = -\frac{2g^2}{g + \mathcal{T}_1(q)}. \qquad (32)$$

The scattering amplitude for $2 \to 2$ scattering in the underlying theory described by the action (19) can be calculated by solving the two-body scattering problem in the potential $V_0(\mathbf{x} - \mathbf{x}')$. The contribution from s-wave scattering is (Landau and Lifshitz, 1980)

$$\mathcal{T} = \frac{16\pi}{q} e^{i\delta_0(q)} \sin[\delta_0(q)], \qquad (33)$$

where $\delta_0(q)$ is the s-wave phase shift. We next write the low-momentum expansion as follows:

$$q \cot[\delta_0(q)] = \left[-\frac{1}{a} + \frac{1}{2} r_s q^2 + \cdots\right]. \qquad (34)$$

This expansion defines the scattering length a and the effective range r_s. Using the identity $e^{ix} \sin(x) = 1/[\cot(x) - i]$, we can expand the T matrix in powers of momentum q. Matching Eqs. (32) and (33) through first order in the external momentum q using Eq. (34), we obtain

$$g = 8\pi a. \qquad (35)$$

The parameter h can be determined by going to the next order in the low-momentum expansion. We shall do this in Sec. III.E. Similarly, the parameter g_3 can be determined by solving the three-body scattering problem in the potential $V_0(\mathbf{x} - \mathbf{x}')$ and demanding that the $3 \to 3$ scattering amplitudes in the full and in the effective theory be the same at low momentum.

Traditionally, the starting point has been the interatomic potential $V_0(\mathbf{x} - \mathbf{x}')$. At low densities, it can be shown that the ladder diagrams are of equal importance and must be summed. The summation of these diagrams can be expressed in terms of an effective interaction Γ that satisfies an integral equation which also involves $V_0(\mathbf{x} - \mathbf{x}')$ (Beliaev, 1958; Fetter and Walecka, 1971). The interatomic potential appearing in Γ can be eliminated in favor of the scattering amplitude for two-particle scattering. In the low-momentum limit, the effective interaction reduces to $8\pi a$. The mean-field self-energies, and therefore the first-order propagator and spectrum, can be expressed in terms of the effective interaction. Thus the spectrum reduces in the low-momentum limit to the Bogoliubov spectrum.

B. Perturbative framework

We next discuss the perturbative framework set up by Braaten and Nieto (1999a, 1999b), which can be used to calculate systematically the low-energy properties of a weakly interacting Bose gas.

We first parametrize the quantum field ψ in terms of a time-independent condensate v and a quantum fluctuating field $\tilde{\psi}$:

$$\psi = v + \tilde{\psi}. \qquad (36)$$

The fluctuating field $\tilde{\psi}$ can be conveniently written in terms of two real fields:

$$\tilde{\psi} = \frac{1}{\sqrt{2}}(\psi_1 + i\psi_2). \qquad (37)$$

Substituting Eqs. (36) and (37) into Eq. (25), we decompose the action into three terms,

$$S[v, \psi_1, \psi_2] = S[v] + S_{\text{free}}[v, \psi_1, \psi_2] + S_{\text{int}}[v, \psi_1, \psi_2], \qquad (38)$$

where we have indicated that the action depends on v, as well, and switched to the variables ψ_1 and ψ_2 instead of ψ^* and ψ. $S[v]$ is the classical action,

$$S[v] = \int dt \int d^d x \left[\mu v^2 - \frac{1}{2} g v^4 \right], \qquad (39)$$

while the free part of the action is

$$S_{\text{free}}[v,\psi_1,\psi_2] = \int dt \int d^d x \left[\frac{1}{2}(\dot\psi_1\psi_2 - \psi_1\dot\psi_2) \right.$$
$$\left. + \frac{1}{2}\psi_1(\nabla^2 + X)\psi_1 + \frac{1}{2}\psi_2(\nabla^2 + Y)\psi_2 \right], \qquad (40)$$

where

$$X = \mu - 3g v^2, \qquad (41)$$

$$Y = \mu - g v^2. \qquad (42)$$

The terms $3gv^2$ and gv^2 in X and Y are often referred to as mean-field self-energies. The interaction part of the action is

$$S_{\text{int}}[v,\psi_1,\psi_2]$$
$$= \int dt \int d^d x \left[\sqrt{2} J \psi_1 + \frac{1}{\sqrt{2}} Z \psi_1 (\psi_1^2 + \psi_2^2) \right.$$
$$\left. - \frac{1}{8} g (\psi_1^2 + \psi_2^2)^2 \right]. \qquad (43)$$

The sources in Eq. (43) are

$$J = [\mu - g v^2] v, \qquad (44)$$

$$Z = -g v. \qquad (45)$$

The propagator that corresponds to the free action $S_{\text{free}}[v,\psi_1,\psi_2]$ in Eq. (40) is

$$D(\omega,p) = \frac{i}{\omega^2 - \epsilon^2(p) + i\varepsilon} \begin{pmatrix} p^2 - Y & -i\omega \\ i\omega & p^2 - X \end{pmatrix}. \qquad (46)$$

Here, $p = |\mathbf{p}|$, where $\mathbf{p}$ is the wave vector, ω is the frequency, and $\epsilon(p)$ is the dispersion relation:

$$\epsilon(p) = \sqrt{(p^2 - X)(p^2 - Y)}. \qquad (47)$$

Note that one can diagonalize the matrix (46) by a field redefinition, which is equivalent to a Bogoliubov transformation in the operator approach. Such a field redefinition, however, makes the interaction terms much more complicated and increases the number of diagrams that one needs to evaluate. For practical purposes, we therefore stick to the above propagator.

The partition function $\mathcal{Z}$ can be expressed as a path integral over the quantum fields ψ_1 and ψ_2 (Negele and Orland, 1988):

$$\mathcal{Z} = \int \mathcal{D}\psi_1 \mathcal{D}\psi_2 \, e^{iS[v,\psi_1,\psi_2]}. \qquad (48)$$

All the thermodynamic observables can be derived from the partition function $\mathcal{Z}$. For instance, the free-energy density $\mathcal{F}$ is given by

$$\mathcal{F}(\mu) = i \frac{\ln \mathcal{Z}}{\mathcal{V}}, \qquad (49)$$

where $\mathcal{V}$ is the spacetime volume of the system. The pressure $\mathcal{P}(\mu)$ is

$$\mathcal{P}(\mu) = -\mathcal{F}(\mu). \qquad (50)$$

The number density n is given by the expectation value $\langle \psi^* \psi \rangle$ in the ground state:

$$n(\mu) = \int \mathcal{D}\psi_1 \mathcal{D}\psi_2 \, (\psi^* \psi) e^{iS[v,\psi_1,\psi_2]}. \qquad (51)$$

It can therefore be expressed as

$$n(\mu) = -\frac{\partial \mathcal{F}(\mu)}{\partial \mu}. \qquad (52)$$

The energy density $\mathcal{E}$ is given by the Legendre transform of the free-energy density $\mathcal{F}$:

$$\mathcal{E}(n) = \mathcal{F}(\mu) + n\mu. \qquad (53)$$

The free energy $\mathcal{F}$ is given by all *connected vacuum diagrams* that are Feynman diagrams with no external legs. The sum of the vacuum graphs is independent of the condensate v. At this point it is convenient to introduce the *thermodynamic potential* $\Omega(\mu,v)$. The thermodynamic potential is given by all one-particle irreducible vacuum diagrams and can be expanded in the number of loops:

$$\Omega(\mu,v) = \Omega_0(\mu,v) + \Omega_1(\mu,v) + \Omega_2(\mu,v) + \cdots, \qquad (54)$$

where the subscript n denotes the contribution from the nth order in the loop expansion. If Ω is evaluated at a value of the condensate that satisfies the condition

$$\bar{v} = \langle \psi \rangle, \qquad (55)$$

all one-particle reducible diagrams (those that are disconnected by cutting a single propagator line) vanish. Thus evaluating the thermodynamic potential at the value of the condensate that satisfies Eq. (55), one obtains the free energy

$$\mathcal{F}(\mu) = \Omega_0(\mu,\bar{v}) + \Omega_1(\mu,\bar{v}) + \Omega_2(\mu,\bar{v}) + \cdots. \qquad (56)$$

Using Eq. (37), condition (55) reduces to $\langle \psi_2 \rangle = 0$ and $\langle \psi_1 \rangle = 0$. The first condition can be automatically satisfied by a suitable choice of the phase of ψ. The second condition is then equivalent to

$$\frac{\partial \Omega(\mu,v)}{\partial v} = 0. \qquad (57)$$

The value of the condensate that satisfies Eq. (57) is denoted by $\bar{v}$. The free energy can also be expanded in powers of quantum corrections around the mean-field result $\mathcal{F}_0(\mu)$:

$$\mathcal{F}(\mu) = \mathcal{F}_0(\mu) + \mathcal{F}_1(\mu) + \mathcal{F}_2(\mu) + \cdots. \qquad (58)$$

The loop expansion (56) of $\mathcal{F}(\mu)$ does not coincide with the expansion (58) of $\mathcal{F}(\mu)$ in powers of quantum corrections because of its dependence on $\bar{v}$. To obtain the expansion of $\mathcal{F}$ in powers of quantum corrections, we must expand the condensate $\bar{v}$ in powers of quantum corrections:

$$\bar{v} = v_0 + v_1 + v_2 + \cdots, \tag{59}$$

where v_0 is the classical minimum, which satisfies

$$\frac{\partial \Omega_0(\mu,v)}{\partial v} = 0. \tag{60}$$

By expanding Eq. (57) about v_0, one obtains the quantum corrections $v_1, v_2, \ldots$ to the condensate. For instance, the first quantum correction v_1 to the classical minimum v_0 is

$$v_1 = -\frac{\partial \Omega_1(\mu,v)}{\partial v}\bigg|_{v=v_0} \bigg/ \frac{\partial^2 \Omega_0(\mu,v)}{\partial v^2}\bigg|_{v=v_0}. \tag{61}$$

The mean-field free-energy density is

$$\mathcal{F}_0(\mu) = \Omega_0(\mu,v_0). \tag{62}$$

Inserting Eq. (59) into Eq. (56) and expanding in powers of $v_1, v_2, \ldots$, we obtain the quantum expansion of the free-energy density. The first quantum correction to the free-energy density is

$$\mathcal{F}_1(\mu) = \Omega_1(\mu,v_0), \tag{63}$$

and the second quantum correction to the free-energy density is

$$\mathcal{F}_2(\mu) = \Omega_2(\mu,v_0) + v_1 \frac{\partial \Omega_1(\mu,v)}{\partial v}\bigg|_{v=v_0}$$

$$+ \frac{1}{2} v_1^2 \frac{\partial^2 \Omega_0(\mu,v)}{\partial v^2}\bigg|_{v=v_0}. \tag{64}$$

Expressions for higher-order corrections to the free energy can be derived in the same way.

The value of the condensate v that minimizes the classical action (39) is given by $v_0 = \sqrt{\mu/g}$. The linear term in Eq. (43) then vanishes since $J=0$. At the minimum of the classical action, both the propagator (46) and the dispersion relation (47) simplify significantly, since we also have $Y=0$. At the minimum, these equations reduce to

$$D(\omega,p) = \frac{i}{\omega^2 - \epsilon^2(p) + i\varepsilon}\begin{pmatrix} p^2 & -i\omega \\ i\omega & \epsilon^2(p)/p^2 \end{pmatrix}, \tag{65}$$

$$\epsilon(p) = p\sqrt{p^2 + 2\mu}. \tag{66}$$

The spectrum (66) was first derived by Bogoliubov (1947). The dispersion relation is gapless and linear for small wave vectors. This reflects the spontaneous breakdown of the U(1) symmetry. The dispersion relation changes from linear to quadratic in the vicinity of $p = \sqrt{2\mu}$, which is called the *inverse coherence length*. For very large wave vectors, the dispersion relation is approximately $\epsilon(p) = p^2 + \mu$, where the second term represents the mean-field energy due to interaction with condensed particles.

We next comment on how traditional approaches fit into the more general perturbative framework discussed in this section. The starting point is the second-quantized grand-canonical Hamiltonian that includes a two-body potential $V_0(\mathbf{x})$:

$$\mathcal{H} = \int d^d x \, \psi^*(\mathbf{x})[-\nabla^2 - \mu]\psi(\mathbf{x})$$

$$+ \frac{1}{2}\int d^d x \int d^d x' \, \psi^*(\mathbf{x})\psi^*(\mathbf{x}')$$

$$\times V_0(\mathbf{x}-\mathbf{x}')\psi(\mathbf{x})\psi(\mathbf{x}'). \tag{67}$$

This Hamiltonian is nonlocal and is often replaced by a local one. This is done by approximating the true two-body potential by a local two-body interaction, whose strength g is tuned to reproduce the scattering length of $V_0(\mathbf{x}-\mathbf{x}')$. This yields

$$\mathcal{H} = \int d^d x \left\{ \psi^*[-\nabla^2 - \mu]\psi + \frac{1}{2}g(\psi^*\psi)^2 \right\}. \tag{68}$$

The grand-canonical Hamiltonian is expressed in terms of creation and annihilation operators that satisfy the standard equal-time commutation relations. Bogoliubov's idea was to treat the $\mathbf{p}=0$ momentum separately (Bogoliubov, 1947). Since this state is macroscopically occupied, to a very good approximation, the creation and annihilation operators for bosons with $\mathbf{p}=0$ commute. Thus they can be treated classically and be replaced by a constant which is the condensate density. This step is equivalent to splitting the quantum field ψ into a condensate v and a fluctuating field $\tilde{\psi}$, as in Eq. (36).

In the Bogoliubov approximation (Bogoliubov, 1947), one makes a quadratic approximation to the Hamiltonian by neglecting terms with three and four operators. Since the resulting Hamiltonian contains products of two annihilation operators and products of two creation operators, it must be diagonalized by a canonical transformation. The resulting quasiparticle spectrum is then given by Eq. (66).

In the Beliaev approximation (Beliaev, 1958), one goes one step further by calculating the leading quantum corrections to the quasiparticle spectrum (66). This is done by including all one-loop diagrams, that is, all diagrams up to second order in the interaction in the self-energies and then calculating the poles of the propagator. The correction to the Bogoliubov spectrum (66) was first calculated by Beliaev (1958) and coincides with a leading-order calculation in the approach outlined here. We shall return to that calculation in Sec. III.D.

The perturbative framework has been formulated in terms of two real fields, ψ_1 and ψ_2. As noted in the Introduction, one has traditionally presented the theory in terms of normal and anomalous Green's functions, $G_{11}(\omega,p)$ and $G_{12}(\omega,p)$, and the self-energies $\Sigma_{11}(\omega,p)$ and $\Sigma_{12}(\omega,p)$. This formulation corresponds to using the fields ψ^* and ψ instead of ψ_1 and ψ_2. In either formulation, one ends up with a 2×2 matrix for the propagator and self-energies, and the amount of work to calculate most quantities is comparable. For readers who want to translate intermediate results to a more familiar language, we note that

$$\Sigma_{11}(\omega,p) = \frac{1}{2}[\Pi_{11}(\omega,p) + \Pi_{22}(\omega,p)], \tag{69}$$

$$\Sigma_{12}(\omega,p)=\frac{1}{2}[\Pi_{11}(\omega,p)-\Pi_{22}(\omega,p)], \qquad (70)$$

where $\Pi_{ij}(\omega,p)$ are the components of the 2×2 self-energy matrix.

We next comment on the Hugenholz-Pines theorem (Hugenholz and Pines, 1958), which ensures that the spectrum does not exhibit a gap. This has been proven to all orders in perturbation theory. It is simply the Goldstone theorem for a dilute Bose gas with a spontaneously broken continuous symmetry. The Hugenholz-Pines theorem is normally given in terms of normal and anomalous self-energies:

$$\mu=\Sigma_{11}(0,0)-\Sigma_{12}(0,0).$$

In terms of the self-energies $\Pi_{ij}(\omega,p)$, the theorem takes a particularly simple form:

$$\mu=\Pi_{22}(0,0). \qquad (71)$$

C. Ground-state energy density and condensate depletion

In this subsection, we calculate the leading quantum correction to the ground-state energy and the depletion of the condensate. While these results are standard textbook material (Fetter and Walecka, 1971), it is instructive to see how they are derived within the present framework.

The mean-field thermodynamic potential $\Omega_0(\mu,v)$ is given by the terms in the classical action (39):

$$\Omega_0(\mu,v)=-\mu v^2+\frac{1}{2}gv^4. \qquad (72)$$

The minimum of the mean-field thermodynamic potential is given by $v_0=\sqrt{\mu/g}$ and the mean-field free energy $\mathcal{F}_0$ is obtained by evaluating Eq. (72) at the minimum:

$$\mathcal{F}_0(\mu)=-\frac{\mu^2}{2g}. \qquad (73)$$

The mean-field number density follows from differentiating Eq. (73) with respect to μ. The chemical potential in the mean-field approximation is then obtained by inversion:

$$\mu_0=gn. \qquad (74)$$

From Eq. (53), the mean-field energy $\mathcal{E}_0$ is easily found to be

$$\mathcal{E}_0(n)=\frac{1}{2}gn^2$$
$$=4\pi a n^2. \qquad (75)$$

The mean-field result for the energy density was first obtained by Bogoliubov (1947).

The one-loop contribution to the thermodynamic potential $\Omega(\mu,v)$ is given by

$$\Omega_1(\mu,v)=i\frac{\ln \mathcal{Z}_0}{\mathcal{V}}, \qquad (76)$$

where $\mathcal{Z}_0$ is the path integral involving the quadratic quantum fluctuations around the mean field,

$$\mathcal{Z}_0=\int \mathcal{D}\psi_1\mathcal{D}\psi_2 \ e^{iS_{\text{free}}[v,\psi_1,\psi_2]}$$
$$=e^{i\int dt\int d^3x(1/2)}\det D^{-1}(\omega,p). \qquad (77)$$

Here $D^{-1}(\omega,p)$ is the inverse of the propagator (46) and det denotes a determinant in the functional sense. Using the fact that $\operatorname{Tr}\ln A=\ln\det A$ for any matrix A, we obtain

$$\Omega_1(\mu,v)=-\frac{1}{2}i\int\frac{d\omega}{2\pi}\int\frac{d^dk}{(2\pi)^d}\ln\det D^{-1}(\omega,k)$$
$$+\Delta_1\Omega. \qquad (78)$$

Here we have added $\Delta_1\Omega$, which is the one-loop counterterm. The counterterm is added to cancel the ultraviolet divergences that one encounters when evaluating the integral in Eq. (78). After integrating over ω using Eq. (A1), we obtain

$$\Omega_1(\mu,v)=\frac{1}{2}\int\frac{d^dk}{(2\pi)^d}\sqrt{(k^2-X)(k^2-Y)}$$
$$+\Delta_1\Omega(\mu,v). \qquad (79)$$

The one-loop contribution $\mathcal{F}_1$ to the free energy is obtained by evaluating Eq. (79) at the classical minimum, where $Y=0$ and $X=-2\mu$. The one-loop free energy then reduces to

$$\mathcal{F}_{0+1}(\mu)=-\frac{\mu^2}{2g}+\frac{1}{2}\int\frac{d^dk}{(2\pi)^d}k\sqrt{k^2+2\mu}+\Delta_1\mathcal{F}(\mu)$$
$$=-\frac{\mu^2}{2g}+\frac{1}{2}I_{0,-1}(2\mu)+\Delta_1\mathcal{F}(\mu), \qquad (80)$$

where the integral $I_{m,n}(\Lambda)$ is defined in the Appendix, and $\Delta_1\mathcal{F}$ is the one-loop counterterm. The integral $I_{0,-1}(\Lambda)$ has quintic, cubic, and linear ultraviolet divergences that are set to zero in dimensional regularization. The counterterm $\Delta_1\mathcal{F}$ is therefore zero, and the limit $d\to3$ is regular. We obtain

$$\mathcal{F}_{0+1}(\mu)=-\frac{\mu^2}{2g}\left[1-\frac{4\sqrt{2\mu g^2}}{15\pi^2}\right]. \qquad (81)$$

It might be useful to see how the renormalization procedure works with a simple ultraviolet cutoff. In that case, the one-loop contribution to the free energy $\mathcal{F}_1$ can be written as

$$\mathcal{F}_1(\mu)=\frac{1}{2}\int^M\frac{d^3k}{(2\pi)^3}k\sqrt{k^2+2\mu}+\Delta_1\mathcal{F}, \qquad (82)$$

where the integral is calculated in $d=3$ dimensions and the superscript M indicates that $|\mathbf{k}|<M$ has been imposed. We can now rewrite this as

$$\mathcal{F}_1(\mu)=\frac{1}{2}\int^M\frac{d^3k}{(2\pi)^3}\left[k\sqrt{k^2+2\mu}-k^2-\mu+\frac{\mu^2}{2k^2}\right]$$
$$+\int^M\frac{d^3k}{(2\pi)^3}\left[k^2+\mu-\frac{\mu^2}{2k^2}\right]+\Delta_1\mathcal{F}. \qquad (83)$$

The first integral is now convergent in the limit $M\to\infty$ and the divergences have been isolated in the second

integral. This first term goes like M^5 and is independent of μ and g. It can therefore be removed by a vacuum-energy counterterm $\Delta_1 \mathcal{E}$. The form of $\Delta_1 \mathcal{F}$ can be found by substituting $g \to g + \Delta_1 g$ and $\mu \to \mu + \Delta_1 \mu$ in $\mathcal{F}_0(\mu)$ and expanding to first order in $\Delta_1 g$ and $\Delta_1 \mu$. Including the vacuum counterterm, we obtain

$$\Delta \mathcal{F}_1(\mu) = -\frac{\mu}{g} \Delta_1 \mu + \frac{\mu^2}{2g^2} \Delta_1 g + \Delta_1 \mathcal{E}. \tag{84}$$

The counterterms needed to cancel the quintic, cubic, and linear divergences can then be found by inspection. One obtains

$$\Delta_1 \mathcal{E} = -\frac{1}{2} \int^M \frac{d^3 k}{(2\pi)^3} k^2, \tag{85}$$

$$\Delta_1 g = \frac{1}{2} g^2 \int^M \frac{d^3 k}{(2\pi)^3} \frac{1}{k^2}, \tag{86}$$

$$\Delta_1 \mu = \frac{1}{2} g \int^M \frac{d^3 k}{(2\pi)^3}. \tag{87}$$

Note that the counterterm $\Delta_1 g$ in Eq. (86) is precisely what is needed to cancel the divergence appearing in the one-loop correction to the scattering length, Eq. (29). This is in accord with our comment on counterterms in footnote 3. The renormalized one-loop free energy can then be written as

$$\mathcal{F}_{0+1}(\mu) = -\frac{\mu^2}{2g} + \frac{1}{2} \int^M \frac{d^3 k}{(2\pi)^3} \left[\epsilon(k) - k^2 - \mu + \frac{\mu^2}{2k^2} \right]. \tag{88}$$

We can now take the limit $M \to \infty$. Evaluating the integral, we recover Eq. (81).

Finally, we mention that the *pseudopotential method* (Huang and Yang, 1957) is an alternative way of treating ultraviolet divergences. One replaces the contact potential $g \delta^3(\mathbf{x})/2$ by the pseudopotential $g \delta^3(\mathbf{x})(\partial/\partial x)x/2$, and one can avoid the ultraviolet divergences by evaluating the partial derivative at the right stage of the calculation. We shall not discuss this method any further.

Using Eqs. (52), (80), and (A7), we obtain the number density in the one-loop approximation

$$n_{0+1}(\mu) = \frac{\mu}{g} - \frac{1}{2} I_{1,1}(2\mu) = \frac{\mu}{g} \left[1 - \frac{\sqrt{2\mu g^2}}{3\pi^2} \right]. \tag{89}$$

Inverting Eq. (89) to obtain the chemical potential as a function of the number density, one finds

$$\mu_{0+1}(n) = gn + \frac{1}{2} g I_{1,1}(2gn)$$

$$= 8\pi a n \left[1 + \frac{32}{3} \sqrt{\frac{na^3}{\pi}} \right]. \tag{90}$$

Note that here and in the following we are replacing the argument μ by gn in the loop integrals $I_{m,n}$, since corrections are of higher order in $\sqrt{na^3}$. Using Eqs. (53), (80), and (89), we obtain the energy density in the one-loop approximation:

$$\mathcal{E}_{0+1}(n) = \frac{1}{2} gn^2 + \frac{1}{2} I_{0,-1}(2gn)$$

$$= 4\pi a n^2 \left[1 + \frac{128}{15} \sqrt{\frac{na^3}{\pi}} \right]. \tag{91}$$

The leading quantum correction to the mean-field result (75) was first derived by Lee, Huang, and Yang (Lee, Huang, and Yang, 1957; Lee and Yang, 1957) for a hard-sphere potential. Later, it was shown that it is universal in the sense that it applies to all short-range potentials with scattering length a (Brueckner and Sawada, 1957; Beliaev, 1958; Lieb, 1963). Note that the result (91) is nonanalytic in the scattering length a. This shows that the result is nonperturbative from the point of view of "naive" perturbation theory, where one uses free-particle propagators. It corresponds to the summation of an infinite set of one-loop diagrams, with repeated insertions of the operator $\frac{3}{2} g v^2 \psi_1^2$. The structure of these diagrams is the same as the ring diagrams first discussed by Gell-Mann and Brueckner for the nonrelativistic electron gas (Gell-Mann and Brueckner, 1957), and they are summed in the same manner. It is interesting to note that each diagram in the series is increasingly divergent in the infrared, but the sum is infrared convergent.

Using Eq. (36) and the parametrization (37), the expression for the number density becomes

$$n = v^2 + \frac{1}{2} \langle \psi_1^2 + \psi_2^2 \rangle. \tag{92}$$

The condensate density n_0 is given by the expectation value $v^2 = |\langle \psi \rangle|^2$. At the mean-field level, one neglects the fluctuations of ψ_1 and ψ_2 and replaces $\langle \psi^* \psi \rangle$ by $|\langle \psi \rangle|^2$. The total number density is then equal to the condensate density. But when quantum fluctuations are taken into account, this is no longer the case. Due to interactions, some of the particles are kicked out of the condensate and are not in the $\mathbf{k}=0$ momentum state. The difference $n - n_0$ is called the depletion of the condensate and is proportional to the diluteness parameter $\sqrt{na^3}$. The one-loop diagrams that contribute to the expectation values $\langle \psi_1^2 \rangle$ and $\langle \psi_2^2 \rangle$ are shown in Fig. 4. The solid line denotes the diagonal propagator for ψ_1, and the dashed line the diagonal propagator for ψ_2. The solid circles denote an insertion of the operator ψ_1^2 or ψ_2^2. Taking these one-loop effects into account, Eq. (92) reduces to

FIG. 4. One-loop diagrams contributing to expectation values $\langle \psi_1^2 \rangle$ and $\langle \psi_2^2 \rangle$.

$$n_{0+1}(n_0) = n_0 + \frac{1}{2}i\int\frac{d\omega}{2\pi}\int\frac{d^dk}{(2\pi)^d}\left[\frac{k^2+\epsilon^2(k)/k^2}{\omega^2-\epsilon^2(k)+i\varepsilon}\right]$$

$$= n_0 + \frac{1}{4}[I_{1,1}(2gn_0) + I_{-1,-1}(2gn_0)]. \quad (93)$$

Using the expressions for the integrals in the Appendix, we obtain

$$n_{0+1}(n_0) = n_0\left[1 + \frac{8}{3}\sqrt{\frac{n_0a^3}{\pi}}\right]. \quad (94)$$

The result (94) for the depletion was first obtained by Bogoliubov (1947). In recent experiments, Cornish *et al.* (2000) were able to vary the *s*-wave scattering length a for ^{85}Rb atoms over a large range by applying a strong external magnetic field and exploiting the existence of a Feshbach resonance at $B \sim 155$ G. Values for $\sqrt{na^3}$ up to approximately 0.1 were obtained and should be sufficiently large to see deviations from the mean field in experiments. In order to observe this quantum phenomenon, it is essential that experiments be carried out at sufficiently low temperature so that the thermal depletion of the condensate is negligible.

D. Collective excitations

The Bogoliubov spectrum is given by Eq. (66) and was derived from the microscopic theory represented by the action (25). It is linear for small momentum p with slope $\sqrt{2\mu}$. The spectrum $\omega(p)$ of collective excitations is given by the poles of the propagator. The poles are the solutions to the equation

$$\det[D_0^{-1}(\omega,p) - \Pi(\omega,p)] = 0, \quad (95)$$

where $D_0(\omega,p)$ is the real-time version of the free propagator (6) and $\Pi(\omega,p)$ is the 2×2 self-energy matrix. The dispersion relation $\omega(p)$ is generally complex and can therefore be written as

$$\omega(p) = \mathrm{Re}\,\omega(p) - i\gamma(p). \quad (96)$$

The real part $\mathrm{Re}\,\omega(p)$ gives the energies of the excitations, while the imaginary part $\gamma(p)$ represents the damping of the excitations. The Bogoliubov spectrum is purely real and therefore, in this approximation, the excitations have an infinite lifetime.

In the following, we calculate the leading quantum correction to the real part of the spectrum in the long-wavelength limit and thus reproduce Beliaev's classic result (Beliaev, 1958). The one-loop Feynman diagrams that contribute to the self-energies are shown in Figs. 5–7.[4] The solid line denotes the diagonal propagator for ψ_1 and the dashed line the diagonal propagator for ψ_2. The off-diagonal propagators for ψ_1 and ψ_2 are represented by lines that are half solid and half dashed. One-loop contributions to self-energies are down by a factor of $\sqrt{na^3}$ compared to the mean-field terms in the inverse propagator. It is therefore consistent to evaluate the self-energies using the mean-field dispersion relation $\epsilon(p)$, since corrections would be suppressed by at least a factor of na^3.

In the following, we calculate the off-diagonal self-energy $\Pi_{12}(\omega,p)$ explicitly. The expression is

$$\Pi_{12}(\epsilon(p),p) = g^2v^2\int\frac{d\omega}{2\pi}\int\frac{d^dk}{(2\pi)^d}\left\{\frac{3[\omega+\epsilon(p)]k^2}{\{[\omega+\epsilon(p)]^2-\epsilon^2(|\mathbf{p}+\mathbf{k}|)+i\varepsilon\}[\omega^2-\epsilon^2(k)+i\varepsilon]}\right.$$
$$\left. -\frac{[\omega+\epsilon(p)]\epsilon^2(k)/k^2}{\{[\omega+\epsilon(p)]^2-\epsilon^2(|\mathbf{p}+\mathbf{k}|)+i\varepsilon\}[\omega^2-\epsilon^2(k)+i\varepsilon]}\right\}. \quad (97)$$

After integrating over ω, we find that the imaginary part of $\Pi_{12}(\epsilon(p),p)$ becomes

$$\mathrm{Im}\,\Pi_{12}(\epsilon(p),p) = -g^2v^2\int\frac{d^dk}{(2\pi)^d}$$
$$\times\left\{\frac{[\epsilon(p)+\epsilon(k)][3k^2/\epsilon(k)-\epsilon(k)/k^2]}{[\epsilon^2(|\mathbf{p}+\mathbf{k}|)-\epsilon^2(p)-\epsilon^2(k)]}\right.$$
$$\left. +\frac{3k^2-\epsilon^2(k)/k^2}{\{[\epsilon(k)+\epsilon(p)]^2-\epsilon^2(|\mathbf{p}+\mathbf{k}|)\}}\right\}. \quad (98)$$

Finally, we expand Eq. (98) in powers of the external momentum p. We simplify using Eqs. (A7)–(A9), whereupon the self-energy reduces to

$$\mathrm{Im}\,\Pi_{12}(\epsilon(p),p) = \frac{1}{8}g(2gv^2)^{3/2}[3I_{1,3}-I_{-1,1}]p$$
$$+ \mathcal{O}(p^3/\sqrt{gv^2}). \quad (99)$$

Notice in particular that $\Pi_{12}(0,0)$ vanishes. This property holds to all orders in perturbation theory and follows from time-reversal invariance. Note also that $\Pi_{21}(\omega,p) = -\Pi_{12}(\omega,p)$, which also holds to all orders in loop expansion. The real part of the self-energies $\Pi_{11}(\epsilon(p),p)$ and $\Pi_{22}(\epsilon(p),p)$ are expanded about zero

---

[4]Note that the sum of all one-particle reducible diagrams that contribute to the self-energies vanishes. This sum is proportional to the derivative of the effective potential and is zero when evaluated at the minimum of the effective potential.
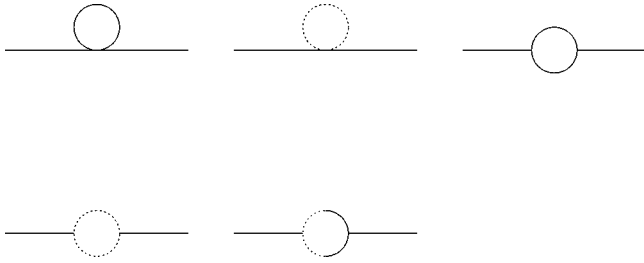
FIG. 5. One-loop diagrams contributing to the self-energy $\Pi_{11}(\omega,p)$.

external momentum in the same way. Including the mean-field self-energies, one finds

$$
\begin{aligned}
\text{Re}\,\Pi_{11}(\epsilon(p),p) = {} & 3gv^2 + \frac{1}{4}g[3I_{1,1}+I_{-1,-1} \\
& - gv^2(9I_{2,3}-6I_{0,1}+I_{-2,-1})] \\
& + \mathcal{O}(p^2),
\end{aligned}
\tag{100}
$$

$$
\begin{aligned}
\text{Re}\,\Pi_{22}(\epsilon(p),p) = {} & gv^2 + \frac{1}{12}g[9I_{1,1}+3I_{-1,-1} \\
& - p^2gv^2(6I_{3,5}-11I_{1,3}+3I_{-1,1})] \\
& + \mathcal{O}(p^4/gv^2).
\end{aligned}
\tag{101}
$$

The expressions for the self-energies $\Pi_{11}(\epsilon(p),p)$, $\Pi_{22}(\epsilon(p),p)$, and $\Pi_{12}(\epsilon(p),p)$ are infrared divergent. The integrals $I_{-2,-1}(2gn_0)$ and $I_{-1,1}(2gn_0)$ both have a logarithmic divergence as the loop momentum k goes to zero. These divergences show up as poles in ϵ in Eqs. (A16) and (A17). However, it is important to point out that they cancel in the final results for physical quantities, as we shall see below.

The real part of Eq. (95) can now be written as

$$
\begin{aligned}
[\omega - \text{Im}\,\Pi_{12}(\epsilon(p),p)]^2 = {} & [p^2-\mu+\text{Re}\,\Pi_{11}(\epsilon(p),p)] \\
& \times [p^2-\mu+\text{Re}\,\Pi_{22}(\epsilon(p),p)].
\end{aligned}
\tag{102}
$$

The next step is to eliminate the chemical potential from Eq. (102) by minimizing the one-loop thermodynamic
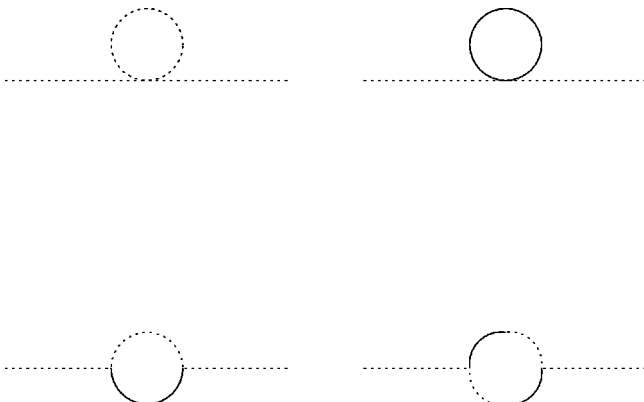

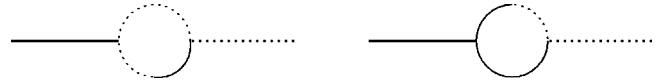FIG. 6. One-loop diagrams contributing to the self-energy $\Pi_{22}(\omega,p)$.

FIG. 7. One-loop diagrams contributing to the self-energy $\Pi_{12}(\omega,p)$.

potential $\Omega_{0+1}(\mu,v)$. This is found by differentiating the sum of Eqs. (72) and (79) with respect to the condensate v and setting it to zero, which yields

$$
0 = -\mu + gv^2 + \frac{1}{4}g\int \frac{d^dp}{(2\pi)^d}\frac{3(p^2-Y)+(p^2-X)}{\sqrt{(p^2-X)(p^2-Y)}}.
\tag{103}
$$

To the order in quantum corrections at which we are calculating, it is consistent to evaluate the one-loop contribution to Eq. (103) at the classical minimum $v=v_0$. Equation (103) then reduces to

$$
0 = -\mu + gv^2 + \frac{1}{4}g[3I_{1,1}+I_{-1,-1}] = -\mu + \Pi_{22}(0,0).
\tag{104}
$$

Equation (104) shows that the Goldstone theorem is satisfied at the stationary point of the thermodynamic potential. Using Eq. (93), we see that the chemical potential obtained from Eq. (90) agrees with Eq. (104). Solving for the chemical potential and substituting this result as well as the self-energies given by Eqs. (99)–(101) into Eq. (102), we obtain

$$
\begin{aligned}
& \left[\omega + \frac{1}{8}g(2gv^2)^{3/2}(3I_{1,3}-I_{-1,1})p\right]^2 \\
& = p^2\left[p^2+2gv^2\left(1-\frac{1}{8}g(9I_{2,3}+I_{-2,-1}-6I_{0,1})\right)\right] \\
& \quad \times \left[1-\frac{1}{12}g^2v^2(6I_{3,5}-11I_{1,3}+3I_{-1,1})\right].
\end{aligned}
\tag{105}
$$

We can now solve for ω in Eq. (105). In the long-wavelength limit $p\ll\sqrt{2gv^2}$, we obtain

$$
\begin{aligned}
\text{Re}\,\omega(p) = {} & p\sqrt{2gv^2}\left[1-\frac{g^2v^2}{24}(6I_{3,5}+7I_{1,3}-3I_{-1,1})\right] \\
& \times \left[1-\frac{1}{16}g(9I_{2,3}-6I_{0,1}+I_{-2,-1})\right] \\
= {} & p\sqrt{2gn_0}\left[1+\frac{28}{3}\sqrt{\frac{n_0a^3}{\pi}}\right].
\end{aligned}
\tag{106}
$$

The infrared-divergent terms that appear in the expressions for the self-energies cancel algebraically after having used the relations (A7)–(A9). The ultraviolet divergences associated with the integrals in Eq. (106) are again power divergences. Thus one immediately obtains a finite result, and this is another example of the convenience of employing dimensional regularization. The result (106) was first obtained by Beliaev (1958). One can easily check that the slope of ω in Eq. (106) is the same as the macroscopic speed of sound c, which one obtains from differentiating the pressure with respect to the

number density (Fetter and Walecka, 1971). This equality was proven to all orders in perturbation theory by Gavoret and Nozières (1964) and by Hohenberg and Martin (1965).

The effective-field-theory approach presented in this section is based on a Cartesian parametrization of the quantum field $\tilde{\psi}$ in Eq. (37). A similar effective-field-theory approach was developed by Popov (1987) and later extended by Liu (1997, 1998). Instead of using a Cartesian parametrization of the field ψ, it was parametrized using the density n and the phase χ:

$$\psi(\mathbf{x},t) = \sqrt{n(\mathbf{x},t)} \ e^{i\chi(\mathbf{x},t)}. \tag{107}$$

The density field is shifted in analogy with the shift in Eq. (36):

$$n(\mathbf{x},t) = v^2 + \sigma(\mathbf{x},t). \tag{108}$$

We recall that condition (55) simplifies calculations, since it makes all one-particle reducible diagrams vanish. This condition is replaced by

$$\langle \sigma \rangle = 0. \tag{109}$$

Using the parametrization (107) together with Eq. (108), we find that the action (25) takes the form

$$S = S[v] + \int dt \int d^d x \left[\frac{1}{v} J\sigma + \frac{1}{2}(\chi\dot{\sigma} - \dot{\chi}\sigma) - \frac{1}{2}g\sigma^2 \right.$$

$$- v^2(\nabla\chi)^2 - \frac{1}{4v^2}(\nabla\sigma)^2 - \sigma(\nabla\chi)^2 + \frac{1}{4v^4}\sigma(\nabla\sigma)^2$$

$$\left. + \cdots \right], \tag{110}$$

where the dots indicate an infinite series of higher-order operators. The classical action $S[v]$ and the source J are given by Eqs. (39) and (44), respectively. After a rescaling of the fields σ and χ, the free propagator corresponding to the action (110) is identical to Eq. (65). However, the interaction vertices are different. In particular, the vertex corresponding to the operator $\sigma(\nabla\chi)^2$ is momentum dependent. One feature of the perturbative expansion that follows from the action (110) is the absence of infrared divergences in individual diagrams (Popov, 1983). The momentum dependence of the trilinear interaction $\sigma(\nabla\chi)^2$ compensates for the singular behavior of the propagator at low momenta. This difference should not be viewed as being fundamental, since infrared divergences always cancel in physical quantities. We have already seen one example of this when we considered the quantum correction to the Bogoliubov dispersion relation. On the other hand, individual diagrams are more severely ultraviolet divergent, but these cancel when the diagrams are added. The above features merely represent a different way of organizing the perturbative calculations. The equality of calculations of physical quantities order by order in perturbation theory simply reflects the reparametrization invariance of the functional integral.

As mentioned before, the imaginary part of the dispersion relation represents the damping of the collective excitations. In the case of a dilute Bose gas, this term was first calculated by Beliaev (1958). In the long-wavelength limit, his calculations showed that the damping rate is proportional to p^5:

$$\gamma(p) = \frac{3p^5}{320\pi n_0}. \tag{111}$$

The imaginary part $\gamma(p)$ is connected with one phonon decaying into two phonons with lower energy, often referred to as Beliaev damping. The action (110) was later used by other authors (Popov, 1983; Liu, 1997, 1998) to rederive Eq. (111). The calculations represent a significant simplification compared to the original derivation.

E. Nonuniversal effects

In the previous subsection, it was shown that the dominant effects of the interaction between the atoms could be subsumed in a single coupling constant called the s-wave scattering length. Thus, to leading order in the low-density expansion, all interatomic potentials with the same s-wave scattering length will have the same properties, and this property is called universality. However, at higher orders in the low-density expansion, physical quantities will depend on the details of the interatomic potential such as the effective range r_s. These are called *nonuniversal effects*. A detailed analysis of nonuniversal effects can be found in the paper by Braaten, Hammer, and Hermans (2001). We discuss these effects next.

Including the operator $[\nabla(\psi^*\psi)]^2$ in Eq. (25), we can again calculate exactly the scattering amplitude for s-wave scattering. Summing the contributions from the diagrams in Fig. 3, we obtain (Braaten *et al.*, 2001)

$$\mathcal{T}(q) = -\left[\frac{1}{2g + 4hq^2} + i\frac{q}{16\pi} \right]^{-1}. \tag{112}$$

The coupling constant h is then related to the effective range r_s of the true potential (Braaten *et al.*, 2001), and it is determined by matching Eqs. (33) and (112) through third order in q. This yields

$$h = 2\pi a^2 r_s. \tag{113}$$

After performing the shift (36), we find that the operator $[\nabla(\psi^*\psi)]^2$ also contributes to the free part of the action. Including the effects of this operator, one obtains a modified propagator and a modified dispersion relation:

$$D(\omega,p) = \frac{i}{\omega^2 - \epsilon^2(p) + i\varepsilon} \begin{pmatrix} p^2 & -i\omega \\ i\omega & \epsilon^2(p)/p^2 \end{pmatrix}, \tag{114}$$

where the new dispersion relation is

$$\epsilon(p) = p\sqrt{(1 + 2hv^2)p^2 + 2gv^2}. \tag{115}$$

The spectrum (115) has the Bogoliubov form with modified coefficients. It is therefore straightforward to recalculate the ground-state energy density and the depletion of the condensate by rescaling the momentum $\mathbf{p} \rightarrow \mathbf{p}\sqrt{1 + 2hv^2}$. For instance, the expression for the number density is analogous to Eq. (93):

$$n_{0+1}(n_0) = n_0 + \frac{1}{4}\left[\int \frac{d^d p}{(2\pi)^d} \frac{p^2}{\epsilon(p)} + \frac{\epsilon^2(p)}{p^2}\right]$$

$$= n_0 + \frac{1}{4}[1 + 2hv^2]^{-(d+1)/2} I_{1,1}$$

$$+ \frac{1}{4}[1 + 2hv^2]^{-(d-1)/2} I_{-1,-1}. \qquad (116)$$

The limit $d \to 3$ is regular, and we obtain

$$n_{0+1}(n_0) = n_0\left[1 + \frac{1}{24\pi^2} \frac{\sqrt{8n_0 g^3}}{(1+2hv^2)^2}(1 - 2hv^2)\right]. \qquad (117)$$

Using Eqs. (35) and (113), and expanding to first order in the effective range r_s, we find

$$n_{0+1}(n_0) = n_0\left[1 + \frac{8}{3}\sqrt{\frac{n_0 a^3}{\pi}} - \frac{32\pi^2 r_s}{a}\left(\frac{n_0 a^3}{\pi}\right)^{3/2}\right]. \qquad (118)$$

Similarly, we can calculate the ground-state energy density. Expanding to first order in the effective range r_s, one finds (Braaten *et al.*, 2001)

$$\mathcal{E}_{0+1}(n) = 4\pi a n^2\left[1 + \frac{128}{15}\sqrt{\frac{na^3}{\pi}}\right.$$

$$\left. - \frac{1024\pi^2 r_s}{15a}\left(\frac{na^3}{\pi}\right)^{3/2}\right]. \qquad (119)$$

Effective field theory can be used to determine at which order in the low-density expansion a given operator starts to contribute to various physical quantities. As an example, we consider the energy density $\mathcal{E}$. Each power of $\psi^*\psi$ contributes a factor of n. Each power of ∇ contributes a factor of $\sqrt{na}$. Each loop order in the quantum loop expansion contributes a factor of $\sqrt{na^3}$. The derivative interaction $[\nabla(\psi^*\psi)]^2$ does not contribute to the energy density at the mean-field level for a homogeneous Bose gas, since ∇v obviously vanishes in this case. It first contributes at the one-loop level, and this gives one factor of $\sqrt{na^3}$. There are two powers of $\psi^*\psi$ and two powers of ∇, which give two factors of n and $\sqrt{na}$, respectively. This yields a contribution proportional to $r_s n^2 (na^3)^{3/2}$, in accordance with the explicit calculation (119).

We next comment on the nonuniversal effects that arise in higher-order calculations of the energy density. For simplicity, we ignore all other coupling constants than g. The leading term is the mean-field contribution given in Eq. (75). A one-loop calculation gives rise to a universal correction proportional to $\sqrt{na^3}$ shown in Eq. (91). At the two-loop level, one encounters two terms. The first is a universal logarithmic correction proportional to $na^3 \ln na^3$. This term was first calculated by Wu (1959). The second term is a nonuniversal term proportional to na^3, first calculated by Braaten and Nieto (1999b). It comes about as follows. At the two-loop level, there is a logarithmic ultraviolet divergence that cannot be canceled by a local two-body counterterm of

the form $\Delta g(\psi^*\psi)^2$. The only way to cancel it is to add to the Lagrangian a local counterterm of the form $\Delta g_3(\psi^*\psi)^3$ and absorb the divergence in the coefficient of this operator. One can see the necessity of such an operator by considering $3 \to 3$ scattering. At the two-loop level, or fourth order in a, there are Feynman diagrams that depend logarithmically on the ultraviolet cutoff. They give an additional momentum-independent contribution to the $3 \to 3$ scattering amplitude. In order to reproduce the low-energy scattering of three atoms, the local momentum-independent operator $\Delta g_3(\psi^*\psi)^3$ must be included in the effective Lagrangian. The counterterm of this operator that removes the logarithimic divergences from the $3 \to 3$ scattering amplitude is then exactly the same counterterm needed to remove the logarithmic divergence in the energy density.

The coefficient g_3 generally depends on the properties of the two-body and three-body potentials. The operator $(\psi^*\psi)^3$ in Eq. (25) takes into account not only the contribution from $3 \to 3$ scattering from a possible three-body potential, but also the contribution from the successive $2 \to 2$ scattering via the potential $V_0(\mathbf{x})$. One way to determine the coefficient g_3 would be to solve the $3 \to 3$ scattering problem for the potential $V_0(\mathbf{x})$. Alternatively, one could determine it from calculating the ground-state energy density of bosons interacting through $V_0(\mathbf{x})$. Such a strategy was recently employed by Braaten, Hammer, and Hermans (2001) using the Monte Carlo calculations of the condensate fraction and the energy density for four different model potentials of Giorgini, Boronat, and Casulleras (1999). The four potentials were a hard-sphere potential with radius a, two soft-sphere potentials with height V_0 and radii $R = 5a$ and $R = 10a$, and a hard-sphere square-well potential with depth V_0 and inner and outer radii of $R = a/50$ and $R = a/10$, respectively. These four potentials all have the same s-wave scattering length a, but different effective ranges r_s. By calculating the energy density for the homogeneous Bose gas in the low-density expansion and matching it to the Monte Carlo results, Braaten, Hammer, and Hermans were able to estimate the coefficient g_3. Due to the large statistical errors, they could not find any deviation from universality in the three-body contact parameter. In order to determine the coefficient more accurately, one needs data with greater precision at various densities.

IV. WEAKLY INTERACTING BOSE GAS AT FINITE TEMPERATURE

In this section, we discuss the weakly interacting Bose gas at finite temperature. We first review the Hartree-Fock-Bogoliubov (HFB) approximation, the Bogoliubov approximation, and the Popov approximation. We then discuss Wilson's renormalization-group approach applied to this problem. Finally, we discuss improved variational approaches to the finite-temperature Bose gas.

A. Hartree-Fock Bogoliubov approximation

The self-consistent Hartree-Fock-Bogoliubov approximation and its relation to the Bogoliubov approximation and the Popov approximation have been discussed in detail (Griffin, 1996; Shi and Griffin, 1998; Hutchinson *et al.*, 2000). The starting point is the action (25) in imaginary time:

$$S[\psi^*,\psi]=\int_0^\beta d\tau\int d^dx\left\{\psi^*\left[\frac{\partial}{\partial\tau}-\mu-\nabla^2\right]\psi\right.$$
$$\left.+\frac{1}{2}g(\psi^*\psi)^2\right\}. \tag{120}$$

The next step is to treat the interaction term using a self-consistent quadratic approximation. After performing the shift (36), there are terms that are cubic and quartic in the quantum field $\tilde{\psi}$. These terms are approximated as

$$\tilde{\psi}^*\tilde{\psi}\tilde{\psi}\approx 2\langle\tilde{\psi}^*\tilde{\psi}\rangle\tilde{\psi}+\langle\tilde{\psi}\tilde{\psi}\rangle\tilde{\psi}^*, \tag{121}$$

$$\tilde{\psi}^*\tilde{\psi}\tilde{\psi}^*\tilde{\psi}\approx 4\langle\tilde{\psi}^*\tilde{\psi}\rangle\tilde{\psi}^*\tilde{\psi}+\langle\tilde{\psi}^*\tilde{\psi}^*\rangle\tilde{\psi}\tilde{\psi}+\langle\tilde{\psi}\tilde{\psi}\rangle\tilde{\psi}^*\tilde{\psi}^*. \tag{122}$$

Terms involving the expectation value of a single field have been omitted since $\langle\tilde{\psi}\rangle=\langle\tilde{\psi}^*\rangle=0$. Moreover, terms involving the expectation values of three or four fields are omitted. The quantities $\langle\tilde{\psi}^*\tilde{\psi}\rangle$ and $\langle\tilde{\psi}\tilde{\psi}\rangle$ are often referred to as the *normal and anomalous averages*, respectively.

We next write the quantum field $\tilde{\psi}=(\psi_1+i\psi_2)/\sqrt{2}$ and insert Eqs. (121) and (122) into the action (120). We then obtain an approximate action, which is quadratic in the fluctuating fields:

$$S[v,\psi_1,\psi_2]=S[v]+S_{\text{free}}[v,\psi_1,\psi_2]+S_{\text{int}}[v,\psi_1,\psi_2], \tag{123}$$

where in analogy with the zero-temperature case, we have defined the classical, free, and interacting parts of the action by

$$S[v]=\int_0^\beta d\tau\int d^dx\left[-\mu v^2+\frac{1}{2}gv^4\right], \tag{124}$$

$$S_{\text{free}}[v,\psi_1\psi_2]=\int_0^\beta d\tau\int d^dx\left[\frac{1}{2}i(\psi_1\dot{\psi}_2-\dot{\psi}_1\psi_2)\right.$$
$$+\frac{1}{2}iW\psi_1\psi_2+\frac{1}{2}\psi_1(-\nabla^2+X)\psi_1$$
$$\left.+\frac{1}{2}\psi_2(-\nabla^2+Y)\psi_2\right], \tag{125}$$

$$S_{\text{int}}[v,\psi_1,\psi_2]=\int_0^\beta d\tau\int d^dx\left\{\left[-\mu+g\left(v^2+2\langle\tilde{\psi}^*\tilde{\psi}\rangle\right.\right.\right.$$
$$\left.\left.+\frac{1}{2}\langle\tilde{\psi}\tilde{\psi}\rangle+\frac{1}{2}\langle\tilde{\psi}^*\tilde{\psi}^*\rangle\right)\right]\sqrt{2}v\psi_1$$
$$+\frac{1}{2}[\langle\tilde{\psi}^*\tilde{\psi}^*\rangle-\langle\tilde{\psi}\tilde{\psi}\rangle]\sqrt{2}v\psi_2\bigg\}, \tag{126}$$

where

$$W=g[\langle\tilde{\psi}\tilde{\psi}\rangle-\langle\tilde{\psi}^*\tilde{\psi}^*\rangle], \tag{127}$$

$$X=-\mu+g\left[3v^2+2\langle\tilde{\psi}^*\tilde{\psi}\rangle+\frac{1}{2}\langle\tilde{\psi}\tilde{\psi}\rangle+\frac{1}{2}\langle\tilde{\psi}^*\tilde{\psi}^*\rangle\right], \tag{128}$$

$$Y=-\mu+g\left[v^2+2\langle\tilde{\psi}^*\tilde{\psi}\rangle-\frac{1}{2}\langle\tilde{\psi}\tilde{\psi}\rangle-\frac{1}{2}\langle\tilde{\psi}^*\tilde{\psi}^*\rangle\right]. \tag{129}$$

Requiring that the terms linear in ψ_1 and ψ_2 in Eq. (126) vanish immediately yields

$$0=\langle\tilde{\psi}^*\tilde{\psi}^*\rangle-\langle\tilde{\psi}\tilde{\psi}\rangle, \tag{130}$$

$$0=-\mu+g\left[v^2+2\langle\tilde{\psi}^*\tilde{\psi}\rangle+\frac{1}{2}\langle\tilde{\psi}\tilde{\psi}\rangle+\frac{1}{2}\langle\tilde{\psi}^*\tilde{\psi}^*\rangle\right]. \tag{131}$$

The equation of motion for the quantum field $\tilde{\psi}$ follows from Eq. (125) and reads

$$\frac{\partial\tilde{\psi}}{\partial\tau}=-[\nabla^2+\mu]\tilde{\psi}+g[2(v^2+\langle\tilde{\psi}^*\tilde{\psi}\rangle)\tilde{\psi}$$
$$+(v^2+\langle\tilde{\psi}\tilde{\psi}\rangle)\tilde{\psi}^*]. \tag{132}$$

The propagator that corresponds to the free part of the action is

$$D(\omega_n,p)=\frac{1}{\omega_n^2+\epsilon^2(p)}\begin{pmatrix}p^2-2g\langle\tilde{\psi}\tilde{\psi}\rangle & \omega_n \\ -\omega_n & p^2+2gv^2\end{pmatrix}, \tag{133}$$

where we have used Eq. (130) to simplify. The dispersion relation is given by

$$\epsilon^2(p)=[p^2-2g\langle\tilde{\psi}\tilde{\psi}\rangle][p^2+2gv^2]. \tag{134}$$

It can be shown that the anomalous average $\langle\tilde{\psi}\tilde{\psi}\rangle$ is negative (Griffin, 1996), so that the dispersion relation (134) makes sense.

Equations (131)–(134) constituting the Hartree-Fock-Bogoliubov approximation. One of the attractive features of this approximation is that it is guaranteed to respect the conservation laws that follow from the underlying symmetries of the field theory. On the other hand, one of the problems with it is that there is a gap in the spectrum (134), which is a consequence of the spontaneously broken symmetry. Thus the HFB approximation violates the Goldstone theorem. Shi and Griffin (1998) have argued that the problem of a gap in the HFB approximation is due to overcounting diagrams that contribute to the anomalous self-energy and are second order in the interaction, making it inconsistent to that order in the interaction.

Another problem with the HFB approximation is that is it computationally difficult to apply. One starts with some initial guess for the condensate density and the chemical potential, as well as the normal and anomalous averages satisfying Eq. (131). One then solves for the infinitely many normal modes in Eq. (132). These nor-

mal modes are then used to calculate the normal and anomalous averages. The procedure is iterated to self-consistency.[5] In this way, one obtains information about the different normal modes. However, since the HFB approximation has a gap, some of this information must be qualitatively incorrect.

The HFB approximation can also be viewed as a variational one (Blaizot and Ripka, 1986), although the equivalence seems to have gone unnoticed in some of the literature. The idea is to make a Gaussian ansatz for the ground-state wave functional and the excitations. The variational parameters are the normal and anomalous self-energies $\Sigma_{11}(\omega_n,p)$ and $\Sigma_{12}(\omega_n,p)$, which are normally taken to be independent of frequency and momentum. The corresponding terms $\Sigma_{11}(\omega_n,p)\psi^*\psi$ and $\Sigma_{12}(\omega_n,p)\psi\psi$ are quadratic in fields and are simply added to and subtracted from the Lagrangian. Expressing the normal and anomalous self-energies in terms of Π_{11} and Π_{22}, the action can be split into a free part and an interacting part according to

$$S_{\text{free}}[v,\psi_1\psi_2]=\int_0^\beta d\tau\int d^dx\left[\frac{1}{2}i(\psi_1\dot{\psi}_2-\dot{\psi}_1\psi_2)\right.$$

$$+\frac{1}{2}\psi_1(-\nabla^2-X)\psi_1$$

$$\left.+\frac{1}{2}\psi_2(-\nabla^2-Y)\psi_2\right], \tag{135}$$

$$S_{\text{int}}[v,\psi_1,\psi_2]=\int_0^\beta d\tau\int d^dx\left[\frac{1}{2}(3gv^2-\Pi_{11})\psi_1^2\right.$$

$$+\frac{1}{2}(gv^2-\Pi_{22})\psi_2^2-\frac{1}{\sqrt{2}}Zv\psi_1(\psi_1^2+\psi_2^2)$$

$$\left.+\frac{1}{8}g(\psi_1^2+\psi_2^2)^2\right], \tag{136}$$

where we have defined

$$X=\mu-\Pi_{11}, \tag{137}$$

$$Y=\mu-\Pi_{22}, \tag{138}$$

$$Z=-gv^2. \tag{139}$$

The propagator that corresponds to the free part of the action is

$$D(\omega_n,p)=\frac{1}{\omega_n^2+\epsilon^2(p)}\begin{pmatrix}p^2-Y & \omega_n\\ -\omega_n & p^2-X\end{pmatrix},$$

where the dispersion relation is given by

$$\epsilon(p)=\sqrt{(p^2-X)(p^2-Y)}. \tag{140}$$

The next step is to calculate the thermodynamic potential in some approximate way including the interaction
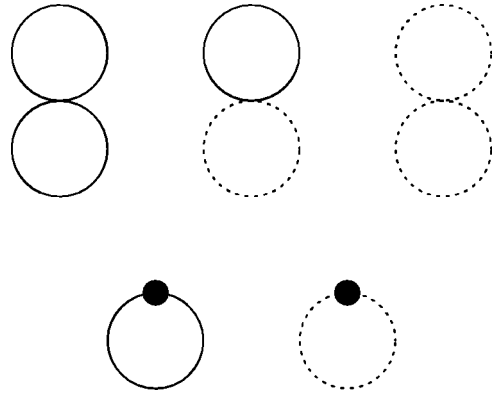

FIG. 8. Vacuum diagrams included in the Gaussian approximation.

term (136), which consists of three- and four-point vertices together with the subtracted self-energies. This is done by calculating the thermodynamic potential approximately according to

$$\Omega=-\mu v^2+\frac{1}{2}gv^4+\text{Tr}\ln D^{-1}+\langle S_{\text{int}}\rangle, \tag{141}$$

where $\langle A\rangle$ is the thermal average of the operator A. The thermodynamic potential then becomes

$$\Omega=-\mu v^2+\frac{1}{2}gv^4+\frac{1}{2}\text{Tr}\ln D^{-1}$$

$$+\frac{1}{4}g\left[\sum_P \frac{p^2-Y}{\omega_n^2+\epsilon^2(p)}\right]\sum_P\left[\frac{p^2-X}{\omega_n^2+\epsilon^2(p)}\right]$$

$$+\frac{3}{8}g\left[\sum_P \frac{p^2-Y}{\omega_n^2+\epsilon^2(p)}\right]^2+\frac{3}{8}g\left[\sum_P \frac{p^2-X}{\omega_n^2+\epsilon^2(p)}\right]^2$$

$$+\frac{1}{2}(3gv^2-\Pi_{11})\sum_P\left[\frac{p^2-Y}{\omega_n^2+\epsilon^2(p)}\right]$$

$$+\frac{1}{2}(gv^2-\Pi_{22})\sum_P\left[\frac{p^2-X}{\omega_n^2+\epsilon^2(p)}\right]. \tag{142}$$

The Feynman diagrams that correspond to the interaction term in Eq. (142) are shown in Fig. 8. The solid circle denotes an insertion of either $3gv^2-\Pi_{11}$ or $gv^2-\Pi_{22}$.

The condensate density v is determined by the stationarity condition

$$\frac{\partial\Omega}{\partial v}=0. \tag{143}$$

Using Eq. (142) for the thermodynamic potential, we find that Eq. (143) becomes

$$0=-\mu+gv^2+\frac{3}{2}g\sum_P\left[\frac{p^2-Y}{\omega_n^2+\epsilon^2(p)}\right]$$

$$+\frac{1}{2}g\sum_P\left[\frac{p^2-X}{\omega_n^2+\epsilon^2(p)}\right]. \tag{144}$$

The self-energies Π_{11} and Π_{22} are determined variationally by requiring that they minimize the free energy:
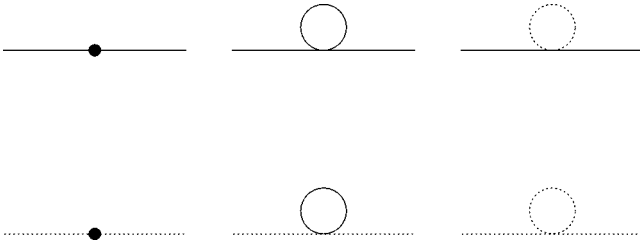
FIG. 9. Feynman diagrams included in the self-energies Π_{11} and Π_{22} in the Gaussian approximation.

$$\frac{\partial \Omega}{\partial \Pi_{11}} = 0, \tag{145}$$

$$\frac{\partial \Omega}{\partial \Pi_{22}} = 0. \tag{146}$$

Equations (145) and (146) are often referred to as gap equations. Their solutions are

$$\Pi_{11} = 3gv^2 + \frac{3}{2}g \sum_P \left[\frac{p^2 - Y}{\omega_n^2 + \epsilon^2(p)} \right]$$

$$+ \frac{1}{2}g \sum_P \left[\frac{p^2 - X}{\omega_n^2 + \epsilon^2(p)} \right], \tag{147}$$

$$\Pi_{22} = gv^2 + \frac{1}{2}g \sum_P \left[\frac{p^2 - Y}{\omega_n^2 + \epsilon^2(p)} \right]$$

$$+ \frac{3}{2}g \sum_P \left[\frac{p^2 - X}{\omega_n^2 + \epsilon^2(p)} \right]. \tag{148}$$

The Feynman diagrams that correspond to the gap equations (147) and (148) are shown in Fig. 9. Inserting Eqs. (147) and (148) into Eq. (140), and using Eq. (144) to eliminate the chemical potential, we obtain the Hartree-Fock-Bogoliubov spectrum (134).

The Gaussian approximation can be made the starting point for a systematic expansion procedure. This expansion was first formulated by Okopinska (1987). Stancu and Stevenson (1990) calculated the leading corrections to the Gaussian approximation for a relativistic ϕ^4 theory in four dimensions. The Feynman diagrams that are included in this next-to-leading-order calculation are the three-loop diagrams, the two-loop setting sun diagrams, the two-loop double bubbles with a single self-energy insertion, and the one-loop diagrams with two insertions of a self-energy.

We next discuss the Bogoliubov and Popov approximations, which are obtained by making certain approximations in the full HFB approximation.

1. Bogoliubov approximation

The Bogoliubov appoximation amounts to neglecting both the normal and the anomalous averages in Eqs. (131)–(134). The chemical potential (131) then reduces to

$$\mu = gv^2. \tag{149}$$

The spectrum (134) is given by

$$\epsilon(p) = p\sqrt{p^2 + 2\mu}, \tag{150}$$

which is gapless. The Bogoliubov approximation has a natural interpretation in terms of Feynman diagrams. It is obtained by neglecting the two-loop diagrams contributing to the thermodynamic potential (142). The self-energies that follow from the gap equations are then given by their mean-field values, so we have $\Pi_{11}(\omega_n, p) = 3gv^2$ and $\Pi_{22}(\omega_n, p) = gv^2$. The stationarity condition (143) simply reduces to Eq. (149). The free energy is obtained by substituting the mean-field values for the self-energies into the thermodynamic potential evaluated at the minimum. This yields

$$\mathcal{F} = -\frac{\mu^2}{2g} + \frac{1}{2} \sum_P \ln[\omega_n^2 + \epsilon^2(p)]$$

$$= -\frac{\mu^2}{2g} + \frac{1}{2}I_{0,-1} + \frac{T}{2\pi^2}\int_0^\infty dp\ p^2 \ln[1 - e^{-\beta\epsilon(p)}]. \tag{151}$$

In the Bogoliubov approximation, one assumes that most particles are in the zero-momentum state. Clearly, this approximation is only valid at very low temperatures where one can ignore the thermal depletion of the condensate.

One can expand the free energy (151) about zero temperature. At sufficiently low temperatures, the thermodynamics are dominated by the phonon part of the spectrum. Using Eqs. (A10) and (A31), the free energy reduces in the limit $T \ll 2\mu$ to

$$\mathcal{F} = -\frac{\mu^2}{2g}\left[1 - \frac{4\sqrt{2\mu g^2}}{15\pi^2}\right] - \frac{\pi^2 T^4}{90(2\mu)^{3/2}}. \tag{152}$$

The other thermodynamic functions follow from the free energy (151). In the low-temperature limit, the number density becomes

$$n = \frac{\mu}{g}\left[1 - \frac{\sqrt{2\mu g^2}}{3\pi^2}\right] - \frac{\pi^2 T^4}{60(2\mu)^{5/2}}. \tag{153}$$

Inverting Eq. (153), we obtain the chemical potential in the limit $T \ll 2gn$:

$$\mu = gn\left[1 + \sqrt{\frac{2ng^3}{3\pi^2}}\right] + \frac{g\pi^2 T^4}{60(2gn)^{5/2}}. \tag{154}$$

Similarly, for temperatures $T \ll 2gn$, the equilibrium energy density is

$$\mathcal{E} = 4\pi an^2\left[1 + \frac{128}{15}\sqrt{\frac{na^3}{\pi}}\right] - \frac{\pi^2 T^4}{90(2gn)^{3/2}}. \tag{155}$$

Using Eq. (92), one can calculate the total number density as a function of the condensate density and temperature:

$$n = n_0 + \frac{1}{2} \sum\!\!\!\!\!\!\int_P \frac{p^2 + \epsilon^2(p)}{\omega_n^2 + \epsilon^2(p)}$$

$$= n_0 + \frac{1}{4}[I_{1,1} + I_{-1,-1}]$$

$$+ \frac{1}{4\pi^2} \int_0^\infty dp \, \frac{p^2[p^2 + \epsilon^2(p)]}{\epsilon(p)} n[\epsilon(p)]. \tag{156}$$

In the limit $T \ll 2gn_0$, one finds

$$n = n_0 \left[1 + \frac{8}{3}\sqrt{\frac{n_0 a^3}{\pi}}\right] + \frac{T^2}{24\sqrt{2gn_0}}. \tag{157}$$

Equations (152)–(157) were first obtained by Lee and Yang (1958). The second term inside the brackets is the quantum depletion of the condensate that was calculated in Sec. III.C. The last term is the thermal depletion.

2. Popov approximation

In the Popov approximation (Popov, 1983), one neglects the anomalous average in Eqs. (131)–(134). The chemical potential (131) reduces to

$$\mu = g[v^2 + 2\langle \tilde{\psi}^* \tilde{\psi}\rangle]. \tag{158}$$

Similarly, the spectrum (134) becomes

$$\epsilon(p) = p\sqrt{p^2 + 2gv^2} \tag{159}$$

and is gapless. Note that the spectrum formally has the same form as the Bogoliubov spectrum, but now the condensate density depends on the temperature. The number density n satisfies

$$n = n_0 + \langle \tilde{\psi}^* \tilde{\psi}\rangle. \tag{160}$$

Equations (158) and (160) constitute the equations of state for the weakly interacting Bose gas in the Popov approximation. For a given temperature T and total number density n, they must be solved simultaneously for the condensate density n_0 and the chemical potential. Note in particular that the condensate density has a strong temperature dependence. For small values of the gas parameter, the condensate density as a function of temperature typically deviates by only a few percent from the result (17) for the ideal gas.

At $T=0$, the expectation value in Eq. (158) is suppressed by a factor of $\sqrt{na^3}$ compared to the mean-field term. This implies that the Popov approximation gives the same results as the Bogoliubov approximation for all thermodynamic quantities up to corrections of the order of the gas parameter $\sqrt{na^3}$. Since the Popov approximation does not include all corrections of order $\sqrt{na^3}$, it is no more accurate than the Bogoliubov approximation at zero temperature.

At higher temperatures, the Popov approximation ought to give a better description than the Bogoliubov approximation, since it takes into account the temperature dependence of the condensate. However, the Popov approximation breaks down in a narrow temperature region around T_c. This can be seen from the fact that the Popov approximation predicts a first-order phase transition for the weakly interacting Bose gas, while universality arguments based on O(2) symmetry tell us that the phase transition is of second order.[6]

The Popov approximation can also be interpreted in terms of Feynman diagrams. This is done by expressing propagators and interactions in terms of normal and anomalous self-energies rather than Π_{11} and Π_{22}. The Feynman diagrams that contribute to the thermodynamic potential in the HFB approximation are still those shown in Fig. 8, but the sum-integrals are now in terms of normal and anomalous propagators, and the symmetry factors are different. The Popov approximation for the thermodynamic potential is then defined by keeping the diagrams that involve normal propagators and neglecting those that involve anomalous ones. The corresponding gap equation, which follows from the variational principle, gives the normal self-energy as the sum of the mean-field contribution $2gv^2$ and the one-loop tadpole diagram that involves the normal propagator. The anomalous self-energy is given by the mean-field contribution gv^2 alone. This definition has been given before (Shi and Griffin, 1985). Finally, the free energy is obtained by substituting the expressions for the self-energies into the thermodynamic potential evaluated at the minimum. The free energy in the Popov approximation has the Bogoliubov form (151).

3. Many-body T matrix and modified Popov approximation

In Sec. III.A, we calculated the exact scattering amplitude for $2 \to 2$ scattering in a vacuum. In the limit where the external momentum goes to zero, the two-body scattering matrix goes to a constant. In the next section, we shall show, using renormalization-group methods, that the effective coupling constant for a weakly interacting Bose gas is temperature dependent and in particular that it vanishes at the critical temperature. This behavior is expected at a second-order phase transition where the correlation length goes to infinity (the effective chemical potential or the effective mass goes to zero) due to the fact that ϕ^4 theory is a trivial theory. It is therefore important to improve on the Popov theory by using an effective temperature-dependent coupling constant. This can be done by using the *many-body T-matrix approximation*. This approximation takes medium effects into account by summing repeated two-body scattering processes of quasiparticles in the gas rather than in the vacuum. This is done by calculating the diagrams in Fig. 3 at finite temperature using the propagator (65). The many-body T matrix $T^{MB}(k,k,K;z)$ depends on the relative momenta of the two atoms **k** and **k** before and

––––––

[6]In Sec. IV.C, we show that the long-distance properties of the dilute Bose gas are given by a classical field theory in three dimensions with an O(2) symmetry. In particular, the infrared Wilson-Fisher fixed point is that of a three-dimensional O(2) model. This model is known to have a second-order phase transition.

after collision, the total center-of-mass momentum **K**, and the center-of-mass energy z. In the following, we neglect this energy and momentum dependence, which is a good approximation (Bijlsma and Stoof, 1996a; Shi and Griffin, 1998).

At zero external momentum p, the one-loop diagram in Fig. 3 is

$$\mathcal{T}_1(0) = 2g^2 \sum_{P} \!\!\!\!\!\!\!\!\!\!\!\!\!\!\!\!\!\! \frac{1}{\omega_n^2 + \epsilon^2(p)}$$

$$= gI_{0,1} + g\frac{1}{\pi^2}\int_0^\infty dp\, \frac{p^2}{\epsilon(p)} n[\epsilon(p)]. \tag{161}$$

By summing the geometric series corrresponding to the diagrams shown in Fig. 3, we find (Bijlsma and Stoof, 1996a; Shi and Griffin, 1998)

$$T^{\mathrm{MB}}(0) = \frac{2g^2}{2g - \mathcal{T}_1(0)}. \tag{162}$$

We next consider the many-body T matrix at low temperature. For $T \ll 2gn_0$, we obtain

$$T^{\mathrm{MB}}(0) = g\left\{1 + \frac{\sqrt{2n_0 g^3}}{4\pi^2}\left[1 - \frac{\pi^2}{6}\left(\frac{T}{n_0 g}\right)^2\right]\right\}. \tag{163}$$

We note in particular that at $T=0$, the many-body T matrix reduces to g up to corrections of order $\sqrt{na^3}$.

The many-body T matrix has been used to obtain an improved approximation from the Gaussian approximation (Bijlsma and Stoof, 1996a). The normal and anomalous self-energies can be easily calculated from Eqs. (147) and (148). We obtain

$$\Sigma_{11} = 2gv^2 + g\sum_{P}\!\!\!\!\!\!\!\!\!\!\!\!\!\!\!\!\!\! \left[\frac{p^2 - Y}{\omega_n^2 + \epsilon^2(p)}\right] + g\sum_{P}\!\!\!\!\!\!\!\!\!\!\!\!\!\!\!\!\!\! \left[\frac{p^2 - X}{\omega_n^2 + \epsilon^2(p)}\right]$$

$$= 2g[v^2 + \langle \tilde{\psi}^* \tilde{\psi}\rangle],$$

$$\Sigma_{12} = gv^2 + g\sum_{P}\!\!\!\!\!\!\!\!\!\!\!\!\!\!\!\!\!\! \left[\frac{p^2 - Y}{\omega_n^2 + \epsilon^2(p)}\right] - g\sum_{P}\!\!\!\!\!\!\!\!\!\!\!\!\!\!\!\!\!\! \left[\frac{p^2 - X}{\omega_n^2 + \epsilon^2(p)}\right]$$

$$= gv^2 + \frac{1}{2g}\Sigma_{12}\mathcal{T}_1(0). \tag{164}$$

The last equation can be easily solved for Σ_{12}. Using Eq. (162), we obtain

$$\Sigma_{12} = T^{\mathrm{MB}}(0)v^2. \tag{165}$$

Thus the normal self-energy $\Sigma_{11}(0,0)$ is given in the Hartree-Fock or one-loop approximation, while the anomalous self-energy $\Sigma_{12}(0,0)$ is given in the many-body T-matrix approximation. This observation motivated Bijlsma and Stoof (1996a) to redo the calculation using the many-body T matrix as an effective interaction. This gives both the normal and anomalous self-energies in the many-body T matrix approximation:

$$\Sigma_{11} = 2T^{\mathrm{MB}}(0)[v^2 + \langle \tilde{\psi}^* \tilde{\psi}\rangle], \tag{166}$$

$$\Sigma_{12} = T^{\mathrm{MB}}(0)v^2. \tag{167}$$

These modified self-energies define a modified Gaussian approximation, which was used to investigate the thermodynamic properties of the homogeneous Bose gas in two and three dimensions. In three dimensions, this approach yields a second-order phase transition, but the critical temperature is the same as that of an ideal gas. At the same time, the effective coupling constant, which is precisely the many-body T matrix, vanishes at the temperature given by Eq. (16) (Shi and Griffin, 1998). However, it turns out that the Hugenholz-Pines theorem is not always satisfied. At very low temperature, it can be shown (Bijlsma and Stoof, 1996a) that the value of v^2 that minimizes the thermodynamic potential does not exactly correspond to the condition $\mu = \Sigma_{11}(0,0) - \Sigma_{12}(0,0)$.

The self-energies (166) and (167) can also be obtained from the HFB equations (128) and (129) by neglecting the anomalous average and replacing the coupling constant g by the many-body T matrix. By making the substitution $g \rightarrow T^{\mathrm{MB}}$ and neglecting the anomalous average in the remaining equations that define the HFB approximation, Hutchinson *et al.* (1998) and Proukakis *et al.* (1998) obtained a gapless approximation.[7] Equations (131), (132), and (134) now become

$$0 = -\mu + T^{\mathrm{MB}}[v^2 + 2\langle \tilde{\psi}^* \tilde{\psi}\rangle], \tag{168}$$

$$\frac{\partial \tilde{\psi}}{\partial \tau} = -[\nabla^2 + \mu]\tilde{\psi} + T^{\mathrm{MB}}[2(v^2 + \langle \tilde{\psi}^* \tilde{\psi}\rangle)\tilde{\psi} + v^2 \tilde{\psi}^*], \tag{169}$$

$$\epsilon^2(p) = p^2[p^2 + 2T^{\mathrm{MB}}v^2]. \tag{170}$$

The modified mean-field approximation does not reproduce known perturbative results at $T=0$. For instance, the prediction for the correction to the Bogoliubov spectrum at long wavelengths differs from Eq. (106). Thus at $T=0$, this approximation is no more accurate than the Bogoliubov or Popov approximations.

B. Other variational approaches

In this subsection, we discuss other variational approaches to the weakly interacting Bose gas. The idea is to define a thermodynamic potential Ω that depends on a set of variational parameters a_i. The free energy and other thermodynamic variables are then given by the thermodynamic potential and its derivative evaluated at the variational minimum $\partial\Omega/\partial a_i = 0$. A variational method can be successful only if the essential physics can be captured by the variational parameters.

1. Φ-derivable approach

The Φ-derivable approximation is an approach in which the full propagator serves as an infinite set of variational parameters. It was first formulated by Luttinger

---

[7]It is *not* gapless in the sense that the value of the condensate v that minimizes the effective potential coincides with $\mu = \Sigma_{11}(0,0) - \Sigma_{12}(0,0)$, as explained above.

and Ward (1960), and by Baym (1962) for nonrelativistic fermions, and later generalized to relativistic field theories by Cornwall, Jackiw, and Tomboulis (1974). A property of the Φ-derivable approximation is that it is conserving, which means that it respects the conservation laws that follow from the global symmetries of the system.

We next apply the Φ-derivable approach to the dilute Bose gas. We shall rederive some of the results obtained by Lundh and Rammer (2002), but the formulation is somewhat different.

The Φ-derivable thermodynamic potential $\Omega[D]$ has the form

$$\Omega[D] = -\mu v^2 + \frac{1}{2}gv^4 + \frac{1}{2}\operatorname{Tr}\ln D^{-1}$$
$$-\frac{1}{2}\operatorname{Tr}\Pi D + \Phi[D], \tag{171}$$

where Π is the exact self-energy, D is the exact propagator, and the interaction potential $\Phi[D]$ is the sum of all *two-particle irreducible vacuum diagrams*. These are diagrams that do not fall apart when two propagator lines are cut. It is understood that both Π and D are 2×2 matrices. Tr denotes the trace in configuration space. The condensate v is found by minimizing the thermodynamic potential in the usual way

$$\frac{\partial\Omega[D]}{\partial v} = 0. \tag{172}$$

Similarly, the variational principle requires that the thermodynamic potential be stationary under variations of the full propagator at fixed D_0. This can be expressed as

$$\frac{\partial\Omega[D]}{\partial D} = 0. \tag{173}$$

If we denote the free propagator by D_0, the Schwinger-Dyson equation for the exact propagator D can be written as

$$D^{-1} = D_0^{-1} + \Pi. \tag{174}$$

Using Eq. (174), we can rewrite Eq. (173)

$$\frac{\partial\Phi[D]}{\partial D} = \frac{1}{2}\Pi. \tag{175}$$

Equation (175) for the self-energy cannot be solved exactly, but one can resort to a systematic approximation. The n-loop Φ-derivable approximation is such an approximation. It is defined by keeping all two-particle irreducible diagrams up to n loops in the thermodynamic potential. Differentiation with respect to the components of the propagator is equivalent to cutting the corresponding lines in the Feynman diagrams. Thus the gap equations for the self-energy in the n-loop Φ-derivable approximation contain all two-particle irreducible diagrams up to $n-1$ loops. It leads to a set of integral equations for the self-energies that generally are extremely difficult to solve. In certain simple cases, where the self-energies are momentum independent, one can solve these equations.
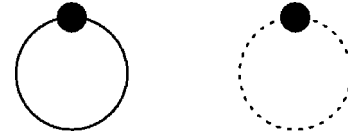

FIG. 10. Vacuum diagrams contributing to the one-loop Φ-derivable approximation $\Phi_1[D]$.

Consider the one-loop Φ-derivable approximation. The diagrams that contribute to $\Phi_1[D]$ are shown in Fig. 10, and the approximation reads

$$\Phi_1[D] = \frac{3}{2}gv^2 \sum_P \frac{p^2 - Y}{\omega_n^2 + \epsilon^2(p)}$$
$$+ \frac{1}{2}gv^2 \sum_P \frac{p^2 - X}{\omega_n^2 + \epsilon^2(p)}. \tag{176}$$

The self-energies are given by

$$\Pi_{11} = 3gv^2, \tag{177}$$
$$\Pi_{22} = gv^2, \tag{178}$$

while Π_{12} and Π_{21} both vanish. Thus the self-energies are those of the Bogoliubov approximation. We next substitute the self-energies (177) and (178) into the thermodynamic potential (171). It turns out that the two terms $-\frac{1}{2}\operatorname{Tr}\Pi D$ and $\Phi_1[D]$ cancel each other, and the one-loop Φ-derivable approximation for the free energy reduces to the Bogoliubov approximation (151).

The two-loop Φ-derivable approximation Φ_2 is very complicated. The two-loop diagrams that contribute to the thermodynamic potential are shown in Fig. 11. The corresponding equation for the self-energy matrix (175) is obtained by cutting the lines in the diagrams. The diagrams that are first order in the interaction are momentum independent and can be easily calculated. The diagrams that are second order in the interaction are momentum dependent. The difficult momentum dependence comes from the self-energy in the propagators. This leads to intractable integral equations for the self-energies. There have been attempts to simplify the two-loop Φ-derivable approximation by making the ansatz
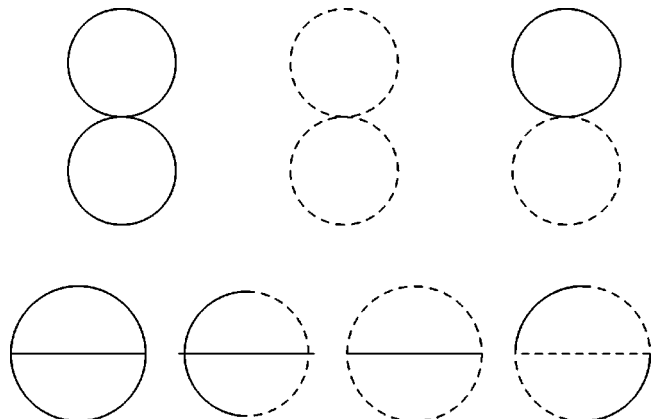

FIG. 11. Vacuum diagrams contributing to the two-loop Φ-derivable approximation $\Phi_2[D]$.

that the self-energy is a momentum-independent mass term (Amelino-Camelia and Pi, 1993). However, such approximations lead to a mass gap and hence violate the Hugenholz-Pines theorem.

Finally, we notice that if one neglects the setting sun diagrams in Fig. 11, the two-loop Φ-derivable approximation reduces to the Gaussian approximation that was discussed in detail in the previous subsection.

2. Optimized perturbation theory

The complexity of the Φ-derivable approach makes the use of simpler variational approaches very appealing. One such approach is optimized perturbation theory. One introduces a finite number of variational parameters. In its simplest form, one introduces a single variational parameter m or μ. In a relativistic field theory, m is a variational mass parameter, while in a nonrelativistic field theory, μ is a variational chemical potential. This method, first formulated by Yukalov (1976), can be extended to include variational coupling constants and a variational kinetic-energy term (Chiku, 2000). At this point, it is important to emphasize that the parameters introduced in optimized perturbation theory are completely arbitrary and that one needs a prescription for them in order to complete a calculation. One prescription is the *principle of minimal sensitivity*, in which one requires that the parameters satisfy a stationarity condition. For instance, one can demand that the free energy be stationary with respect to variations of these parameters. Another criterion is the *principle of fastest apparent convergence*. This condition requires that the difference between a physical quantity calculated at two different loop orders be as small as possible.

The starting point is the action (120). We rewrite the corresponding Lagrangian by introducing an effective chemical potential μ_1, an effective coupling constant λ, and a counting variable δ in the following manner:

$$\mathcal{L} = \psi^* \left[\frac{\partial}{\partial \tau} - \nabla^2 - \mu_1 - \delta(\mu - \mu_1) \right] \psi + \frac{1}{2} \lambda (\psi^* \psi)^2$$
$$+ \frac{1}{2} \delta(g - \lambda)(\psi^* \psi)^2 + \cdots . \tag{179}$$

If we set $\delta = 1$, we immediately recover the Lagrangian that corresponds to the action (120). Optimized perturbation theory is defined by the power counting rule that δ be of the order $\lambda \sim g$. We carry out calculations in powers of λ and, at the end of the calculations, we set $\delta = 1$. It is important to note that the power counting rules also should be applied to the counterterms. The ultraviolet divergences that appear in optimized perturbation theory are removed by the counterterms determined in the standard loop expansion for perturbation theory at $T = 0$.

The introduction of μ_1 and λ represents a reorganization of the perturbative series, which is a selective resummation of higher-order graphs. But it is important to emphasize that there is no overcounting of diagrams. Every diagram is counted once with the correct symme-

try factor. If calculated to all orders, the results for physical quantities would be independent of these parameters. However, at any finite order in perturbation theory, they do depend on these parameters.

When we perform the shift (36), the free propagator takes the form

$$D(\omega_n, p) = \frac{1}{\omega_n^2 + \epsilon^2(p)} \begin{pmatrix} p^2 - Y & \omega_n \\ -\omega_n & p^2 - X \end{pmatrix}, \tag{180}$$

where

$$X = \mu_1 - 3\lambda v^2, \tag{181}$$

$$Y = \mu_1 - \lambda v^2, \tag{182}$$

$$\epsilon(p) = \sqrt{(p^2 - X)(p^2 - Y)}. \tag{183}$$

The mean-field thermodynamic potential is

$$\Omega_0 = -\mu_1 v^2 + \frac{1}{2} \lambda v^4. \tag{184}$$

The one-loop contribution to the thermodynamic potential reads

$$\Omega_1 = -\delta(\mu - \mu_1) v^2 + \frac{1}{2} \delta(g - \lambda) v^4$$
$$+ \frac{1}{2} \sum_P \ln[\omega_n^2 + (p^2 - X)(p^2 - Y)]. \tag{185}$$

The one-loop thermodynamic potential is then given by the sum of Eqs. (184) and (185). Setting $\delta = 1$, we obtain

$$\Omega_{0+1} = -\mu v^2 + \frac{1}{2} g v^4$$
$$+ \frac{1}{2} \sum_P \ln[\omega_n^2 + (p^2 - X)(p^2 - Y)]. \tag{186}$$

At this point, we would like to discuss the Goldstone theorem in connection with optimized perturbation theory. There is some confusion in the literature whether optimized perturbation theory violates Goldstone's theorem. Depending on the choice of the parameters μ_1 and λ, the mean-field dispersion relation $\epsilon(p)$ in Eq. (183) may or may not be gapless when evaluated at the minimum of the effective potential. Beyond the mean-field approximation, however, the dispersion relation is not given by Eq. (183), but rather by

$$\det[D_0^{-1}(\omega_n, p) - \Pi(\omega_n, p)] = 0, \tag{187}$$

where $D_0(\omega, p)$ is the propagator (6) and $\Pi(\omega_n, p)$ is the 2×2 self-energy matrix. The solution to Eq. (187) is gapless, order by order, in optimized perturbation theory. We can easily check this at the one-loop level. Differentiating the effective potential (186) with respect to the condensate and requiring that v be a stationary point yields

$$0 = -\mu + gv^2 + \frac{1}{2}\lambda \sum_P \frac{3(p^2 - Y) + (p^2 - X)}{\omega_n^2 + \epsilon^2(p)}$$

$$= -\mu + \Pi_{22}(0,0), \tag{188}$$

where $\Pi_{22}(0,0)$ is an imaginary-time version of Eq. (101) and corresponds to the self-energy diagrams displayed in Fig. 6. Equation (188) ensures that Goldstone's theorem is satisfied at one loop.

We next discuss various choices of the parameters μ_1 and λ. Although in principle they are arbitrary, from a physics point of view, some choices are better motivated than others. One requirement one might impose is that the results reduce in the limit $T \to 0$ to the results one obtains by applying the perturbative framework discussed in the previous section. One very simple choice is

$$\mu_1 = gv^2, \tag{189}$$

$$\lambda = g. \tag{190}$$

This choice leads to the dispersion relation (66). Another choice is motivated by the principle of minimal sensitivity, where one demands that the parameters satisfy

$$\frac{\partial \Omega}{\partial \mu_1} = 0, \tag{191}$$

$$\frac{\partial \Omega}{\partial \lambda} = 0. \tag{192}$$

At the one-loop level, the only solution to Eqs. (191) and (192) is the trivial solution $\mu_1 = \lambda = 0$ (Chiku, 2000). Only at higher orders are there nontrivial solutions. A very promising choice is

$$\mu_1 = \mu, \tag{193}$$

$$\lambda = T^{\mathrm{MB}}. \tag{194}$$

The many-body T matrix has several desirable features. Up to corrections of order $\sqrt{na^3}$, it reduces to the s-wave scattering length at $T = 0$. Thus the choice of Eqs. (193) and (194) will reproduce the results for the weakly interacting Bose gas at $T = 0$. Furthermore, it also takes into account medium effects by summing repeated two-particle scattering in the gas.

Relativistic ϕ^4 theory at finite temperature has been studied using optimized perturbation theory (Chiku and Hatsuda, 1998; Chiku, 2000). The one-loop calculation that was carried out (Chiku and Hatsuda, 1998) predicts a first-order phase transition, while the two-loop calculation (Chiku, 2000) predicts a second-order phase transition. Thus it is very likely that a two-loop calculation using optimized perturbation theory is capable of correctly describing this important aspect of the phase transition while incorporating the Goldstone theorem. Second, optimized perturbation theory provides an ideal framework for calculating the energy shifts and damping

rates of collective excitations of a Bose-Einstein condensate. Clearly, however, more work is needed.

In the paper by Haugset *et al.* (1998), the authors construct an improved one-loop thermodynamic potential by including the self-energy $\Pi_{22}(0,0)$ in the propagator. The calculation of the improved one-loop effective potential is equivalent to summing up all the ring diagrams, except that the two-loop diagram is counted twice. One must then subtract by hand the term that was overincluded. From the viewpoint of optimized perturbation theory, this overcounting comes about because the one-loop diagram with a self-energy insertion was omitted (in addition to the setting sun diagrams). Thus a consistent power counting according to the rules above is necessary to avoid problems with overcounting of Feynman diagrams.

C. Renormalization-group approach

One very powerful method of quantum field theory is the Wilson renormalization group (RG; Wilson and Kogut, 1974; Polchinski, 1984). The basic idea is to separate the momentum modes in the path integral into fast modes and slow modes by a cutoff. One then integrates out the fast modes. This yields an effective action for the slow modes, in which the coefficients of the original operators are renormalized and new operators are induced. By lowering the cutoff infinitesimally, one obtains a set of differential equations for the parameters in the effective action. Integrating out all modes down to $k = 0$ yields the full effective action.

Renormalization-group techniques have been applied to the homogeneous Bose gas at finite temperature by several authors (Bijlsma and Stoof, 1996a; Andersen and Strickland, 1999; Metikas and Alber, 2002). The first quantitative study was carried out by Bijlsma and Stoof. In that paper, they considered the one-loop diagrams that contribute to the effective chemical potential, effective four-point vertex, etc. By introducing a cutoff, as explained above, they derived a set of coupled differential equations. They then solved these equations numerically and obtained the condensate density as a function of the temperature and the critical temperature as a function of the s-wave scattering length. They also derived equations for the fixed points and calculated critical exponents.

A somewhat different renormalization-group approach was used by Andersen and Strickland (1999). It is based on a derivative expansion of the effective action $\Gamma[v]$ (Morris, 1994a, 1994b), which is obtained by integrating out the quantum and thermal fluctuations. If one imposes an infrared cutoff k, one can expand the corresponding effective action $\Gamma_k[v]$ as

$$\Gamma_k[v] = \int_0^\beta d\tau \int d^dx \left\{ V_k(v) + \frac{1}{2} i Z_k^{(1)}(v) \epsilon_{ij} v_i \frac{\partial}{\partial \tau} v_j \right.$$

$$\left. + \frac{1}{2} Z_k^{(2)}(v)(\nabla v_i)^2 + \cdots \right\}, \tag{195}$$

where $i,j = 1,2$, and repeated indices are summed over.

V_k is the effective potential, $Z_k^{(1)}$ and $Z_k^{(2)}$ are wave-function normalization constants, ϵ_{ij} is the Levi-Civita symbol, and v_i is the ith component of the condensate v. The dots indicate all higher-order terms in the derivative expansion. Here and in the following, the subscript k indicates a dependence on the infrared cutoff. By lowering the cutoff k, one obtains a set of coupled integral equations for the functions $V_k, Z_k^{(1)}, Z_k^{(2)}, \ldots$. The leading order in the derivative expansion is defined by setting the coefficients $Z_k^{(1)}$ and $Z_k^{(2)}$ to unity and the coefficients of all higher derivative operators in Eq. (195) to zero. This is called the *local-potential approximation*. In the following, we restrict ourselves to the local potential approximation and derive a flow equation for the effective potential $V_k(v)$.

1. One-loop effective potential

We are now ready to calculate quantum and thermal corrections to the classical potential. We compute the one-loop effective potential which we shall "RG improve" in Sec. IV.C.2. This method of deriving RG flow equations is conceptually and technically simpler than the direct application of exact or momentum-shell RG techniques (Andersen and Strickland, 1999).

The one-loop effective potential reads

$$V = V_0 + \frac{1}{2} \operatorname{Tr} \ln D^{-1}(\omega_n, p)$$

$$= -\mu v^2 + \frac{1}{2} g v^4 + \frac{1}{2} \sum_{\substack{\int \\ P}} \ln[\omega_n^2 + \epsilon^2(p)], \qquad (196)$$

where the mean-field potential has been denoted by $V_0 = -\mu v^2 + \frac{1}{2} g v^4$. We proceed by dividing the modes in the path integral into slow and fast modes separated by an infrared cutoff k. This is done by introducing a cutoff function $R_k(p)$, or *regulator*, which we keep general for the moment. We add the term

$$S_k[\psi_1, \psi_2] = -\int_0^\beta d\tau \int d^d x \frac{1}{2} R_k(\sqrt{-\nabla^2})$$

$$\times [\psi_1 \nabla^2 \psi_1 + \psi_2 \nabla^2 \psi_2], \qquad (197)$$

to the action Eq. (120). The argument p of the function $R_k(p)$ has been replaced by $\sqrt{-\nabla^2}$ in coordinate space. After performing the shift (36), we have the modified propagator

$$D_k(\omega_n, p) = \frac{1}{\omega_n^2 + \epsilon_k^2(p)} \begin{pmatrix} p^2[R_k(p)+1]+V_0' & \omega_n \\ -\omega_n & p^2[R_k(p)+1]+V_0'+2V_0''v^2 \end{pmatrix}, \qquad (198)$$

where a prime on V_0 denotes differentiation with respect to v^2. The modified dispersion relation is

$$\epsilon_k(p) = \sqrt{\{p^2[R_k(p)+1]+V_0'\}}$$

$$\times \sqrt{\{p^2[R_k(p)+1]+V_0'+2V_0''v^2\}}. \qquad (199)$$

By a judicious choice of $R_k(p)$, we can suppress the low-momentum modes in the path integral and leave the high-momentum modes essentially unchanged. It is useful to introduce a *blocking function* $f_k(p)$ which is defined by

$$R_k(p) = \frac{1 - f_k(p)}{f_k(p)}. \qquad (200)$$

The blocking function satisfies

$$\lim_{p \to 0} f_k(p) = 0, \quad \lim_{p \to \infty} f_k(p) = 1. \qquad (201)$$

These properties ensure that the low-momentum modes are suppressed by making them very heavy, while the high-momentum modes are left essentially unchanged. Typical blocking functions are shown in Fig. 12.

The sharp cutoff function $R_k(p)$ is defined by the blocking function $f_k(p) = \theta(p-k)$, and is shown in Fig. 12 (solid line). It provides a sharp separation between fast and slow modes. When the sharp cutoff is used, the slow modes become completely suppressed in the path

integral, while the fast modes are completely unaltered. The advantage of using a sharp cutoff is that certain integrals can be done analytically, and the integro-differential RG equation is reduced to a differential RG equation.

The solutions to approximate renormalization-group equations (e.g., the truncation of the derivative expansion at some finite order) depends on the regulator function $R_k(p)$. There have been several papers on the optimal choice of the cutoff function (Andersen and Strickland, 1999; Litim, 2000, 2001). Here we consider the class of smooth blocking functions

$$f_k^m(p) = \frac{p^m}{p^2 + k^m}. \qquad (202)$$

In the limit $m \to \infty$, we recover the sharp blocking function. In Sec. IV.C.3, we shall see that a smooth regulator is better than the sharp one, but it comes at the expense of more complicated numerics.

We return to the one-loop effective potential in Eq. (196). Using the inverse propagator $D_k^{-1}(\omega_n, p)$, we find that the modified one-loop effective potential becomes

$$V_k = V_0 + \frac{1}{2} \sum_{\substack{\int \\ P}} \ln[\omega_n^2 + \epsilon_k^2(p)]. \qquad (203)$$

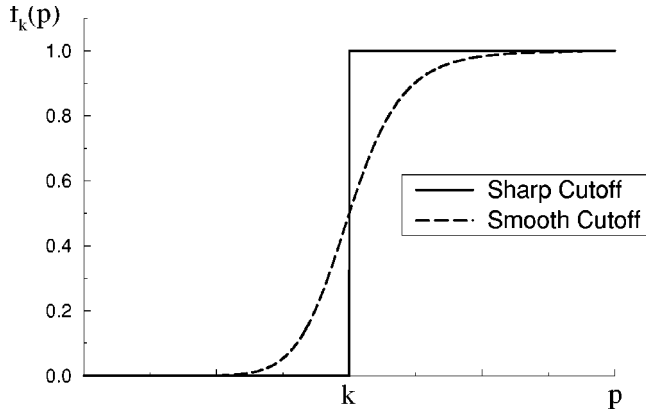Upon summation over the Matsubara frequencies, we obtain

FIG. 12. Typical balancing function: solid line, sharp blocking function; and dashed line, a typical smooth blocking function.

$$V_k = V_0 + \int \frac{d^d p}{(2\pi)^d} \left\{ \frac{1}{2} \epsilon_k(p) + T \ln[1 - e^{-\beta \epsilon_k(p)}] \right\}.$$

(204)

The first term in the brackets is the $T=0$ part and represents the zero-point fluctuations. The second term includes thermal effects. Differentiation with respect to the infrared cutoff k yields

$$k \frac{\partial}{\partial k} V_k = -k \int \frac{d^d p}{(2\pi)^d} \left(\frac{\partial R_k(p)}{\partial k} \right) \frac{1}{2\epsilon_k(p)}$$
$$\times \{1 + 2n[\epsilon_k(p)]\} \{p^2[R_k(p)+1] + V_0'$$
$$+ V_0'' v^2\}.$$

(205)

Equation (205) is an integro-differential equation for the one-loop effective potential. It is obtained by integrating out each mode independently, where the feedback from the fast modes to the slow modes is completely ignored. Since all modes are integrated out independently, this is sometimes called the *independent-mode approximation* (Liao and Strickland, 1995). The lack of feedback leads to a poor tracking of the effective degrees of freedom. The situation is remedied by applying the renormalization group, which effectively sums up important classes of diagrams.

2. Renormalization-group improvement

The easiest way of deriving the RG-improved version of Eq. (205) is simply to make it self-consistent by replacing V_0 by V_k everywhere. This yields

$$k \frac{\partial}{\partial k} V_k = -k \int \frac{d^d p}{(2\pi)^d} \left(\frac{\partial R_k(p)}{\partial k} \right) \frac{1}{2\epsilon_k(p)}$$
$$\times \{1 + 2n[\epsilon_k(p)]\} \{p^2[R_k(p)+1] + V_k'$$
$$+ V_k'' v^2\},$$

(206)

where the RG-improved dispersion relation is

$$\epsilon_k(p) = \sqrt{\{p^2[R_k(p)+1] + V_k'\}}$$
$$\times \sqrt{\{p^2[R_k(p)+1] + V_k' + 2V_k'' v^2\}},$$

(207)

and the primes in Eqs. (206) and (207) again denote differentiation with respect to v^2. The self-consistent equation (206) is not a perturbative approximation, but is exact to leading order in the derivative expansion. This equation has been rigorously derived using the path-integral representation and the derivative expansion of the effective action (Andersen and Strickland, 1999). There are other ways of regulating the one-loop expression (196) and subsequently "RG-improving" it. However, they do not always resum perturbation theory correctly (with all higher-order diagrams included and all combinatorical coefficients correct). These issues have been studied in detail by Litim and Pawlowski (2002; see also Canet *et al.*, 2003).

Note that since $V_{k=0}'$ vanishes at the minimum of the effective potential, the dispersion relation in the broken phase reduces to

$$\epsilon_{k=0}(p) = p \sqrt{p^2 + 2V_{k=0}'' v^2}.$$

(208)

Thus the Goldstone theorem is automatically satisfied for temperatures below T_c.

In the calculations that follow, we shall restrict ourselves to using a sharp cutoff function. The integral over p in Eq. (206) can be done analytically, resulting in a differential RG equation. In this case, Eq. (206) reduces to

$$k \frac{\partial}{\partial k} V_k = -\frac{1}{2} S_d k^d \{\epsilon(k) + 2T \ln[1 - e^{-\beta\epsilon(k)}]\},$$

(209)

where

$$S_d = \frac{\Omega_d}{(2\pi)^d},$$

(210)

and Ω_d is the area of a d-dimensional sphere whose expression is given in the Appendix.

Since the factor $\partial R_k(p)/\partial k$ forces $p=k$, we have defined $\epsilon(k) = \epsilon_k(p=k)$, where the dispersion relation $\epsilon(k)$ is

$$\epsilon(k) = \sqrt{[k^2 + V_k'][k^2 + V_k' + 2V_k'' v^2]}.$$

(211)

In order to solve Eq. (209), one must impose the correct boundary condition on the effective potential V_k. For $k = \infty$, no modes have been integrated out and V_k reduces to the classical potential V_0. In practice, one must impose the boundary condition at a large but finite value $k = \Lambda$.

Equation (209) has been solved numerically for the effective potential $V_{k=0}(v)$ with the above boundary condition in $d=3$ dimensions for different values of T, as shown in Fig. 13. We have normalized the condensate v as well as the effective potential by the appropriate powers of the ultraviolet cutoff Λ. The curves clearly show that the phase transition is second order. For $T < T_c$, the effective potential has a small imaginary part, and we have shown only the real part in Fig. 13. The imaginary part of the effective potential does, however, vanish for $T \geq T_c$. The effective chemical potential $\mu_{k=0}$ as well as the effective quartic coupling constant $g_{k=0}$ are shown in Fig. 14, and both quantities vanish at the
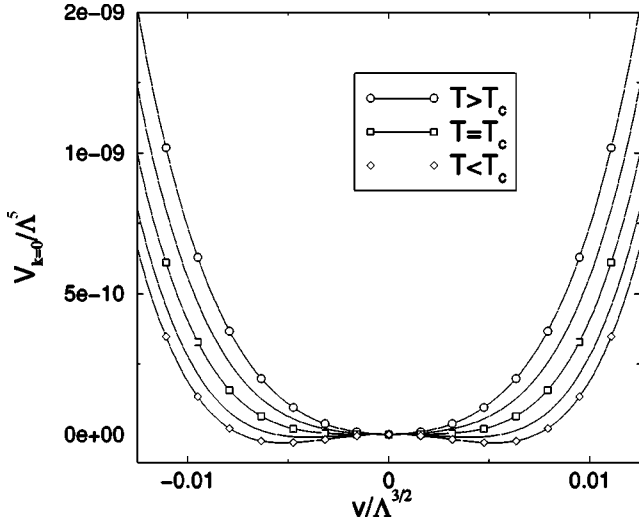
FIG. 13. Real part of the RG-improved effective potential $V_{k=0}(v)$ for various values of the temperature. The phase transition is clearly second order.

critical point. The corresponding operators are relevant and must therefore vanish at T_c, and we see that the renormalization-group approach correctly describes the behavior near criticality. Moreover, it can be shown that the sextic coupling $g_{k=0}^{(6)}$ goes to a nonzero constant at the critical temperature.

3. Critical behavior and critical exponents

In order to investigate critical behavior near fixed points, we write the flow equation in dimensionless form using the dimensionless quantities

$$\bar{\beta} = \beta k^2 \tag{212}$$

$$\bar{v} = \beta^{1/2} k^{(2-d)/2} v \tag{213}$$

$$\bar{V}_k = \beta k^{-d} V_k, \tag{214}$$

$$\bar{\epsilon}(k) = k^{-2}\epsilon(k). \tag{215}$$
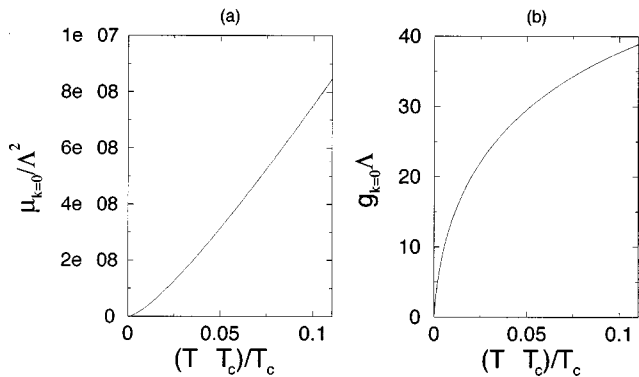
Equation (209) can then be written as

FIG. 14. The effective chemical potential $\mu_{k=0}$ and the effective quartic coupling $g_{k=0}$ near the critical temperature. Both vanish at T_c.

$$0 = \left[k\frac{\partial}{\partial k} - \frac{1}{2}(d-2)\bar{v}\frac{\partial}{\partial \bar{v}} + d \right]\bar{V}_k$$
$$+ \frac{1}{2}S_d\bar{\beta}\bar{\epsilon}(k) + S_d \ln[1 - e^{-\bar{\beta}\bar{\epsilon}(k)}]. \tag{216}$$

The *critical potential* is obtained by setting to zero the derivative with respect to k in Eq. (216). Expanding in powers of $\bar{\beta}\bar{\epsilon}(k)$, we obtain

$$\left[-\frac{1}{2}(d-2)\bar{v}\frac{\partial}{\partial \bar{v}} + d \right]\bar{V}_k = -\frac{1}{2}S_d\bar{\beta}\bar{\epsilon}(k) - S_d \ln[\bar{\beta}\bar{\epsilon}(k)]. \tag{217}$$

Taking the limit $\bar{\beta} \to 0$ and ignoring the term which is independent of v leads to

$$\left[-\frac{1}{2}(d-2)\bar{v}\frac{\partial}{\partial \bar{v}} + d \right]\bar{V}_k = -\frac{1}{2}S_d(\ln[1 + \bar{V}'_k]$$
$$+ \ln[1 + \bar{V}'_k + 2\bar{V}''_k\bar{v}^2]). \tag{218}$$

This is the same equation as obtained by Morris (1998) for a relativistic O(2)-symmetric scalar theory in d dimensions to leading order in the derivative expansion. Therefore the results for the critical behavior at leading order in the derivative expansion will be the same as those obtained in the d-dimensional O(2) model at zero temperature.

The above also demonstrates that the system behaves as a d-dimensional one as the temperature becomes much higher than any other scale in the problem. Thus the system goes from being $(d+1)$ dimensional at low temperature to being effectively d dimensional at high temperature, and this is often called *dimensional cross-over*. It is also referred to as dimensional reduction. The nonzero Matsubara modes decouple, and the system can be described in terms of a classical field theory for the $n=0$ modes in d dimensions (Landsman, 1989). We return to this subject in Sec. V, where we discuss the calculation of the critical temperature of a dilute Bose gas.

The RG equation (206) satisfied by $V_k[v]$ is highly nonlinear, and a direct measurement of the critical exponents from the numerical solutions is very time consuming. This becomes even worse as one goes to higher orders in the derivative expansion, and so it is important to have an additional reliable approximation scheme for calculating critical exponents. In the following we perform a polynomial expansion (Nicoll *et al.*, 1974) of the effective potential, expand around $v=0$, and truncate at Nth order:

$$V_k = -\mu_k v^2 + \frac{1}{2}g_k v^4 + \sum_{n=3}^{N} \frac{g_k^{(2n)}}{n!} v^{2n}. \tag{219}$$

The polynomial expansion turns the partial differential equation (209) into a set of coupled ordinary differential equations. In order to demonstrate the procedure we shall show how the fixed points and critical exponents are calculated at the lowest nontrivial order of trunca-

tion ($N=2$). We write the equations in dimensionless form using Eqs. (212)–(215) and

$$\bar{\mu}_k = k^{-2}\mu_k, \quad \bar{g}_k = \beta^{-1}k^{d-4}g_k. \tag{220}$$

We then obtain the following set of equations:

$$k\frac{\partial}{\partial k}\bar{\mu}_k = -2\bar{\mu}_k + S_d\bar{\beta}\bar{g}_k\{1+2n[\bar{\epsilon}(k)]\} \tag{221}$$

$$k\frac{\partial}{\partial k}\bar{g}_k = (d-4)\bar{g}_k + S_d\bar{\beta}\bar{g}_k^2\left[\frac{1}{2(1-\bar{\mu}_k)}\{1+2n[\bar{\epsilon}(k)]\}\right.$$

$$\left. +\bar{\beta}n[\bar{\epsilon}(k)]\{1+n[\bar{\epsilon}(k)]\}\right]. \tag{222}$$

A similar set of equations was first obtained by Bijlsma and Stoof (1996a) by considering the one-loop diagrams that contribute to the running of the effective chemical potential, the effective quartic coupling constant, etc.

The equations for the fixed points are

$$k\frac{\partial}{\partial k}\bar{\mu}_k = 0, \quad k\frac{\partial}{\partial k}\bar{g}_k = 0. \tag{223}$$

If we introduce the variables r and s through the relations

$$r=\frac{\bar{\mu}_k}{1-\bar{\mu}_k}, \quad s=\frac{\bar{g}_k}{(1-\bar{\mu}_k)^2}, \tag{224}$$

and expand the equations in powers of $\bar{\beta}(1-\bar{\mu}_k)$, the RG equations can be written as

$$\frac{\partial r}{\partial k} = -2[1+r][r-S_d s], \tag{225}$$

$$\frac{\partial s}{\partial k} = -s[4-d+4r-9S_d s]. \tag{226}$$

We have the trivial Gaussian fixed point $(r,s)=(0,0)$ as well as the infinite-temperature Gaussian fixed point $(-1,0)$. Finally, for $d<4$ there is the infrared Wilson-Fisher fixed point $((4-d)/5,(4-d)/(5S_d))$ (Wilson and Kogut, 1974).

Setting $d=3$ and linearizing Eq. (225) around the fixed point, we find the eigenvalues $(\lambda_1,\lambda_2)=(-1.278,1.878)$. The critical exponent ν is given by the inverse of the largest eigenvalue: $\nu=1/\lambda_2=0.532$. This procedure can now be repeated including a larger number N of terms in the expansion Eq. (219). The result for ν is plotted in Fig. 15 as a function of the number of terms in the polynomial expansion (dashed line). Our result agrees with that of Morris, who considered the relativistic O(2) model in $d=3$ at zero temperature (Morris, 1998). The critical exponent ν oscillates around the average value 0.73. The value of ν never converges as $N\to\infty$, but continues to fluctuate. For comparison, we have also showed the results using the smooth regulator function (202) with $m=5$. Clearly, the convergence properties have improved signficantly.

Our result should be compared to experiment on ^{4}He and the ϵ expansion, which both give a value of 0.67 (Zinn-Justin, 1989). The result $\nu=0.73$ is a leading-order
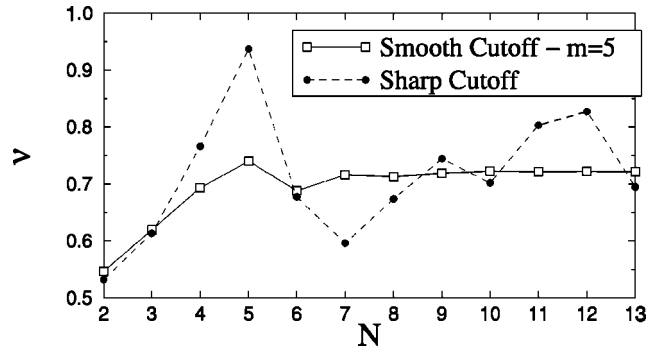

FIG. 15. The critical exponent ν as a function of number of terms N in the polynomial expansion.

result in the derivative expansion of the effective action (195). The next-to-leading order in the derivative expansion involves a set of coupled equations for the potential V_k and the wave-function normalization terms $Z_k^{(1)}$ and $Z_k^{(2)}$. These equations were derived by Morris (1998). A calculation of the critical exponent gives a value of $\nu=0.65$. One expects the critical exponent ν to converge towards 0.67 as one includes more terms in the derivative expansion.

We close this section by comparing the two approaches discussed here (Bijlsma and Stoof, 1996a; Andersen and Strickland, 1999). The renormalization-group equation (209) that we obtained in the local potential approximation is highly nonlinear. We made a further approximation by expanding the effective potential in a power series, which turns the partial differential equation (209) into a set of coupled ordinary differential equations. These flow equations were first obtained by Bijlsma and Stoof (1996a) by considering the one-loop diagrams that contribute to the various n-point functions, while neglecting their momentum dependence. However, the two sets of RG equations differ if one includes the momentum dependence of the one-loop graphs and goes beyond the local potential approximation (Liao and Strickland, 1995; Andersen and Strickland, 1999).

D. Beliaev-Popov approximation

In Sec. III.B, we discussed in some detail the Beliaev approximation at zero temperature. We recall that this approximation is defined by all one-loop diagrams contributing to the self-energies. It was shown that the resulting dispersion relation is gapless. Popov (1983) generalized the Beliaev approximation to finite temperature, and hence it is often called the Beliaev-Popov approximation (Shi and Griffin, 1998). He calculated the one-loop diagrams in the limit of zero external energy and momentum. However, one has to be careful because the limits $\omega\to0,\mathbf{p}\to0$ and $\mathbf{p}\to0,\omega\to0$ do not commute at finite temperature. Later, Shi and Griffin gave a detailed discussion of the Beliaev-Popov approximation and explicit formal expressions for the normal and anomalous self-energies at finite temperature and arbitrary external energy ω and momentum $\mathbf{p}$. An analy-

sis of the Beliaev-Popov approximation similar to the one presented at zero temperature in Sec. III would probably be significantly simpler. For instance, it follows immediately from the finite-temperature version of Eq. (104) that the chemical potential is free of the infrared divergences that separately plague the expressions for $\Sigma_{11}(0,0)$ and $\Sigma_{12}(0,0)$. The expression for the chemical potential is

$$\mu = gv^2 + \frac{1}{2}g \sum_P \frac{4p^2 - 4\mu + 6gv^2}{\omega_n^2 + \epsilon^2(p)}$$

$$= gv^2 + \frac{1}{4}g[3I_{1,1} + I_{-1,-1}]$$

$$+ \frac{1}{2\pi^2}g \int_0^\infty dp \frac{p^2(2p^2 - 2\mu + 3gv^2)}{\epsilon(p)} n[\epsilon(p)].$$

(227)

In the high-temperature limit, where $\beta g v^2 \ll 1$, one finds

$$\mu = gv^2 \left[1 - \frac{3}{8\pi^2} \frac{T}{gv^2} \sqrt{2g^3v^2} \right].$$

(228)

Thus at high temperature, the dimensionless expansion parameter has an extra factor of T/gv^2 compared to the zero-temperature case, where it is $\sqrt{g^3v^2}$.

So far our description of the dilute Bose gas has been in terms of spontaneous breaking of the U(1) symmetry and has used a chemical potential to ensure that the mean number of particles is constant. There exist alternative approaches that are number conserving. Such an approach was first introduced by Giradeau and Arnowitt as early as in 1959 (Giradeau and Arnowitt, 1959). This approach is variational in nature and, like the HFB approximation, it exhibits a gap in the dispersion relation. However, it was later shown by Takano (1961) that the gap is removed if one takes into account cubic terms in the Hamiltonian in a consistent manner. More recently, Morgan (1999) discussed in detail number-conserving approaches and generalized them to trapped Bose gases. The starting point is the Hamiltonian, including interaction terms describing binary collisions written in terms of pair operators that conserve particle number. These operators are defined by

$$\alpha_i = \beta_0^\dagger a_i,$$

(229)

where a_i are the standard annihilation operators and $\beta_0 = (1 + a_0^\dagger a_0)^{-1/2} a_0$. The Hamiltonian can then be divided into terms containing zero, one, two, three, and four creation/annihilation operators. The terms that contain up to two operators are then diagonalized, while the cubic and quartic terms are treated as perturbations using first- and second-order perturbation theory. The validity of perturbation theory is the usual requirement that $\sqrt{na^3} \ll 1$ at $T=0$. At high temperature, it follows from Eq. (228) that the requirement be $T\sqrt{g^3v^2}/gv^2 \ll 1$. In the zero-temperature limit, the calculations reproduce several known results presented in Sec. III. The Hamiltonian can be used to calculate the ground-state energy density $\mathcal{E}$ (rather than the free-energy density $\mathcal{F}$),

and a calculation involving the quadratic terms yields the result of Bogoliubov given in Eq. (91). A second-order calculation reproduces the $na^3 \ln(na^3)$ term of Wu (1959), but one is faced with a logarithmic ultraviolet-divergent term which is proportional to na^3. As we argued in Sec. III.E, the correct way to treat this divergence is to absorb it in the coefficient of the operator $(\psi^*\psi)^3$, which represents $3 \rightarrow 3$ scattering. The approach also reproduces Beliaev's results for the phonon spectrum (106) and the damping rate (111). Finally, we mention that the modified Popov approximation (Hutchinson et al., 1998; Proukakis et al., 1998) has also been examined within the framework of number-conserving approaches (Morgan, 1999).

V. CALCULATIONS OF T_c

The critical temperature for an ideal Bose gas is given by Eq. (16). A natural question to ask is: what is the leading-order effect of a weak two-body interaction on the critical temperature of a homogeneous Bose gas? This question has been around for almost 50 years, but only very recently has the issue been settled. It has been discussed in detail by Baym et al. (1999, 2001), and we follow their paper to some extent. Various approaches to the problem have also been discussed very recently by Haque (2003).

In the following, we assume that the interaction is repulsive, which corresponds to a positive scattering length a. One might think that the effect of a repulsive interaction is to decrease the critical temperature of a Bose gas. For instance, the superfluid transition in liquid ^{4}He takes place at a lower temperature than that of an ideal gas of the same density. However, liquid ^{4}He is not weakly interacting, and it turns out that the leading effect of the interactions in the dilute Bose gas is to increase T_c.

The first paper in which a quantitative prediction appears is by Lee and Yang (1957). In that paper, the authors predict that the critical temperature increases compared to that of an ideal Bose gas and that the increase is proportional to $\sqrt{a}$. Later, the same authors predicted that the shift is linear with a (Lee and Yang, 1958). This prediction was purely qualitative, since neither sign nor magnitude were given. A couple of years later, Glassgold et al. (1960) also predicted an increase of T_c proportional to $\sqrt{a}$. A couple of decades later, the problem was revisited by Toyoda (1982). He predicted a decrease of the critical temperature proportional to $\sqrt{a}$. Since the sign agrees with the measurements on ^{4}He, there seemed to be at least qualitative agreement between theory and experiment. Long ago, Huang claimed an increase in T_c proportional to $a^{3/2}$ (Huang, 1964), and, very recently, he has claimed in another paper that T_c increases proportional to $\sqrt{a}$ (Huang, 1999). From this selection of papers, it is clear that there has been considerable confusion about how T_c depends parametrically on the scattering length. What these, as well as other attempts to calculate T_c (Schakel, 1994; Wilkens

et al., 2000) have in common, is that they are based on perturbation theory. However, Bose condensation in a dilute gas is governed by long-distance physics that is inherently nonperturbative. These issues will be discussed later.

There have also been other approaches to the calculation of T_c. Bijlsma and Stoof have carried out renormalization-group calculations of the critical temperature (Bijlsma and Stoof, 1996a). This approach was discussed in the previous section, and it predicts that the leading shift is proportional to $a \ln a$. Since this approach is purely numerical, it is difficult to take the limit $a \to 0$ and thus obtain the correct dependence on a in the dilute limit. Very recently, there was a calculation of T_c based on the exact renormalization group by Ledowski, Hasselmann, and Kopietz (2003). They calculated the momentum-dependent two-point function and showed that the leading behavior is proportional to the scattering length a.

The first Monte Carlo simulations for hard-sphere bosons in the low-density regime were done by Grüter *et al.* (1997). In that paper, the authors predicted a positive linear shift after extrapolating to the limit $a \to 0$. This result was somewhat surprising since some early Monte Carlo simulations, as well as the experiments on ^{4}He, show a decrease in T_c due to repulsive interactions. Later, it was shown rigorously, using effective-field-theory methods, that the parametric dependence of T_c is indeed linear in a (Baym *et al.*, 1999, 2001). Thus in the dilute limit, we can write

$$\frac{\Delta T_c}{T_c^0} = c n^{1/3} a, \tag{230}$$

where c is a constant that is to be determined. The problem of determining the constant c has been attacked by analytical as well as numerical methods in recent years. These methods include high-precision Monte Carlo simulations, $1/N$ expansions, self-consistent calculations involving summation of bubble and ladder diagrams, and variational perturbation theory. We shall discuss these in Secs. V.B.1–V.B.3.

A. Hartree-Fock approximation and breakdown of perturbation theory

In this subsection, we shall briefly discuss the Hartree-Fock approximation and show that it predicts no shift in the critical temperature. We approach the phase transition from above, so the condensate density v is zero.

In an ideal gas, the number density of excited particles is given by Eq. (13), which can be written as

$$n_{\mathrm{ex}} = \frac{1}{\lambda_T^3} g_{3/2}(z), \tag{231}$$

where the function $g(z)$ is the polylogarithmic function

$$g_l(z) = \sum_{n=1}^{\infty} \frac{z^n}{n^l}, \tag{232}$$
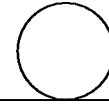
and $z = e^{\beta\mu}$ is the fugacity.

FIG. 16. Self-energy diagram in the Hartree-Fock approximation.

The simplest way to include the effects of interactions is to include the self-energy in the Hartree-Fock approximation. The Feynman graph is the tadpole diagram shown in Fig. 16. The tadpole is independent of the external momentum, and the expression for the Hartree-Fock self-energy is

$$\Sigma_{\mathrm{HF}} = 2g \sum_P \!\!\!\!\!\!\!\!\!\!\!\!\int \frac{p^2 - \mu}{\omega_n^2 + (p^2 - \mu)^2} = 2gn, \tag{233}$$

where we have used Eqs. (13) and (A30). Thus a particle with momentum **p** effectively has the energy $\epsilon(p) = p^2 + 2gn$, where the term $2gn$ arises from the mean field of the other particles. We can now generalize Eq. (231) by writing

$$n = \frac{1}{\lambda_T^3} g_{3/2}(e^{\beta(\mu - 2gn)}). \tag{234}$$

Equation (234) shows that we must increase the chemical potential by an amount $\Delta\mu = \Sigma_{\mathrm{HF}}$ to keep the same number density as that of an ideal gas at the same temperature. It shows in particular that μ must approach Σ_{HF} from below to obtain the critical number density at a given temperature. Thus the critical temperature remains the same. The conclusion is that including a constant mean-field shift in the single-particle energies cannot change the critical temperature of a Bose gas. This is an example of the fact that mean-field theories effectively treat interacting gases as ideal gases with modified parameters and thus predict the same T_c.

Calculations using the Hartree-Fock approximation have been carried out by Huang (1999). He applies a virial expansion to Eq. (234) and obtains a change in the critical temperature which is proportional to $a^{1/2}$. However, this is an artifact of the approximation, as can be seen by including more terms in the expansion. This was discussed in some detail by Baym (1999, 2001). A correct treatment was given by Pethick and Smith (2002). Similarly, the summation of ring diagrams (Haugset *et al.*, 1998) in the effective potential does not change T_c. The reason is that these diagrams are evaluated at zero external momentum and therefore merely correspond to a redefinition of the chemical potential.

We have seen that a leading perturbative calculation in the scattering length a gives no corrections to the critical temperature of a dilute Bose gas. One might try to improve on this result by going to higher orders in perturbation theory. The Feynman diagrams contributing to the self-energy at second order in perturbation theory are shown in Fig. 17.

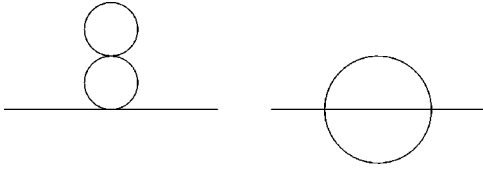If we focus on the contribution from the $n=0$ Matsubara mode, the diagrams read

FIG. 17. Two-loop self-energy diagrams.

$$\Sigma^{2a}(0,\mathbf{p}) = -4g^2T^2 \int \frac{d^dk}{(2\pi)^d} \int \frac{d^dq}{(2\pi)^d}$$

$$\times \frac{1}{(k^2-\mu)(q^2-\mu)^2}, \qquad (235)$$

$$\Sigma^{2b}(0,\mathbf{p}) = -2g^2T^2 \int \frac{d^dk}{(2\pi)^d} \int \frac{d^dq}{(2\pi)^d}$$

$$\times \frac{1}{(k^2-\mu)(q^2-\mu)(|\mathbf{p}+\mathbf{q}+\mathbf{k}|^2-\mu)}, \qquad (236)$$

where the chemical potential acts as an infrared cutoff in the integral. The left diagram is independent of the external momentum. If we use the mean-field criterion that $\mu \to 0$ at the transition, the integral is linearly divergent in the infrared. The right diagram depends on the external momentum $\mathbf{p}$. For $\mu=0$, it is logarithmically divergent as the external momentum goes to zero. As one goes to higher orders in the perturbation expansion, the diagrams become increasingly infrared divergent for $\mu=0$. If we denote a generic self-energy diagram with n loops by Σ_n, we have (Baym $et\ al.$, 1999, 2001)

$$\Sigma_n \sim T\left(\frac{a}{\lambda_T}\right)^2 \left(\frac{a^2}{\mu\lambda_T^4}\right)^{(n-2)/2}. \qquad (237)$$

This shows that perturbation theory breaks down in the critical region due to infrared divergences. Physically, these infrared divergences are screened, and this can be taken into account by summing certain classes of diagrams from all orders of perturbation theory. An example of this is the summation of bubble or ladder diagrams. We return to this issue at the end of this section.

B. Dimensional reduction

In Sec. IV.C, we saw that the renormalization-group equations at high temperature reduce to those of a three-dimensional O(2)-symmetric theory. This is an example of dimensional reduction and, for the dilute Bose gas, it can be understood as follows. In the imaginary time formalism, the fields are decomposed into modes that are characterized by their Matsubara frequency $\omega_n = 2\pi nT$. At distances much larger than the thermal wavelength, and for temperatures sufficiently close to the critical temperature, the time-derivative term for $n \neq 0$ is much larger than both the kinetic-energy term and the effective chemical potential term. This implies that the nonstatic Matsubara modes decouple, and the long-distance physics can be described in terms of an effective

three-dimensional field theory for the $n=0$ mode. The fact that the long-distance physics associated with the phase transition is well separated from the typical momentum scale T associated with the nonzero Matsubara modes makes effective-field-theory methods ideal for studing the phase transition.

An effective three-dimensional theory that describes the long-distance physics can be constructed using the methods of effective field theory (Georgi, 1993). Once the symmetries of the theory have been identified, one writes down the most general Lagrangian $\mathcal{L}_{\text{eff}}$ that is consistent with these symmetries. In the present case, we simply have a complex scalar field with an O(2) symmetry. In addition, there is a three-dimensional rotational symmetry. The effective three-dimensional theory is then described by the action

$$S_{\text{eff}} = \int d^3x \left[-\frac{1}{2}\phi^*\nabla^2\phi + \frac{1}{2}\mu_3\phi^*\phi \right.$$
$$\left. + \frac{1}{24}u(\phi^*\phi)^2 + \cdots \right], \qquad (238)$$

where we have used the conventional normalization of an O(2)-invariant theory. The dots indicate operators with more derivatives and more fields. Examples are $[\nabla(\phi^*\phi)]^2$ and $(\phi^*\phi)^3$. The relation between the parameters in the effective theory and in the full theory can be determined by perturbative matching; one requires that the effective theory (238) reproduce static correlators at long distances $R \gg 1/T$ to a specified accuracy. The reason why the parameters of the effective three-dimensional theory can be determined in perturbation theory is that the coefficients of the effective theory encode the short-distance physics at the scale T, which is perturbative, and that the matching procedure does not involve the nonperturbative long-distance physics.

At the tree level, the matching can be done simply by inspection. By comparing the action (120) that describes the full four-dimensional theory with the action (238) that describes the effective three-dimensional theory, we can read off the relation between the fields in the two theories. This yields

$$\psi = \sqrt{\frac{T}{2}}\phi. \qquad (239)$$

Similarly, by matching the other terms in the action in the two theories at the tree level and using Eq. (239), one easily finds

$$\mu_3 = -\mu, \qquad (240)$$

$$u = 3gT. \qquad (241)$$

Higher-order operators, as well as corrections to the coefficients of the operators in Eq. (238), can be ignored at the order of interest in the diluteness expansion. For instance, the coefficient of the operator $[\nabla(\phi^*\phi)]^2$ is proportional to a^2/λ_T. From dimensional analysis, it follows that the contribution to physical quantities from this operator is then suppressed by a factor of $n^{1/3}a$ com-

pared to the operator $(\phi^*\phi)^2$. The contribution to physical quantities from other operators are analyzed in a similar manner.

For an ideal Bose gas, the critical temperature is given by Eq. (16). Equivalently, the critical number density n_c^0 at fixed temperature satisfies $n_c^0\lambda_T^3=\zeta(\frac{3}{2})$. Due to the repulsive interactions in the dilute Bose gas, the critical number density changes. The first-order change in the critical temperature $\Delta T_c=T_c-T_c^0$ is related to the first-order change $\Delta n_c=n_c-n_c^0$ in the critical number density at fixed T_c by (Baym *et al.*, 1999, 2001)

$$\frac{\Delta T_c}{T_c^0}=-\frac{2}{3}\frac{[n_c(T_c)-n_c^0(T_c)]}{n}$$

$$=-\frac{1}{3}\frac{T^0\Delta\langle\phi^*\phi\rangle}{n_c^0}. \qquad (242)$$

The factor 2/3 in the first line comes from the relation $T^0\propto(n^0)^{2/3}$. The last equality follows from the fact that $n=\langle\psi^*\psi\rangle$ and that the contribution from the zeroth Matsubara mode is $\frac{1}{2}T\langle\phi^*\phi\rangle$, which follows from Eq. (239).

In order to calculate the critical temperature, we must evaluate the quantity $\Delta\langle\phi^*\phi\rangle$. We discuss this next.

1. $1/N$ expansion

The $1/N$ expansion is a nonperturbative method that has been widely used in high-energy and condensed-matter physics (Bréźin and Wadia, 1993; Moshe and Zinn-Justin, 1998). In condensed-matter physics, it has been used to study the critical behavior of $O(N)$ spin models and calculate their critical exponents (Zinn-Justin, 1989). The idea is to generalize a Lagrangian with a fixed number of fields to N fields, and then let N be a variable. The expansion is defined as an expansion in powers of $1/N$ while gN is held fixed (g is the coupling constant). The method is nonperturbative in the sense that, for calculations at every order in $1/N$, there are Feynman diagrams contributing from all orders of perturbation theory. In this way, one sums up graphs from all orders of perturbation theory. One hopes that this expansion captures some of the essential physics that cannot be captured by perturbative methods.

The critical temperature was recently calculated by Baym, Blaizot, and Zinn-Justin (Baym *et al.*, 2000) in

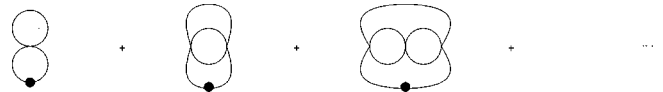FIG. 18. Three-loop Feynman diagrams contributing to $\Delta\langle\phi^2\rangle$.

FIG. 19. Feynman diagrams contributing to $\Delta\langle\phi^2\rangle$ to leading order in $1/N$.

the large-N limit. The next-to-leading-order result was obtained by Arnold and Tomášik (2000).

In the present case, the Lagrangian (238) is generalized to a scalar field theory with N real components. The Lagrangian is now $O(N)$ invariant and reads

$$\mathcal{L}_{\text{eff}}=-\frac{1}{2}\phi_i\nabla^2\phi_i+\frac{1}{2}\mu_3\phi_i^2+\frac{1}{24}u(\phi_i\phi_i)^2, \qquad (243)$$

where i runs from 1 to N. Summation over i is implicitly understood. The large-N limit is obtained by taking $N\to\infty$, while keeping uN constant.

Generally, the diagrams that contribute to $\Delta\langle\phi^2\rangle$ can be obtained from vacuum diagrams by inserting an operator ϕ^2. For example, at the three-loop level there are two diagrams that contribute, and they are shown in Fig. 18. The solid circle denotes an insertion of the operator ϕ^2. It can be shown that the first diagram is suppressed by a factor of $1/N$ relative to the second.

The Feynman diagrams that contribute to $\Delta\langle\phi^2\rangle$ at leading order in $1/N$ are shown in Fig. 19. These diagrams are called bubble diagrams, and the bubble summation is thus exact in the large-N limit. The expression for the expectation value $\Delta\langle\phi_i^2\rangle$ then becomes

$$\Delta\langle\phi_i^2\rangle=-N\int\frac{d^dp}{(2\pi)^d}\frac{1}{p^4}\Sigma(p), \qquad (244)$$

where $\Sigma(p)$ is the self-energy. The Feynman diagrams for the self-energy are obtained from those in Fig. 19 by cutting the propagator line that goes through the solid circles. The self-energy diagrams are shown in Fig. 20.

After mass renormalization, so that $\Sigma(0)=0$, the expression for the self-energy is (Zinn-Justin, 1989)

$$\Sigma(p)=\frac{2}{N}\int\frac{d^dk}{(2\pi)^d}\frac{1}{6/Nu+\mathcal{T}_1(k)}\left[\frac{1}{|\mathbf{p}+\mathbf{k}|^2}-\frac{1}{k^2}\right], \qquad (245)$$

where $\mathcal{T}_1(k)$ is the one-loop contribution to the four-point function

$$\mathcal{T}_1(k)=\int\frac{d^dq}{(2\pi)^d}\frac{1}{q^2|\mathbf{q}+\mathbf{k}|^2}. \qquad (246)$$

In the Appendix, we show how to calculate the function $\mathcal{T}_1(k)$ in dimensional regularization. One finds

$$\mathcal{T}_1(k)=M^{2\epsilon}\frac{\Gamma\left(2-\frac{d}{2}\right)\Gamma\left(\frac{d}{2}-1\right)}{2^{2d-3}\pi^{(d-1)/2}\Gamma\left(\frac{d-1}{2}\right)}k^{d-4}. \qquad (247)$$
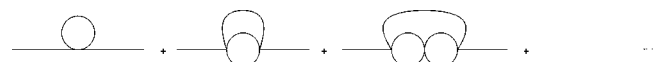

FIG. 20. Feynman graphs contributing to the self-energy to leading order in $1/N$.

The next step is to evaluate the integral over p in Eq. (244). Using Eq. (A21), we obtain

$$\int \frac{d^d p}{(2\pi)^d} \frac{1}{p^4} \left[\frac{1}{|\mathbf{p}+\mathbf{k}|^2} - \frac{1}{k^2} \right]$$

$$= M^{2\epsilon} \frac{\Gamma\left(3-\frac{d}{2}\right)\Gamma\left(\frac{d}{2}-2\right)}{2^{2d-4}\pi^{(d-1)/2}\Gamma\left(\frac{d-3}{2}\right)} k^{d-6}. \tag{248}$$

Inserting Eqs. (247) and (248) into Eq. (245), we obtain

$$\Delta\langle\phi_i^2\rangle = -M^{2\epsilon} \frac{\Gamma\left(3-\frac{d}{2}\right)\Gamma\left(\frac{d}{2}-2\right)}{2^{2d-5}\pi^{(d-1)/2}\Gamma\left(\frac{d-3}{2}\right)}$$

$$\times \int \frac{d^d k}{(2\pi)^d} \frac{k^{d-6}}{a+bk^{d-4}}, \tag{249}$$

where

$$a = 6/Nu, \tag{250}$$

$$b = M^{2\epsilon} \frac{\Gamma\left(2-\frac{d}{2}\right)\Gamma\left(\frac{d}{2}-1\right)}{2^{2d-3}\pi^{(d-1)/2}\Gamma\left(\frac{d-1}{2}\right)}. \tag{251}$$

The final step consists of integrating over k. Using Eq. (A22) in the Appendix we obtain

$$\Delta\langle\phi_i^2\rangle = M^{4\epsilon} a^{(d-2)/(d-4)} b^{(3-d)/(d-4)}$$

$$\times \frac{\Gamma\left(3-\frac{d}{2}\right)\Gamma\left(\frac{d}{2}-2\right)\Gamma\left(\frac{2-d}{4-d}\right)\Gamma\left(\frac{6-d}{4-d}\right)}{2^{3d-6}\pi^{d-1/2}\Gamma\left(\frac{d-3}{2}\right)}. \tag{252}$$

The limit $d\to 3$ is regular and one obtains

$$\Delta\langle\phi_i^2\rangle = -\frac{Nu}{96\pi^2}. \tag{253}$$

Inserting the result (253) into Eq. (242), we obtain the critical temperature to leading order in $1/N$:

$$\frac{\Delta T_c}{T_c^0} = \frac{8\pi}{3\left[\zeta\left(\frac{3}{2}\right)\right]^{4/3}} a n^{1/3} \approx 2.33 n^{1/3} a, \tag{254}$$

where we have used that $u=3gT$ and $g=8\pi a$ and set $N=2$. Thus T_c *increases* linearly with a. As noted before (Baym *et al.*, 2000), the result (254) is independent of N. However, it is only valid in the limit $N\to\infty$.

The $1/N$ correction to the above result has recently been calculated by Arnold and Tomášik (2000). This is a very lengthy and technically complicated calculation. For instance, the integrals that one encounters at order $1/N$ are difficult to evaluate in $3-2\epsilon$ dimensions. Instead, Arnold and Tomášik always reduced their dia-

grams to unambiguous integrals in three dimensions that are simpler to evaluate. We shall not review the calculation, but merely state the result. Through next-to-leading order in $1/N$, the shift in T_c is

$$\frac{\Delta T_c}{T_c^0} = \frac{8\pi}{3\left[\zeta\left(\frac{3}{2}\right)\right]^{4/3}} \left[1 - \frac{0.5272}{N}\right] n^{1/3} a. \tag{255}$$

For $N=2$, this gives a correction of only 26%:

$$\frac{\Delta T_c}{T_c^0} = 1.71 n^{1/3} a. \tag{256}$$

2. Monte Carlo simulations

The action (238) can also be used as the starting point for numerical calculations of the critical temperature and other nonuniversal effects of a dilute Bose gas. This is done by putting the theory on a lattice and using Monte Carlo methods to solve the theory nonperturbatively. Such numerical simulations have been carried out by several groups (Grüter *et al.*, 1997; Holzmann and Krauth, 1999; Arnold and Moore, 2001a, 2001b; Kashurnikov *et al.*, 2001; Arnold *et al.*, 2002). This approach has been discussed in considerable detail by Arnold *et al.* (2002). The value of the coefficient in Eq. (230) reported by Grüter *et al.* (1997) is $c\simeq 0.34$, while Holzmann and Krauth (1999) obtained $c\simeq 2.3$. The most recent values reported by Arnold and Moore (2001a, 2001b) and by Kashurnikov *et al.* (2001) are $c\simeq 1.32$ and $c\simeq 1.29$, respectively. One source of discrepancy lies in the nonlinear corrections to T_c as a function of a at the densities where the simulations of Grüter *et al.* (1997) were performed. Holzmann and Krauth (1999) expanded the integrand in the path integral in powers of the interaction and kept only the first term in that expansion. This perturbative treatment of the interaction is incorrect, since the physics close to the phase transition is inherently nonperturbative. This is in contrast to the Monte Carlo simulations based on the action (238) (Arnold and Moore, 2001a, 2001b; Kashurnikov *et al.*, 2001). These calculations agree within error bars. We shall regard these lattice results as the correct result for the coefficient c in Eq. (230).

3. Other calculations

In this subsection, we briefly discuss other calculations of the shift in T_c in the dilute Bose gas. Generally, the expectation value $\langle\phi^2\rangle$ can be written as

$$\langle\phi^2\rangle = \int \frac{d^d k}{(2\pi)^d} \frac{1}{k^2+\mu_3+\Sigma(k)}, \tag{257}$$

where $\Sigma(k)$ is the self-energy function. The critical point is determined by the condition that the correlation length becomes infinite, or equivalently that the effective chemical potential $\mu_3+\Sigma(0)$ vanishes:

$$\mu_3+\Sigma(0)=0. \tag{258}$$

In the absence of interactions, the condition (258) reduces to the well known $\mu_3 = 0$. Using Eq. (258) to eliminate the chemical potential μ_3, we can write Eq. (242) as

$$\Delta\langle\phi^2\rangle = \int \frac{d^d k}{(2\pi)^d}\left[\frac{1}{k^2+\Sigma(k)-\Sigma(0)}-\frac{1}{k^2}\right]. \quad (259)$$

The next step is to make an approximation for the self-energy function appearing in Eq. (259). In the previous section, we used the large-N expression for the self-energy (245). Baym *et al.* (1999, 2001) considered three different equations for the self-energy.

- The one-bubble approximation:
  The self-energy is approximated by the second diagram in Fig. 17:

$$\Sigma(p)-\Sigma(0) = -2g^2 T\int\frac{d^d k}{(2\pi)^d}\,\mathcal{T}_1(k)$$

$$\times\left[\frac{1}{|\mathbf{p}+\mathbf{k}|^2+\Sigma(|\mathbf{p}+\mathbf{k}|)-\Sigma(0)}\right.$$

$$\left.-\frac{1}{k^2+\Sigma(k)-\Sigma(0)}\right]. \quad (260)$$

- The bubble-summation approximation:
  The self-energy is approximated by the bubble sum in Fig. 20:

$$\Sigma(p)-\Sigma(0) = -2g^2 T\int\frac{d^d k}{(2\pi)^d}\frac{\mathcal{T}_1(k)}{1+2g\mathcal{T}_1(k)}$$

$$\times\left[\frac{1}{|\mathbf{p}+\mathbf{k}|^2+\Sigma(|\mathbf{p}+\mathbf{k}|)-\Sigma(0)}\right.$$

$$\left.-\frac{1}{k^2+\Sigma(k)-\Sigma(0)}\right], \quad (261)$$

- The ladder-summation approximation:
  The self-energy is approximated by the ladder sum similar to the bubble sum,

$$\Sigma(p)-\Sigma(0) = \int\frac{d^d k}{(2\pi)^d}\frac{\mathcal{T}_1(k)}{1+g\mathcal{T}_1(k)}$$

$$\times\left[\frac{1}{|\mathbf{p}+\mathbf{k}|^2+\Sigma(|\mathbf{p}+\mathbf{k}|)-\Sigma(0)}\right.$$

$$\left.-\frac{1}{k^2+\Sigma(k)-\Sigma(0)}\right]. \quad (262)$$

Note that Eqs. (260)–(262) have been made self consistent by replacing the free propagators on the right-hand side by the interacting propagators.

Equations (260)–(262) have been solved numerically, and the results were used to evaluate Eq. (259) to obtain the corresponding shifts in T_c. The results for the coefficient c are 3.8, 2.5, and 1.6, respectively, and thus within a factor of 3. Note also that the prediction for the shift in T_c from the non-self-consistent bubble summation (the leading $1/N$ result with $N=2$) is very close to the result from the self-consistent bubble summation.

We can gain more insight into the mechanism behind the increase in T_c by looking at the modification of the spectrum for small momenta. Let us consider the non-self-consistent bubble sum

$$\epsilon(k) = k^2 + \Sigma(k) - \Sigma(0), \quad (263)$$

where

$$\Sigma(k) = \int\frac{d^d k}{(2\pi)^d}\frac{\mathcal{T}_1(k)}{1+g\mathcal{T}_1(k)}\frac{1}{|\mathbf{p}+\mathbf{k}|^2}. \quad (264)$$

For small momenta k, the difference $\Sigma(k)-\Sigma(0)$ can be approximated by (Baym *et al.*, 1999, 2001)

$$\Sigma(k)-\Sigma(0) = -\frac{2}{3\pi^2}k^2\left(\ln\frac{k}{k_c}-\frac{1}{3}\right), \quad k\ll k_c, \quad (265)$$

where $k_c = 8\pi^2 a/\lambda_T^2$ is the screening wave number. The logarithmic term in Eq. (265) indicates a modified spectrum for small wave numbers $\sim k^{2-\eta}$ and thus a hardening of the spectrum compared to the noninteracting case (the spectrum is of the form k^α, where $\alpha<2$). The hardening results from correlations among particles with low momentum, which leads to a decrease in the critical density and thus an increase in the critical temperature. Other approximations show a different functional dependence of the difference $\Sigma(k)-\Sigma(0)$ at small k, but the basic mechanism remains the same, namely, a hardening of the spectrum at the critical temperature. It has been pointed out (Baym and Holzmann, 2003) that the hardening of the spectrum for the $n=0$ Matsubara mode takes place exactly only at T_c. The Bogoliubov operator inequality guarantees that the spectrum remains quadratic away from T_c.

Variational methods have also been used recently (de Souza Cruz *et al.*, 2001, 2002; Braaten and Radescu, 2002) to calculate T_c. The basic idea is to compute Eq. (259) using an effective three-dimensional Lagrangian that has been reorganized according to the discussion in Sec. IV.B.2. The Lagrangian is written as $\mathcal{L}=\mathcal{L}_0+\mathcal{L}_{int}$, where

$$\mathcal{L}_0 = -\frac{1}{2}\phi_i\nabla^2\phi_i+\frac{1}{2}m^2\phi_i^2, \quad (266)$$

$$\mathcal{L}_{int} = \frac{1}{2}\delta(\mu_3-m^2)\phi_i^2+\frac{1}{24}\delta u(\phi_i\phi_i)^2, \quad (267)$$

and i runs from 1 to N. Calculations are carried out by using δ as a formal expansion parameter, expanding to a given order in δ, and setting $\delta=1$ at the end of the calculation. Finally, we need to give a prescription for the mass parameter m. In the calculations below, we shall use the criterion of minimal sensitivity. In this context, it reads

$$\frac{\partial\Delta\langle\phi^2\rangle}{\partial m}=0. \quad (268)$$

If we wish to apply variational methods to calculating the shift in T_c, we need to generalize the quantity $\Delta\langle\phi^2\rangle$

appearing in Eq. (259) to the field theory defined by Eqs. (266) and (267). We must be able to expand this quantity in powers of δ, and it must reduce to $\Delta\langle\phi^2\rangle$ when $\delta=1$. Several prescriptions for generalizing $\Delta\langle\phi^2\rangle$ have been proposed in the literature (de Souza Cruz *et al.*, 2001, 2002; Braaten and Radescu, 2002). Some of these prescriptions are well behaved in the limit $N \to\infty$, and some of them are not. Since the result for the shift in T_c is known analytically in this limit, this a desirable property for a prescription. Two generalizations that have this property have been considered (Braaten and Radescu, 2002):

$$\Delta_a\langle\phi^2\rangle=N\int\frac{d^dk}{(2\pi)^d}\left[\frac{1}{k^2+\Sigma(k)-\Sigma(0)}-\frac{1}{k^2}\right], \quad (269)$$

$$\Delta_b\langle\phi^2\rangle=N\int\frac{d^dk}{(2\pi)^d}\left[\frac{1}{k^2+m^2(1-\delta)+\Sigma(k)-\Sigma(0)}\right.$$
$$\left.-\frac{1}{k^2+m^2(1-\delta)}\right]. \quad (270)$$

In the following, we shall consider $\Delta_a\langle\phi^2\rangle$. The strategy is to calculate the difference $\Sigma(k)-\Sigma(0)$ in a powers series in δ, substitute the result into Eq. (269), and finally expand the resulting integral in powers of δ. The Feynman diagram that contributes to the self-energy to first order in δ is the leftmost diagram in Fig. 17. It is independent of the external momentum, and so the difference $\Sigma(k)-\Sigma(0)$ vanishes. The first nonzero contribution to the quantity $\Sigma(k)-\Sigma(0)$ is then given by the two-loop diagram in Fig. 17. The expression is

$$\Sigma_2(k)-\Sigma_2(0)=\delta^2\frac{N(N+2)}{18}u^2\int\frac{d^3p}{(2\pi)^3}\int\frac{d^3q}{(2\pi)^3}$$
$$\times\left[\frac{1}{p^2+m^2}\frac{1}{q^2+m^2}\frac{1}{(p+q+k)^2+m^2}\right.$$
$$\left.-\frac{1}{p^2+m^2}\frac{1}{q^2+m^2}\frac{1}{(p+q)^2+m^2}\right], \quad (271)$$

where the subscript n indicates the order in the loop expansion. We have set $d=3$ since the integral is finite in three dimensions. The integral is calculated in the Appendix. Using Eq. (A26), we obtain

$$\Sigma_2(k)-\Sigma_2(0)=\delta^2\frac{N(N+2)}{18}u^2\frac{1}{(4\pi)^2}$$
$$\times\left[1-\frac{3m}{k}\arctan\frac{k}{3m}-\frac{1}{2}\ln\frac{k^2+9m^2}{9m^2}\right]. \quad (272)$$

The self-energy (272) is itself second order in δ. The second-order result for $\Delta_a^{(2)}\langle\phi^2\rangle$ is then obtained by expanding Eq. (269) in powers of the subtracted self-energy and keeping only the first term:

$$\Delta_a^{(2)}\langle\phi^2\rangle=\int\frac{d^3k}{(2\pi)^3}\frac{1}{k^4}[\Sigma_2(k)-\Sigma_2(0)], \quad (273)$$

where the superscript indicates the order of δ. Using Eq. (A27),

$$\Delta_a^{(2)}\langle\phi^2\rangle=-\frac{1}{108(4\pi)^3}\frac{1}{m}\delta^2u^2N(N+2). \quad (274)$$

The minimal-sensitivity criterion (268) has no solution at second order in δ because Eq. (274) is a monotonic function of m. Thus one has to go to the third order in order to obtain a value for m. The result for $\Delta_a^{(3)}\langle\phi^2\rangle$ reads (Braaten and Radescu, 2002)

$$\Delta_a^{(3)}\langle\phi_i^2\rangle=-\frac{1}{108(4\pi)^3}\frac{1}{m}\delta^2u^2N(N+2)\left(1+\frac{1}{2}\delta\right)$$
$$-\delta^3\frac{N(N+2)(N+8)}{18}u^3I_3, \quad (275)$$

where

$$I_3=-\frac{1}{24(4\pi)^4}\left[\pi^2+16\ln\frac{3}{4}+12\mathrm{Li}_2(-1/3)\right]\frac{1}{m^2}. \quad (276)$$

Here

$$\mathrm{Li}_n(x)=\sum_{i=1}^{\infty}\frac{x^i}{i^n} \quad (277)$$

is the polylogarithmic function. At this order, the minimal-sensitivity criterion has a single real solution:

$$m=1.04u\frac{N+8}{24\pi}. \quad (278)$$

The resulting value for $\Delta_a^{(2)}\langle\phi_i^2\rangle$ is

$$\Delta_a^{(2)}\langle\phi_i^2\rangle=0.4813\frac{N+2}{N+8}\left(-\frac{Nu}{96\pi^2}\right). \quad (279)$$

When we set $N=2$, the prefactor becomes 0.19. The lattice result (Arnold and Moore, 2001a, 2001b) is

$$\Delta\langle\phi_i^2\rangle=(0.284\pm0.004)\left(-\frac{Nu}{96\pi^2}\right). \quad (280)$$

Thus the third-order approximation differs from the lattice Monte Carlo result by 66%. Similarly, it was found (Braaten and Radescu, 2002) that the fourth-order approximation differs from the numerical simulations by 61%. Braaten and Radescu (2002) also studied the convergence of the linear δ expansion to the exact result in the large-N limit. It was shown that it converges to the lattice Monte Carlo result (254), but that the convergence is rather slow.

A straightforward application of the linear delta expansion to field-theoretic problems has recently been criticized by Kleinert (Kleinert, 2003; Kleinert and Hamprecht, 2003). One must take into account the correct Wegner exponent (Wegner, 1972) that governs the approach to the strong-coupling limit. The method is then called variational perturbation theory (Kleinert, 1998a, 1998b, 1999). The failure to take into account the correct Wegner exponent is the reason why one finds complex-valued solutions in the linear delta expansion. These

TABLE I. The critical temperature for a dilute Bose gas obtained by various analytic and numerical methods.

$\dfrac{\Delta T_c}{T_0} = 2.33 n^{1/3} a,$	leading order $1/N$ (Baym *et al.*, 2000)
$\dfrac{\Delta T_c}{T_0} = 1.71 n^{1/3} a,$	next-to-leading order $1/N$ (Arnold and Tomasik, 2000)
$\dfrac{\Delta T_c}{T_0} = (1.32 \pm 0.02) n^{1/3} a,$	lattice (Arnold and Moore, 2001a, 2001b)
$\dfrac{\Delta T_c}{T_0} = (1.29 \pm 0.05) n^{1/3} a,$	lattice (Kashurnikov *et al.*, 2001)
$\dfrac{\Delta T_c}{T_0} = 0.7 n^{1/3} a,$	one-bubble approximation (Holzmann *et al.*, 1999)
$\dfrac{\Delta T_c}{T_0} = 3.8 n^{1/3} a,$	one-bubble self-consistent approximation (Baym *et al.*, 1999, 2001)
$\dfrac{\Delta T_c}{T_0} = 2.5 n^{1/3} a,$	ladder-summation approximation (Baym *et al.*, 1999, 2001)
$\dfrac{\Delta T_c}{T_0} = 1.6 n^{1/3} a,$	bubble-summation approximation (Baym *et al.*, 1999, 2001)
$\dfrac{\Delta T_c}{T_0} = (1.27 \pm 0.11) n^{1/3} a,$	seven-loop variational perturbation theory (Kastening, 2004)
$\dfrac{\Delta T_c}{T_0} = (1.23 \pm) n^{1/3} a,$	renormalization group in three dimensions (Ledowski *et al.*, 2003)
$\dfrac{\Delta T_c}{T_0} = (1.3 \pm 0.4) n^{1/3} a,$	simulations of classical field theory (Davis and Morgan, 2003)

matters are highly technical and beyond the scope of this paper. Interested readers are referred to the textbook by Kleinert and Schulte-Frolinde (2001). Variational perturbation theory has very recently been applied in a seven-loop calculation by Kastening (2004, see also Kastening, 2003; and Kleinert, 2003 for five and and six-loop calculations). The result for the coefficient is $c = 1.28 \pm 0.1$, which is in excellent agreement with lattice field-theory results. We also note that seven-loop calculations have been carried out for the case $N = 1$ and $N = 4$ as well. The values for the coefficient c are 1.07 ± 0.10 and 1.54 ± 0.11, respectively. These results are also in good agreement with the lattice simulation of Sun (2003), who obtained the values 1.09 and 1.59, respectively.

We close this section by listing in Table I the predictions for the shift in the critical temperature that were obtained by the various methods we have discussed.

VI. CONCLUSIONS

In the present paper, we have extensively discussed the dilute Bose gas at zero and finite temperature. Using effective-field-theory methods, we set up a systematic perturbative framework that can be used to calculate any quantity of the dilute Bose gas at zero temperature. Within this framework many of the classic results for the weakly interacting Bose gas are derived in an efficient and economical manner. Nonuniversal effects are an-

other application in which effective-field-theory methods are ideal. For instance, such methods were used to solve the long-standing problem of calculating the full order-na^3 correction to the ground-state energy density of a weakly interacting Bose gas. Similarly, it would be of interest to calculate higher-order corrections to the condensate density and compare the result with numerical results (Giorgini *et al.*, 1999). The strength of the effective-field-theory approach lies in the fact that it is systematic. To any given order in the low-energy expansion, only a finite number of terms in the effective Lagrangian contribute to a physical quantity, and this allows us to make definite predictions. Although effective field theories are nonrenormalizable in the traditional sense of the word, one can carry out renormalization systematically order by order in the low-energy expansion.

We have also discussed different approaches to the dilute Bose gas at finite temperature. Although both the Bogoliubov and Popov approximations are gapless, they break down at sufficiently high temperature. Since the interactions between excited bosons are ignored in the Bogoliubov approximation, it is only valid at very low temperatures, where one can neglect the thermal depletion of the condensate. The Popov approximation can be used at much higher temperatures. However, being a mean-field theory, it breaks down in the critical region. It incorrectly predicts a first-order phase transition with

the same T_c as the ideal Bose gas. The full HFB approximation violates the Hugenholz-Pines theorem, which any reasonable approximation should incorporate. The modified Popov approximation based on the many-body T matrix is an improvement over the original Popov approximation because it correctly predicts a second-order phase transition. The renormalization-group equations that have been derived (Bijlsma and Stoof, 1996a; Andersen and Strickland, 1999) show that the critical properties of the dilute Bose gas are given by a three-dimensional spin model with a continuous O(2) symmetry. Explicit numerical calculations demonstrate that the system undergoes a second-order phase transition where the effective coupling constant vanishes at the critical point. Of the other approaches to the thermodynamics of the dilute Bose gas, optimized perturbation theory is probably the most promising. It is a systematically improvable expansion with significant flexibility with respect to the choice of parameters. This approximation also respects the Goldstone theorem order by order in the perturbative expansion. To go beyond one loop for the free energy in optimized perturbation theory is a difficult, but not impossible, task. The complicated setting sun diagrams that appear at the two-loop level are most easily calculated using a method in which one separates the diagrams into contributions from zero, one, and two Bose-Einstein distribution functions (Andersen, Braaten, and Strickland, 2000).

Calculating the shift in the critical temperature of a weakly interacting Bose gas has been a long-standing problem. Using effective-field-theory methods to obtain an effective three-dimensional field theory combined with high-precision lattice calculations has settled the issue in a very elegant way. The next-to-leading-order result in the $1/N$ expansion shows that this expansion works surprisingly well for T_c; for $N=2$, the result is 29% higher than the predictions from the lattice simulations. Among other notable calculations, we mention the application of variational perturbation theory through seven loops. The agreement with lattice data for $N=1, 2$, and 4 is convincing.

This summarizes our current understanding of some aspects of the homogeneous Bose gas at zero and finite temperature. Significant progress has been made in the last ten years, but there are still open problems. We hope that this review has stimulated the reader to further research in the field.

APPENDIX: CALCULATIONAL DETAILS, NOTATION, AND CONVENTIONS

In this appendix, we give some calculational details that may be useful for the reader who is interested in going through the calculations in detail. We also define our notation and conventions used throughout the paper.

1. Zero temperature

All the zero-temperature calculations are carried out in real time. Loop integrals are integrals over real energies ω and over three-dimensional momenta $\mathbf{k}$. The integrals over ω are evaluated using contour integration.

The specific integrals needed are

$$\int \frac{d\omega}{2\pi} \ln[\omega^2 - \epsilon^2(p)] = i\epsilon(p), \tag{A1}$$

$$\int \frac{d\omega}{2\pi} \frac{1}{[\omega^2 - \epsilon^2(p)]} = -\frac{i}{2\epsilon(p)}, \tag{A2}$$

$$\int \frac{d\omega}{2\pi} \frac{1}{[\omega^2 - \epsilon^2(p)]^2} = \frac{i}{4\epsilon^3(p)}. \tag{A3}$$

Some momentum integrals are divergent in the infrared or in the ultraviolet, or both. Dimensional regularization can be used to regularize both ultraviolet and infrared divergences in three-dimensional integrals over momenta. The spatial dimension is generalized to $d=3-2\epsilon$ dimensions. The continuum limit is taken by replacing sums over wave vectors by integrals in $d=3-2\epsilon$ dimensions:

$$\frac{1}{V} \sum_{\mathbf{p}} \rightarrow M^{2\epsilon} \int \frac{d^d p}{(2\pi)^d}. \tag{A4}$$

Here, M is a renormalization scale that ensures that the integral also has the canonical dimension for $d \neq 3$. In the following, we absorb the factor $M^{2\epsilon}$ in the measure, and so it will not appear explicitly. Integrals are evaluated at a value of d for which they converge and then analytically continued to $d=3$.

The integral $I_{m,n}$ is defined by

$$I_{m,n}(\Lambda) = \int \frac{d^d p}{(2\pi)^d} \frac{p^{2m}}{p^n (p^2 + \Lambda^2)^{n/2}}. \tag{A5}$$

With dimensional regularization, $I_{m,n}$ is given by the formula

$$I_{m,n}(\Lambda) = \frac{\Omega_d}{(2\pi)^d} M^{2\epsilon} \Lambda^{d+2m-2n}$$

$$\times \frac{\Gamma\left(\frac{d-n}{2} + m\right) \Gamma\left(n - m - \frac{d}{2}\right)}{2\Gamma\left(\frac{n}{2}\right)}, \tag{A6}$$

where $\Omega_d = 2\pi^{d/2}/\Gamma(d/2)$ is the area of a d-dimensional sphere.

The integrals $I_{m,n}$ satisfy the relations

$$\frac{d}{d\Lambda^2}I_{m,n}=-\frac{n}{2}I_{m+1,n+2}, \tag{A7}$$

$$(d+2m-n)I_{m,n}=nI_{m+2,n+2}, \tag{A8}$$

$$\Lambda^2 I_{m,n}=I_{m-1,n-2}-I_{m+1,n}. \tag{A9}$$

The first relation follows directly from the definition of $I_{m,n}$. The second relation follows from integration by parts, while the last is simply an algebraic relation.

The specific integrals we need in the calculations are listed below. In the limit $d\rightarrow 3$, they become

$$I_{0,-1}=\frac{\Lambda^5}{15\pi^2}, \tag{A10}$$

$$I_{1,1}=\frac{\Lambda^3}{3\pi^2}, \tag{A11}$$

$$I_{-1,-1}=-\frac{\Lambda^3}{6\pi^2}, \tag{A12}$$

$$I_{4,5}=-\frac{4\Lambda}{3\pi^2}, \tag{A13}$$

$$I_{2,3}=-\frac{\Lambda}{\pi^2}, \tag{A14}$$

$$I_{0,1}=-\frac{\Lambda}{2\pi^2}, \tag{A15}$$

$$I_{-2,-1}=-\frac{\Lambda}{4\pi^2}\left[\frac{1}{\epsilon}+4-L-\gamma+\ln(\pi)\right], \tag{A16}$$

$$I_{-1,1}=-\frac{1}{4\Lambda\pi^2}\left[\frac{1}{\epsilon}+2-L-\gamma+\ln(\pi)\right], \tag{A17}$$

where $L=\ln(\Lambda^2/M^2)$. The integrals $I_{-1,1}$ and $I_{-2,-1}$ are both logarithmically divergent in the infrared and this shows up as a pole in ϵ.

We also need to calculate some integrals in d dimensions that depend on the external momentum k. The integral $\mathcal{T}_1(k)$ defined in Eq. (246) is

$$\mathcal{T}_1(k)=\int\frac{d^d q}{(2\pi)^d}\frac{1}{q^2|\mathbf{q}+\mathbf{k}|^2}. \tag{A18}$$

By introducing a Feynman parameter y, we can write the integral as

$$T(k)=\int_0^1 dy\int\frac{d^d q}{(2\pi)^d}\frac{1}{(q^2+m^2)^2}, \tag{A19}$$

where $m^2=y(1-y)k^2$. First integrating over q, and then over y gives

$$T(k)=M^{2\epsilon}\frac{\Gamma\left(2-\frac{d}{2}\right)}{(4\pi)^{d/2}}\int_0^1 dy\,m^{d-4}$$

$$=M^{2\epsilon}\frac{\Gamma\left(2-\frac{d}{2}\right)\Gamma\left(\frac{d}{2}-1\right)}{2^{2d-3}\pi^{(d-1)/2}\Gamma\left(\frac{d-1}{2}\right)}k^{d-4}. \tag{A20}$$

Other integrals needed are calculated in the same manner. Specifically, we need the integrals

$$\int\frac{d^d p}{(2\pi)^d}\frac{1}{p^4}\left[\frac{1}{|\mathbf{p}+\mathbf{k}|^2}-\frac{1}{k^2}\right]$$

$$=M^{2\epsilon}\frac{\Gamma\left(3-\frac{d}{2}\right)\Gamma\left(\frac{d}{2}-2\right)}{2^{2d-4}\pi^{(d-1)/2}\Gamma\left(\frac{d-3}{2}\right)}k^{d-6}, \tag{A21}$$

$$\int\frac{d^d p}{(2\pi)^d}\frac{p^{d-6}}{a+bp^{d-4}}$$

$$=-M^{2\epsilon}\frac{\Gamma\left(\frac{2-d}{4-d}\right)\Gamma\left(\frac{6-d}{4-d}\right)}{2^{d-1}\pi^{d/2}\Gamma\left(\frac{d}{2}\right)}a^{(d-2)/(d-4)}b^{(3-d)/(d-4)}. \tag{A22}$$

Note that the integral in Eq. (A21) vanishes in $d=3$ dimensions due to the factor $\Gamma(-\epsilon)$ in the denominator. The integral (A22) has a pole in ϵ. When these integrals are combined, the limit $d\rightarrow 3$ is regular.

We need to evaluate the subtracted two-loop self-energy in the linear delta expansion. The expression is

$$\Sigma_2(k)-\Sigma_2(0)=\int\frac{d^d p}{(2\pi)^d}\int\frac{d^d q}{(2\pi)^d}$$

$$\times\left[\frac{1}{p^2+m^2}\frac{1}{q^2+m^2}\frac{1}{(p+q+k)^2+m^2}\right.$$

$$\left.-\frac{1}{p^2+m^2}\frac{1}{q^2+m^2}\frac{1}{(p+q)^2+m^2}\right]. \tag{A23}$$

This integral is ultraviolet finite and can be calculated directly in three dimensions by going to coordinate space:

$$\Sigma_2(k)-\Sigma_2(0)=\int d^3r[e^{i\mathbf{k}\cdot\mathbf{r}}-1]V^3(r), \tag{A24}$$

where $V(r)$ is the Fourier transform of the propagator,

$$V(r)=\int\frac{d^3 p}{(2\pi)^3}\frac{e^{i\mathbf{p}\cdot\mathbf{r}}}{p^2+m^2}=\frac{1}{4\pi r}e^{-mr}. \tag{A25}$$

This is the usual Yukawa potential. Integrating over r yields

$$\Sigma_2(k)-\Sigma_2(0)=\frac{1}{(4\pi)^2}\left[1-\frac{3m}{k}\arctan\frac{k}{3m}\right.$$

$$\left.-\frac{1}{2}\ln\frac{k^2+9m^2}{9m^2}\right]. \tag{A26}$$

Finally, we need to evaluate the integral

$$\Delta_a^{(2)}\langle\phi^2\rangle=\int\frac{d^d k}{(2\pi)^d}\frac{1}{k^4}[\Sigma_2(k)-\Sigma_2(0)].$$

The integral is finite in the ultraviolet and can thus be evaluated directly in three dimensions. One obtains

$$\Delta_a^{(2)}\langle\phi^2\rangle = -\frac{1}{6(4\pi)^3}\frac{1}{m}. \tag{A27}$$

2. Finite temperature

In the imaginary-time formalism for thermal field theory, the four-momentum $P=(\omega_n,\mathbf{p})$ is Euclidean with $P^2=\omega_n^2+\mathbf{p}^2$. The Euclidean energy p_0 has discrete values: $\omega_n=2n\pi T$ for bosons, where n is an integer. Loop diagrams involve sums over ω_n and integrals over $\mathbf{p}$. With dimensional regularization, the integral is generalized to $d=3-2\epsilon$ spatial dimensions. We define the dimensionally regularized sum-integral by

$$\sumint_P \equiv M^{2\epsilon}T\sum_{\omega_n=2n\pi T}\int\frac{d^d p}{(2\pi)^d}. \tag{A28}$$

Again, the factor $M^{2\epsilon}$ is absorbed in the measure for convenience.

We also need to evaluate the various sums over Matsubara frequencies. They can be calculated by a standard contour trick, where one rewrites the sum as a contour integral in the complex energy plane (Kapusta, 1989). Specifically, we need the following sums:

$$\sum_n \ln[\omega_n^2+\omega^2]=\beta\omega+2\ln[1-e^{-\beta\omega}], \tag{A29}$$

$$\sum_n \frac{1}{\omega_n^2+\omega^2}=\frac{\beta}{2\omega}[1+2n(\omega)], \tag{A30}$$

where $n(\omega)=1/(e^{\beta\omega}-1)$ is the Bose-Einstein distribution function.

We also need to expand some sum-integrals about zero temperature. The phonon part of the spectrum then dominates the temperature-dependent part of the sum-integral. We can therefore approximate the Bogoliubov dispersion relation $\epsilon(p)$ by $p\sqrt{2\mu}$, and this gives the leading temperature correction. The specific sum-integrals needed are

$$\sumint_P \ln[\omega_n^2+\epsilon^2(p)]$$

$$=I_{0,-1}+\frac{T}{\pi^2}\int_0^\infty dp\,p^2\ln[1-e^{-\beta\epsilon(p)}]$$

$$=\frac{(2\mu)^{5/2}}{15\pi^2}-\frac{\pi^2T^4}{45(2\mu)^{3/2}}+\cdots, \tag{A31}$$

$$\sumint_P \frac{\epsilon^2(p)/p^2}{\omega_n^2+\epsilon^2(p)}=\frac{1}{2}I_{-1,-1}+\frac{1}{2\pi^2}\int_0^\infty dp\,\epsilon(p)n[\epsilon(p)]$$

$$=-\frac{(2\mu)^{3/2}}{12\pi^2}+\frac{T^2}{12\sqrt{2\mu}}+\cdots, \tag{A32}$$

$$\sumint_P \frac{p^2}{\omega_n^2+\epsilon^2(p)}=\frac{1}{2}I_{1,1}+\frac{1}{2\pi^2}\int_0^\infty dp\,\frac{p^4}{\epsilon(p)}n[\epsilon(p)]$$

$$=\frac{(2\mu)^{3/2}}{6\pi^2}+\frac{\pi^2T^4}{30(2\mu)^{5/2}}+\cdots, \tag{A33}$$

$$\sumint_P \frac{1}{\omega_n^2+\epsilon^2(p)}=\frac{1}{2}I_{0,1}+\frac{1}{2\pi^2}\int_0^\infty dp\,\frac{p^2}{\epsilon(p)}n[\epsilon(p)]$$

$$=-\frac{\sqrt{2\mu}}{4\pi^2}+\frac{\pi^2T^2}{12(2\mu)^{3/2}}+\cdots. \tag{A34}$$

REFERENCES

Al Khawaja, U., J. O. Andersen, N. P. Proukakis, and H. T. C. Stoof, 2002, Phys. Rev. A **66**, 013615.

Amelino-Camelia, G., and S.-Y. Pi, 1993, Phys. Rev. D **47**, 2356.

Andersen, J. O., U. Al Khawaja, and H. T. C. Stoof, 2002, Phys. Rev. Lett. **88**, 070407.

Andersen, J. O., E. Braaten, and M. Strickland, 2000, Phys. Rev. D **62**, 045004.

Anderson, M. H., J. R. Ensher, M. R. Matthews, C. Wieman, and E. A. Cornell, 1995, Science **269**, 198.

Andersen, J. O., and M. Strickland, 1999, Phys. Rev. A **60**, 1442.

Arnold, P., and G. D. Moore, 2001a, Phys. Rev. Lett. **87**, 120401.

Arnold, P., and G. D. Moore, 2001b, Phys. Rev. E **64**, 066113.

Arnold, P., G. D. Moore, and B. Tomášik, 2002, Phys. Rev. A **65**, 013606.

Arnold, P., and B. Tomášik, 2000, Phys. Rev. A **62**, 063604.

Baym, G., 1962, Phys. Rev. **127**, 1391.

Baym, G., J.-P. Blaizot, M. Holzmann, F. Laloë, and D. Vautherin, 1999, Phys. Rev. Lett. **83**, 1703.

Baym, G., J.-P. Blaizot, M. Holzmann, F. Laloë, and D. Vautherin, 2001, Eur. Phys. J. B **24**, 107.

Baym, G., J.-P. Blaizot, and J. Zinn-Justin, 2000, Europhys. Lett. **49**, 150.

Baym, G., and M. Holzmann, 2003, Phys. Rev. Lett. **90**, 040402.

Beliaev, S. T., 1958, Sov. Phys. JETP **7**, 289.

Bijlsma, M., and H. T. C. Stoof, 1996a, Phys. Rev. A **54**, 5085.

Bijlsma, M., and H. T. C. Stoof, 1996b, Phys. Rev. A **55**, 498.

Blaizot, J.-P., and G. Ripka, 1986, *Quantum Theory of Finite Systems* (MIT, Cambridge).

Bogoliubov, N. N., 1947, J. Phys. (Moscow) **11**, 23.

Bose, S. N., 1924, Z. Phys. **26**, 178.

Braaten, E., and H.-W. Hammer, 2003, Phys. Rev. A **67**, 042706.

Braaten, E., H.-W. Hammer, and S. Hermans, 2001, Phys. Rev. A **63**, 063609.

Braaten, E., and A. Nieto, 1999a, Phys. Rev. A **60**, 2330.

Braaten, E., and A. Nieto, 1999b, Eur. Phys. J. B **11**, 143.

Braaten, E., and E. Radescu, 2002, Phys. Rev. A **66**, 063601.

Bradley, C. C., C. A. Sackett, J. J. Tollett, and R. G. Hulet, 1995, Phys. Rev. Lett. **75**, 1687.

Brezin, E., and S. R. Wadia, 1993, Eds., *The Large-N Expansion in Quantum Field Theory and Statistical Physics* (World Scientific, Singapore).

Bruecker, K. A., and K. Sawada, 1957, Phys. Rev. **106**, 1117.

Canet, L., B. Delamotte, D. Mouhanna, and J. Videl, 2003, Phys. Rev. D **67**, 065004.

Caswell, W. E., and G. P. Lepage, 1986, Phys. Lett. **167B**, 437.

Chiku, S., 2000, Prog. Theor. Phys. **104**, 1129.

Chiku, S., and T. Hatsuda, 1998, Phys. Rev. D **58**, 076001.

Cornish, L., N. R. Claussen, J. L. Roberts, E. A. Cornell, and C. Wieman, 2000, Phys. Rev. Lett. **85**, 1795.

Cornwall, J. M., R. Jackiw, and E. Tomboulis, 1974, Phys. Rev. D **10**, 2428.

Dalfovo, F., S. Giorgini, L. P. Pitaevskii, and S. Stringari, 1999, Rev. Mod. Phys. **71**, 463.

Davis, K. B., M. O. Mewes, M. R. Andrews, N. J. van Druten, D. S. Durfee, D. M. Kurn, and W. Ketterle, 1995, Phys. Rev. Lett. **75**, 3969.

Davis, M. J., and S. A. Morgan, 2003, Phys. Rev. A **68**, 053615.

de Souza Cruz, F. F., M. B. Pinto, and R. O. Ramos, 2001, Phys. Rev. B **64**, 014515.

de Souza Cruz, F. F., M. B. Pinto, R. O. Ramos, and P. Sena, 2002, Phys. Rev. A **65**, 053613.

Duncan, A., and M. Moshe, 1988, Phys. Lett. B **215**, 352.

Einstein, A., 1924, Sitz. Ber. Preussischen Akad. Wiss. Phys. Math. Kl. **261**, 3.

Feshbach, H., 1962, Ann. Phys. (N.Y.) **19**, 287.

Fetter, A., and J. D. Walecka, 1971, *Quantum Theory of Many-particle Systems* (McGraw-Hill, New York).

Gasser, J., and H. Leutwyler, 1984, Ann. Phys. (N.Y.) **158**, 142.

Gasser, J., and H. Leutwyler, 1985, Nucl. Phys. B **250**, 465.

Gavoret, J., and P. Nozières, 1964, Ann. Phys. (N.Y.) **28**, 349.

Gell-Mann, M., and K. A. Brueckner, 1957, Phys. Rev. **106**, 364.

Georgi, H., 1993, Annu. Rev. Nucl. Part. Sci. **43**, 209.

Giorgini, S., J. Boronat, and J. Casulleras, 1999, Phys. Rev. A **60**, 5129.

Giradeau, M., and R. Arnowitt, 1959, Phys. Rev. **113**, 755.

Glassgold, A. E., A. N. Kaufmann, and K. M. Watson, 1960, Phys. Rev. **120**, 660.

Goldstone, J., 1961, Nuovo Cimento **19**, 154.

Griffin, A., 1996, Phys. Rev. B **53**, 9341.

Grüter, P., D. Ceperly, and F. Laloe, 1997, Phys. Rev. Lett. **79**, 3549.

Haque, M., 2003, cond-mat/0302076.

Haugset, T., H. Haugerud, and F. Ravndal, 1998, Ann. Phys. (N.Y.) **266**, 27.

Hohenberg, P. H., and P. H. Martin, 1965, Ann. Phys. (N.Y.) **34**, 291.

Holzmann, M., P. Grüter, and F. Laloe, 1999, Eur. J. Phys. **10**, 739.

Holzmann, M., and W. Krauth, 1999, Phys. Rev. Lett. **83**, 2687.

Huang, K., 1964, in *Studies in Statistical Mechanics*, Vol. 2, edited by J. de Boer and G. E. Uhlenbeck (North-Holland, Amsterdam), p. 3.

Huang, K., 1999, Phys. Rev. Lett. **83**, 3770.

Huang, K., and C. N. Yang, 1957, Phys. Rev. **105**, 767.

Hugenholz, N. M., and D. Pines, 1958, Phys. Rev. **116**, 489.

Hugenholz, N. M., and D. Pines, 1959, Phys. Rev. **116**, 489.

Hutchinson, D. A. W., K. Burnett, R. J. Dodd, S. A. Morgan, M. Rusch, E. Zaremba, N. P. Proukakis, M. Edwards, and C. W. Clark, 2000, J. Phys. B **33**, 3825.

Hutchinson, D. A. W., R. J. Dodd, and K. Burnett, 1998, Phys. Rev. Lett. **81**, 2198.

Inouye, S., M. R. Andrews, J. Stenger, H.-J. Miesner, D. M. Stamper-Kurn, and W. Ketterle, 1998, Nature (London) **392**, 151.

Kaplan, D., 1995, Effective field theories: Lectures given at the 7th Summer School in Nuclear Physics Symmetries, Seattle, WA, 18–30 June 1995, nucl-th/9506035.

Kapusta, J. I., 1989, *Finite Temperature Field Theory* (Cambridge University, Cambridge, England).

Kashurnikov, V. A., N. V. Prokof'ev, and B. V. Svistunov, 2001, Phys. Rev. Lett. **87**, 120402.

Kastening, B., 2003, Phys. Rev. A **68**, 061601(R).

Kastening, B., 2004, Phys. Rev. A **69**, 043613.

Kleinert, H., 1998a, Phys. Lett. B **434**, 74.

Kleinert, H., 1998b, Phys. Rev. D **57**, 2264; **58**, 107702 (addendum).

Kleinert, H., 1999, Phys. Rev. D **60**, 085001.

Kleinert, H., 2003, Mod. Phys. Lett. B **17**, 1011.

Kleinert, H., and B. Hamprecht, 2003, Phys. Rev. D **68**, 065001.

Kleinert, H., and V. Schulte-Frolinde, 2001, *Critical Properties of ϕ^4-Theories*, 1st ed. (World Scientific, Singapore).

Landau, L. D., 1947, J. Phys. (Moscow) **11**, 91.

Landau, L. D., and E. M. Lifshitz, 1980, *Quantum Mechanics* (Pergamon, New York), Vol. 3.

Landsman, N. P., 1989, Nucl. Phys. B **322**, 498.

Ledowski, S., N. Hasselmann, and P. Kopietz, 2003, cond-mat/0311043.

Lee, T. D., K. Huang, and C. N. Yang, 1957, Phys. Rev. **106**, 1135.

Lee, T. D., and C. N. Yang, 1957, Phys. Rev. **105**, 1119.

Lee, T. D., and C. N. Yang, 1958, Phys. Rev. **112**, 1419.

Leggett, A. J., 2001, Rev. Mod. Phys. **73**, 307.

Lepage, G. P., 1989, in *From Actions to Answers: Proceedings of the TASI'89 Summer School*, Boulder, CO, 1989, edited by T. DeGrand and D. Toussant (World Scientific, Singapore), p. 483.

Liao, S.-B., and M. Strickland, 1995, Phys. Rev. D **52**, 3653.

Lieb, E. H., 1963, Phys. Rev. **130**, 2518.

Litim, D. F., 2000, Phys. Lett. B **486**, 92.

Litim, D. F., 2001, Phys. Rev. D **64**, 105007.

Litim, D. F., and J. M. Pawlowski, 2002, Phys. Rev. D **65**, 081701.

Liu, W. V., 1997, Phys. Rev. Lett. **79**, 4056.

Liu, W. V., 1998, Int. J. Mod. Phys. B **12**, 2103.

Lundh, E., and J. Rammer, 2002, Phys. Rev. A **66**, 033607.

Luttinger, J. M., and J. D. Ward, 1960, Phys. Rev. **118**, 1417.

Metikas, G., and G. Alber, 2002, J. Phys. B **35**, 4223.

Morgan, S., 1999, J. Phys. B **33**, 3847.

Morris, T. R., 1994a, Phys. Lett. B **329**, 241.

Morris, T. R., 1994b, Phys. Lett. B **334**, 355.

Morris, T. R., 1998, Int. J. Mod. Phys. B **12**, 1343.

Moshe, M., and J. Zinn-Justin, 1998, Phys. Rep. **385**, 69.

Negele, J. W., and H. Orland, 1988, *Quantum Many-Particle Systems* (Addison-Wesley, New York).

Nicoll, J. F., T. S. Chang, and H. E. Stanley, 1974, Phys. Rev. Lett. **33**, 540.

Okopinska, A., 1987, Phys. Rev. D **35**, 1835.

Pethick, C. J., and H. Smith, 2002, *Bose-Einstein Condensation in Dilute Gases* (Cambridge University Cambridge, England).

Petrov, D. S., M. Holzmann, and G. V. Shlyapnikov, 2000, Phys. Rev. Lett. **84**, 2551.

Petrov, D. S., G. V. Shlyapnikov, and J. T. M. Walraven, 2000, Phys. Rev. Lett. **85**, 3745.

Pitaevskii, L. P., and S. Stringarii, 2003, *Bose-Einstein Condensation* (Oxford University, Oxford, UK).

Polchinski, J., 1984, Nucl. Phys. **231**, 269.

Popov, V. N., 1983, *Functional Integrals in Quantum Field Theory and Statistical Physics* (Reidel, Dordrecht).

Popov, V. N., 1987, *Functional Integrals and Collective Excitations* (Cambridge University, Cambridge, England).

Proukakis, N. P., S. A. Morgan, S. Choi, and K. Burnett, 1998, Phys. Rev. A **58**, 2435.

Sawada, K., 1959, Phys. Rev. **116**, 1344.

Schakel, A. M. J., 1994, Int. J. Mod. Phys. B **8**, 2021.

Shi, H., and A. Griffin, 1998, Phys. Rep. **304**, 1.

Stancu, I., and P. M. Stevenson, 1990, Phys. Rev. D **42**, 2710.

Stevenson, P. M., 1981, Phys. Rev. D **23**, 2916.

Stwalley, W. C., 1976, Phys. Rev. Lett. **37**, 1628.

Sun, X., 2003, Phys. Rev. E **67**, 066702.

't Hooft, G., and J. M. G. Veltman, 1972, Nucl. Phys. B **44**, 189.

Takan, F., 1961, Phys. Rev. **123**, 699.

Tiesinga, E., B. J. Verhaar, and H. T. C. Stoof, 1993, Phys. Rev. A **47**, 4114.

Toyoda, T., 1982, Ann. Phys. (N.Y.) **141**, 154.

Wegner, F. J., 1972, Phys. Rev. B **5**, 1891.

Wilkens, M., F. Illuminati, and M. Kraмer, 2000, J. Phys. B **33**, L779.

Wilson, K., and J. Kogut, 1974, Phys. Rep. **12**, 75.

Wu, T. T., 1959, Phys. Rev. **115**, 1390.

Yan, Z.-C., J. F. Babb, A. Dalgarno, and G. W. F. Drake, 1996, Phys. Rev. A **54**, 2824.

Yukalov, V. I., 1976, Moscow Univ. Phys. Bull. **31**, 10.

Zinn-Justin, J., 1989, *Quantum Field Theory and Critical Phenomena* (Oxford University, New York).